

Controllable hydrogen bonded self-association for the formation of multifunctional antimicrobial materials

Lisa J. White, Jessica E. Boles, Nyasha Allen, Luke S. Alesbrook, J. Mark Sutton, Charlotte K. Hind, Kira L. F. Hilton, L. R. Blackholly, Rebecca J. Ellaby, George T. Williams, Daniel P. Mulvihill* and Jennifer R. Hiscock*

Table of Contents

Controllable self-association leads to the formation of multifunctional antimicrobial materials	1
Experimental	2
Biological experiments ¹	3
Chemical structures	5
Chemical synthesis.....	5
NMR	6
Characterisation NMR.....	6
Inversion Test.....	9
Dynamic light scattering data	27
Rheological data.....	30
Amplitude sweep	30
Frequency sweep	36
Fluorescence microscopy, scanning electron microscopy and energy dispersive X-ray analysis.....	42
MIC ₅₀ Growth Curves.....	56
USA 300 Methicillin-resistant <i>Staphylococcus aureus</i> (MRSA)	56
<i>Escherichia coli</i> DH10 β (<i>E. coli</i>)	59
Hydrogel antimicrobial efficacy experiments	62
References	66

Experimental

General remarks: A positive pressure of nitrogen and oven dried glassware were used for all reactions. All solvents and starting materials were purchased from known chemical suppliers or available stores and used without any further purification unless specifically stipulated. The NMR spectra were obtained using a Bruker AV2 400 MHz or AVNEO 400 MHz spectrometer. The data was processed using ACD Labs, MestReNova or Topspin software. NMR Chemical shift values are reported in parts per million (ppm) and calibrated to the centre of the residual solvent peak set (s = singlet, br = broad, d = doublet, t = triplet, q = quartet, m = multiplet). The melting point for each compound was measured using Stuart SMP10 melting point apparatus. High resolution mass spectrometry was performed using a Bruker microTOF-Q mass spectrometer and spectra recorded and processed using Bruker's Compass Data Analysis software. Infrared spectra were obtained using a Shimadzu IR-Affinity-1 model Infrared spectrometer. The data are analysed in wavenumbers (cm^{-1}) using IRsolution software. DLS and Zeta Potential studies were carried out using Anton Paar LitesizerTM 500 and processed using KalliopeTM Professional. Cellular growth curve measurements were obtained using a Thermo Scientific Multiscan Go 1510-0318C plate reader and recorded using the SkanIt Software 4.0. Rheological measurements were recorded on an Anton Parr modular compact rheometer (MCR302) using cylinder probe ST10-4V-8.8/97.5. The pH was determined using a Fisherbrand hydrous 300 pH detector. SEM analysis was performed using a Hitachi S3400 N scanning electron microscope, with a 20 Kv accelerating voltage at a vacuum level of <1 pa. The corresponding images were processed using Oxford Instruments AZtex software.

Fluorescence microscopy: Samples were visualised using an Olympus IX71 microscope with PlanApo 100x OTIRFM-SP 1.49 NA lens mounted on a PIFOC z-axis focus drive (Physik Instrumente, Karlsruhe, Germany), fitted onto an ASI motorised stage (ASI, Eugene, OR), with the sample holder, objective lens and environmental chamber held at the required temperature. Samples were illuminated using LED light sources (Cairn Research Ltd, Faversham, UK) with DC/ET350/50x excitation and DC/457/50m emission filters (Chroma, Bellows Falls, VT). Samples were visualised using a Zyla 5.5 (Andor) CMOS camera, and the system was controlled with Metamorph software (Molecular Devices).

Sample preparation: The appropriate salt solution (1 mL, 0.505 M) was added to 5 mg of the compound in a glass vial and heated to 60 °C. This solution was then transferred to a glass slide where it was then covered by a further glass slide before being mounted onto the microscope stage. Images were analysed using Fiji software with the SRRF plugin.

Mass spectrometry: Approximately 1 mg of each compound was dissolved in 1 mL of methanol. This solution was further diluted 100-fold before undergoing analysis where 10 μL of each sample was then injected directly into a flow of 10 mM ammonium acetate in 95 % water (flow rate = 0.02 mL/min).

DLS studies: All vials used for preparing the samples were clean and dry. All solvents used were filtered to remove any particulates that may interfere with the results obtained. Samples of differing concentrations were obtained through serial dilution of a concentrated solution. All samples underwent an annealing process, in which they were heated to 40 °C before being allowed to cool to 25 °C. A series of 9 or 10 runs were recorded at 25 °C.

Zeta potential studies: All vials used for preparing the samples were clean and dry. All solvents used were filtered to remove any particulates that may interfere with the results obtained. All samples underwent an annealing process in which the various solutions were heated to approximately 40 °C before cooling to room temperature, allowing each sample to reach a thermodynamic minimum. The final zeta potential value given is an average of the number of experiments conducted at 25 °C.

Rheometer hydrogel preparation and experimental: Each experiment was run in triplicate. The appropriate salt solution (1 mL, 0.505 M) was added to 5 mg of the compound in a glass vial with an internal diameter of 1 cm and heated to approximately 60 °C, until dissolved. The sample was positioned on the rheometer and set with a relaxation time of 60 minutes. Oscillatory amplitude experiments maintained a frequency of 10 rad s⁻¹ and performed with the amplitude of oscillation from 0.01 % up to 100 % at 298 K. Oscillatory frequency sweep experiments maintained a constant shear strain (γ) of 0.0925 % with an increasing frequency from 0.1–100 rad s⁻¹ at 298 K.

Scanning Electron Microscopy (SEM) and xerogel sample preparation: A sample of hydrogel containing the compound (5 mg) in the appropriate salt solution (1 mL, 0.505 M) was dehydrated to form a xerogel. The sample was then positioned on a carbon tab, which was then mounted on an aluminium stub.

pH determination: The pH meter was calibrated to pH 4, pH 7 and pH 10 using standardized calibration solutions supplied by Oakton. **Salt solution preparation:** All salts were obtained from commercial sources and diluted in 100 mL of distilled H₂O. **Sample preparation:** Samples were prepared for testing by dilution of 2 g of the hydrogel in 20 mL of distilled H₂O and placed in the refrigerator for 2 hours. Before testing the samples were removed from the refrigerator and allowed to acclimatize to room temperature. Measurements were taken in triplicate and the average recorded.

Hydrogel preparation: The appropriate salt solution (1 mL, 0.505 M) was added to the specified quantity of the compound in a glass vial and heated to approximately 60 °C until dissolved then left at room temperature to allow gelation to occur. Gel formation was achieved through an annealing process in which the pre-gel mixture was heated until the gelator (**1**) had dissolved. At this point, the samples were sealed and allowed to cool to room temperature, before undergoing an inversion test to confirm the formation of a hydrogel. The formation of hydrogels was attempted through the addition of the salt solution only, as well as the use of mechanical agitation by a vortexer and sonication. That neither of these conditions yielded hydrogels, is indicative of the stability of the self-associated aggregates.

Salt Solution triggered gelation: The appropriate salt solution (0.1 mL, 5.05 M) was added to the compound (1.5 mg in 0.9 mL of H₂O) in a glass vial.

Mechanically triggered gelation: The appropriate salt solution (0.1 mL, 5.05 M) was added to the compound (1.5 mg in 0.9 mL of H₂O) in a glass vial, mixed using a vortex for 1 minute and left at room temperature for 12 hours to allow gelation to occur.

Biological experiments¹

Preparation of Luria Broth media (LB): Yeast extract (5 g), tryptone (10 g) and sodium chloride (10 g) were dissolved in dH₂O (1 L) then divided into bottles and autoclaved.

Preparation of Luria Broth (LB) agar plates: Agar (6 g) was added to LB (400 mL) and autoclaved. Once cool, the LB agar was poured into sterile petri dishes under sterile conditions and allowed to set. LB plates were stored at 4 °C until use.

Preparation of McFarland standard: Barium chloride (1%, 50 μ L) was added to sulfuric acid (1%, 9.95 mL) and mixed together. The optical density was recorded at 600 nm.

Preparation of antimicrobial compounds for MIC₅₀ calculations: Compounds were dissolved into 5 % ethanol to make up solutions on the day of experiment. Eight concentrations of SSA were made up with final well concentrations of 5 % ethanol.

Preparation of bacterial plates: Sterile LB agar plates were streaked using the desired bacteria (either *Escherichia coli* DH10 β or USA300 *Methicillin-Resistant Staphylococcus aureus*) then incubated at 37 °C overnight.

Preparation of Inoculum: An initial culture was made up by inoculating LB media (5 mL) with at least 4 single colonies of the desired bacteria under sterile conditions and incubating at 37 °C overnight. The following day, a subculture was made up using LB (5 mL) and the initial culture (50 μ L), then incubated at 37 °C until the culture had reached an optical density of 0.4 at 600 nm. Density was adjusted using sterile dH₂O to equal 0.5 McFarland standard ($10^7 - 10^8$ cfu/mL), then a 1:10 dilution was carried out using sterile dH₂O (900 μ L) and the McFarland adjusted suspension (100 μ L). A final dilution (1:100) was carried using the 1:10 suspension (150 μ L) and LB (14.85 mL) before use to achieve a final cell concentration of 10^5 cfu/mL.

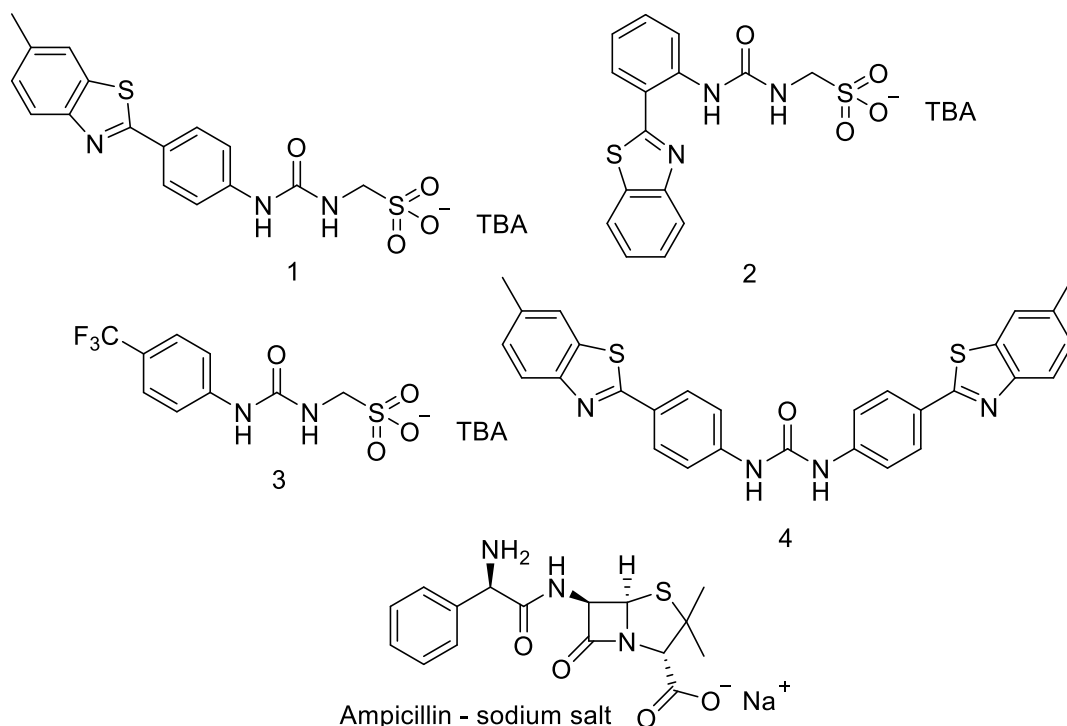
Preparation of 96 well microplate for MIC₅₀: The 1:100 cell suspension (150 μ L) was dispensed into individual wells under sterile conditions. Compounds (30 μ L) were added to the wells to equal a total volume of 180 μ L in the wells. Each experimental condition was repeated (n = 6) and the experiment was repeated on different days. The plates were sealed using parafilm, then incubated at 37 °C in a microplate reader for 18-25 hours. Absorbance readings were taken at 600 nm every 15 min. Data was used to generate growth curves.

Calculation of MIC₅₀: Growth curves were plotted using OD₆₀₀ absorbance readings in Microsoft[®] Excel[®] 2013. OD₆₀₀ absorbance readings 900 minutes from the start of each of these growth cultures for each concentration of drug were plotted in Origin[®] 2015. The resultant curve was normalised and fitted using the Boltzmann fit to define concentration able to reduce the measured cell growth by 50 % (MIC₅₀) for each compound or molecule combination.

Agar well diffusion assay: An initial culture and subsequent sub-culture was created as previously described. LB Agar was made up by mixing LB (200 mL) and agar (3.0 g), then autoclaved. Once autoclaved, the molten agar was placed in a 50 °C water bath until this temperature had equilibrated. The molten agar was then inoculated using the subculture (15 mL), then swirled to mix. The inoculated agar was added to sterile petri dishes (6 mL) then allowed to set under sterile conditions. A sterile cutter was used to remove a disk from the inoculated agar, creating a well in the plate, and the bottom was sealed using fresh agar (5 μ L). Once set, the desired solution or gel required was pipetted into the well (50 μ L) and then placed into a 37 °C incubator for 18 hours then imaged using an ESPON perfection V750 PRO.

Surface diffusion assay: An initial culture and subsequent sub-culture was created as previously described. LB Agar was made up by mixing LB (200 mL) and agar (3.0 g), then autoclaved. Once autoclaved, the molten agar was placed in a 50 °C water bath until this temperature had equilibrated. The molten agar was then inoculated using the subculture (15 mL), then swirled to mix. The inoculated agar was added to sterile petri dishes (6 mL) then allowed to set under sterile conditions. The molten compound gel solutions were pipetted into an empty sterile petri dish (50 μ L). Once gel had set, this was carefully placed onto the center of the set agar plates, then placed into a 37 °C incubator for 18 hours and imaged using an ESPON perfection V750 PRO.

Chemical structures



Chemical synthesis

Compound 1: This compound was synthesised in line with our previously published methods. Proton NMR were found to match our previously published values.²¹H NMR (400 MHz, DMSO-*d*₆): δ : 9.19 (s, 1H), 7.91 – 7.84 (m, 4H), 7.57 (d, *J* = 8.74 Hz, 2H), 7.32 – 7.29 (m, 1H), 6.80 (t, *J* = 5.88 Hz, 1H), 3.93 (d, *J* = 5.88 Hz, 2H), 3.15 – 3.12 (m, 8H), 2.43 (s, 3H), 1.59 – 1.51 (m, 8H), 1.34 – 1.25 (m, 8H), 0.92 (t, *J* = 7.32 Hz, 12H).

Compound 2: This compound was synthesised in line with our previously published methods. Proton NMR were found to match our previously published values.²¹H NMR (400 MHz, DMSO-*d*₆): δ : 10.67 (s, 1H) 8.45 (d, *J* = 7.77 Hz, 1H), 8.30 (d, *J* = 7.79 Hz, 1H), 8.15 (d, *J* = 7.92 Hz, 1H), 7.85 (br d, *J* = 7.72 Hz, 2H), 7.58 (t, *J* = 7.58 Hz, 1H), 7.47 (tt, *J* = 11.69, 7.49 Hz, 2H), 7.10 (t, *J* = 7.52 Hz, 1H), 3.97 (s, 2H), 3.23 – 2.99 (m, 8H), 1.62 – 1.44 (m, 8H), 1.41 – 1.19 (m, 8H), 0.92 (t, *J* = 7.32 Hz, 12H).

Compound 3: This compound was synthesised in line with our previously published methods. Proton NMR were found to match our previously published values.³¹H NMR (400 MHz, 298.15 K, DMSO-*d*₆): δ : 9.24 (s, 1H), 7.55 (dd, *J* = 8.72 Hz, 4H), 6.88 (s, 1H), 3.92 (d, *J* = 5.96 Hz, 2H), 3.17 - 3.13 (m, 8H), 1.60-1.52 (m, 8H), 1.34 - 1.25 (m, 8H), 0.92 (t, *J* = 7.36 Hz, 12H).

Compound 4: Triphosgene (0.31 g, 1.00 mM) was added to a stirring solution of 4-(6-methylbenzothiazol)aniline (0.50 g, 2.00 mM) in ethyl acetate (30 mL) and the mixture heated at reflux for 4 hours. 4-(6-methylbenzothiazol)aniline (0.50 g, 2.00 mM) was then added to the reaction mixture and heated at reflux overnight, filtered and the solid washed with ethyl acetate (10 mL). The impurities were removed through the recrystallization, followed by filtration of the solid from methanol. The filtration was then taken to dryness to give the pure product as a yellow solid with a yield of 84 % (0.85 g, 1.68 mM); Melting Point: > 200 °C; ¹H NMR (400 MHz, DMSO-*d*₆): δ : 9.19 (s, 2H), 8.02 (d, *J* = 8.72 Hz, 4H), 7.91 (ds, 4H), 7.69 (d, *J* = 8.52 Hz, 4H), 7.35 (d, *J* = 8.44 Hz, 2H), 2.47 (s, 6H);

$^{13}\text{C}\{^1\text{H}\}$ NMR (100 MHz, $\text{DMSO-}d_6$): δ : 166.4 (CO), 152.5 (ArC), 152.3 (ArC), 142.8 (ArC), 135.4 (ArC), 134.8 (ArC), 128.3 (ArCH), 127.1 (ArC), 122.5 (ArCH), 122.2 (ArCH), 118.1 (ArCH), 21.5 (CH_3); IR (film): ν = 3270 (NH stretch), 1687, 1100, 995; HRMS ($\text{C}_{29}\text{H}_{22}\text{N}_4\text{OS}_2$) (ESI $^-$): m/z : act: 507.8847 [$\text{M} + \text{H}^+$] $^-$ cal: 506.1235 [M].

NMR

Characterisation NMR

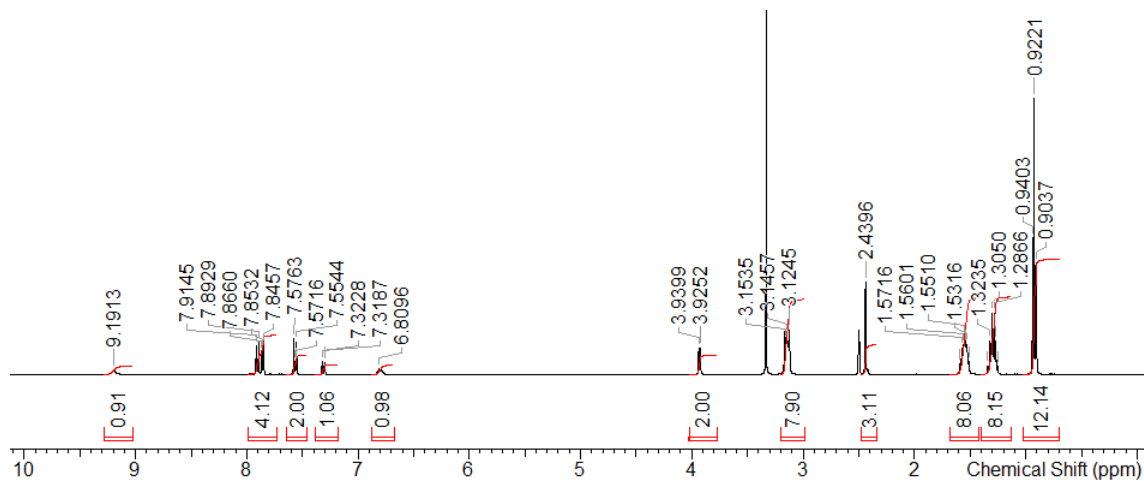


Figure S1 - ^1H NMR spectrum of compound **1** in $\text{DMSO-}d_6$ conducted at 298.15 K.

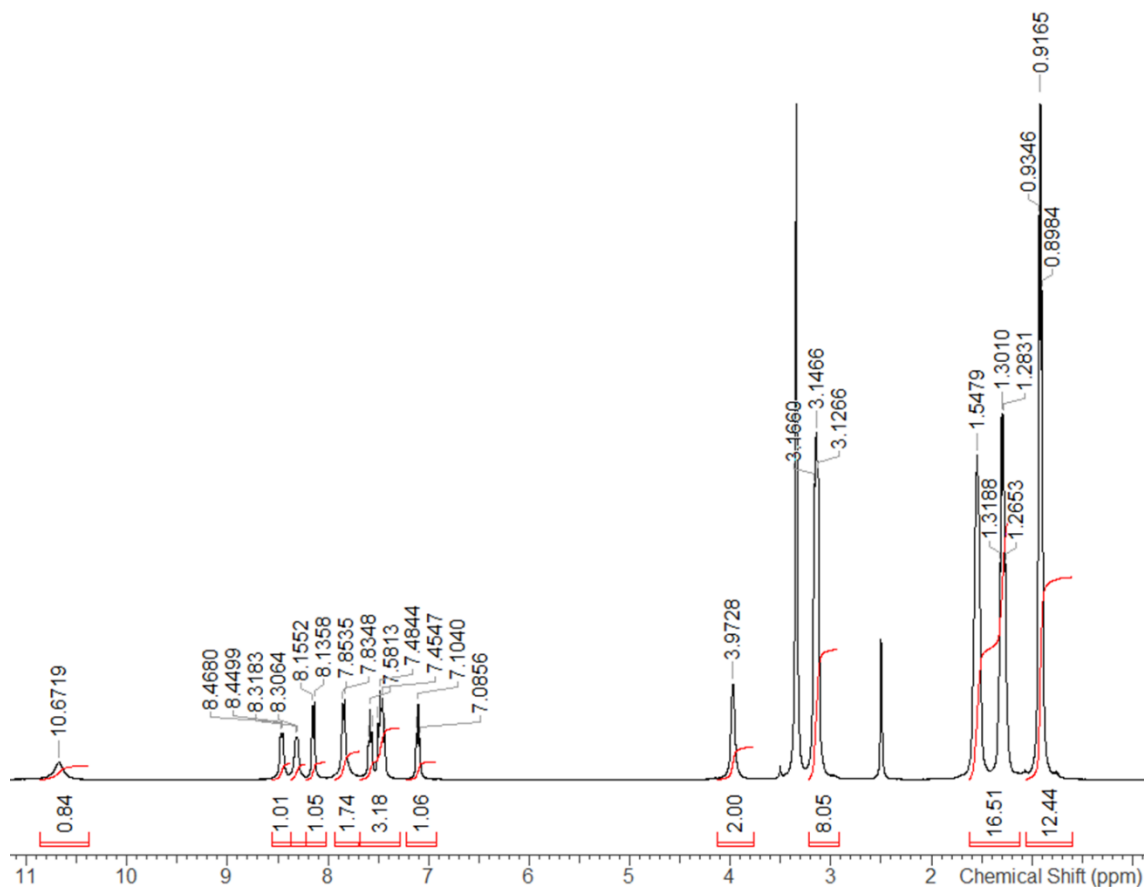


Figure S2 - ^1H NMR spectrum of compound **2** in $\text{DMSO-}d_6$ conducted at 298.15 K.

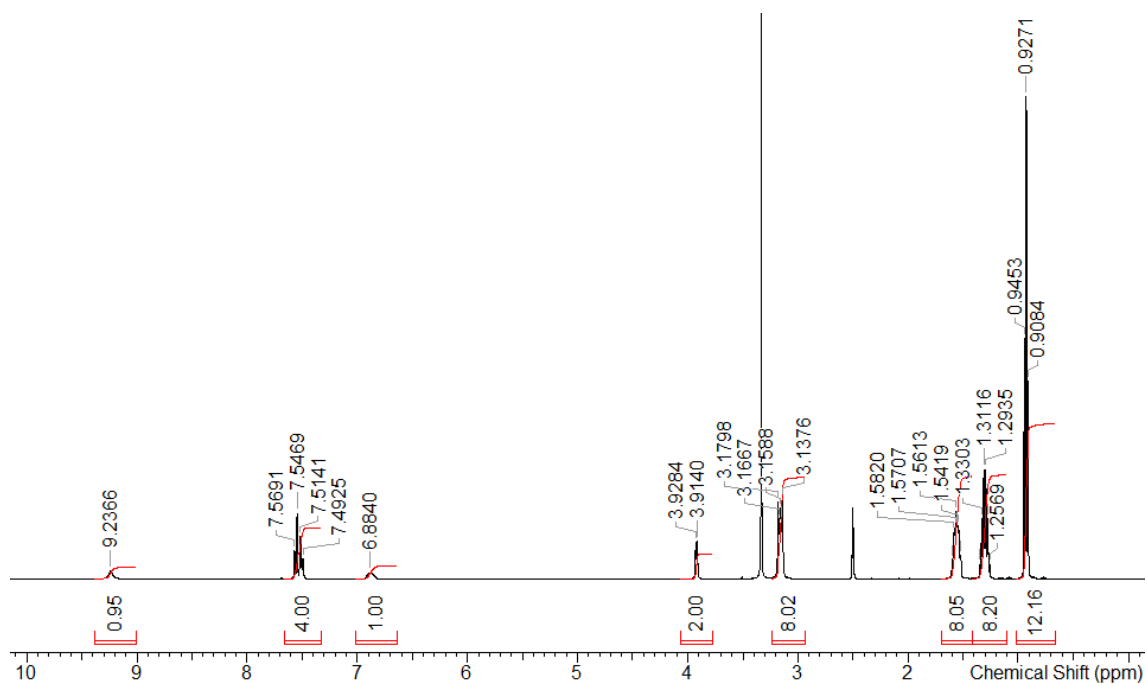


Figure S3 - ^1H NMR spectrum of compound **3** in $\text{DMSO-}d_6$ conducted at 298.15 K.

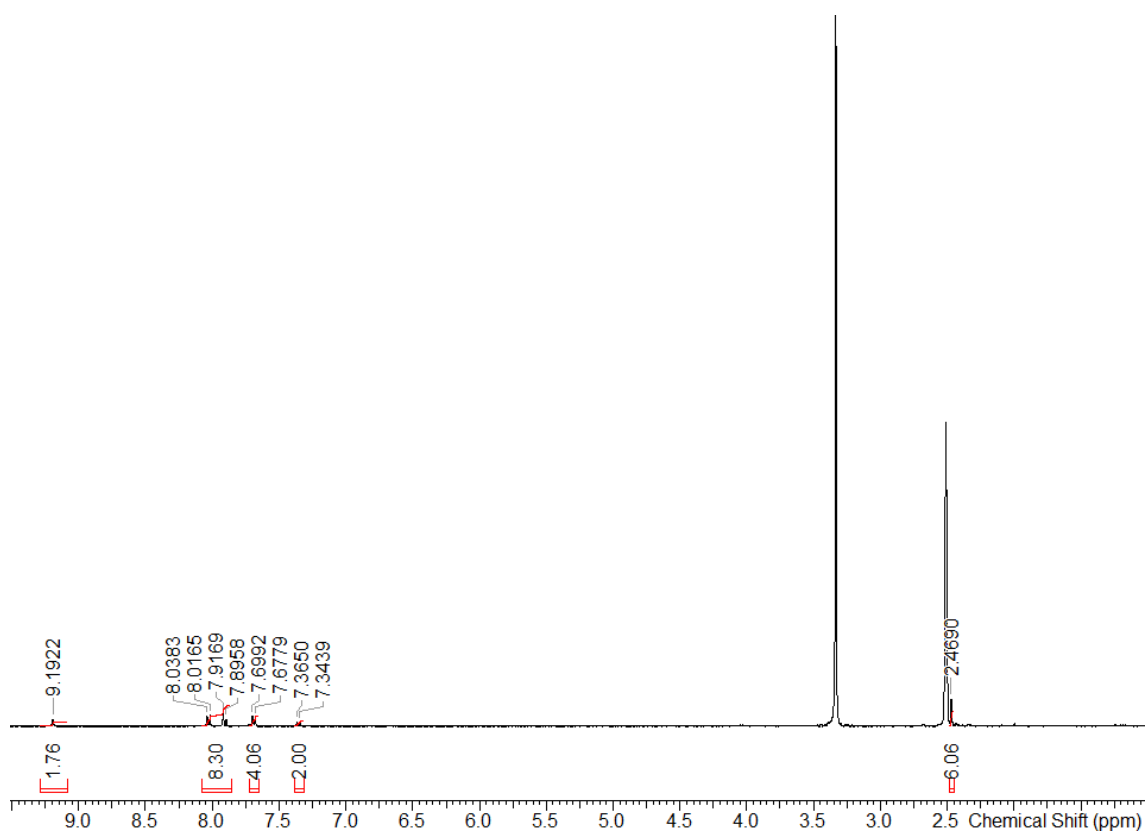


Figure S4 - ^1H NMR spectrum of compound **4** in $\text{DMSO-}d_6$ conducted at 298.15 K.

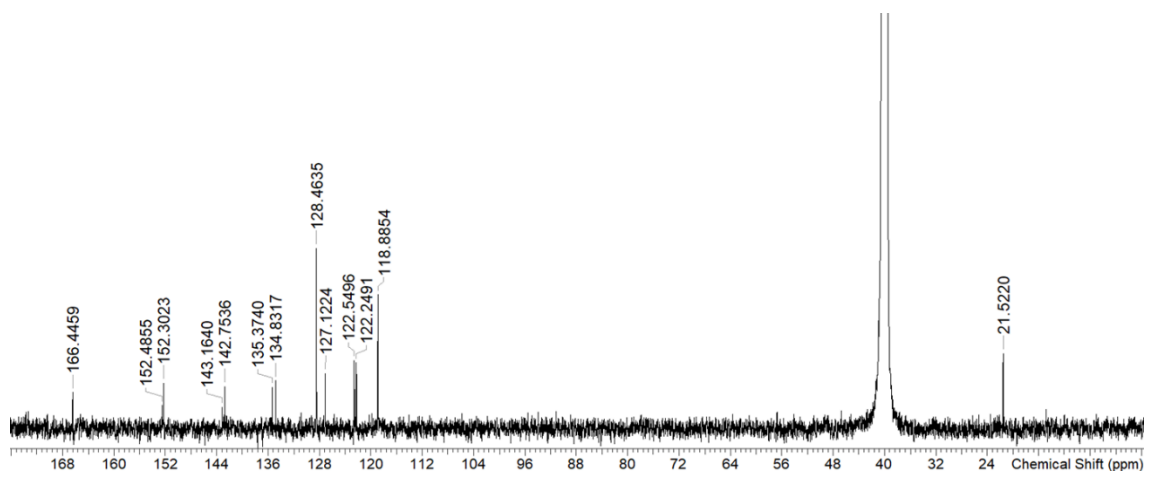


Figure S5 - $^{13}\text{C}\{^1\text{H}\}$ NMR spectrum of compound **4** in $\text{DMSO-}d_6$ conducted at 298.15 K.

Inversion Test

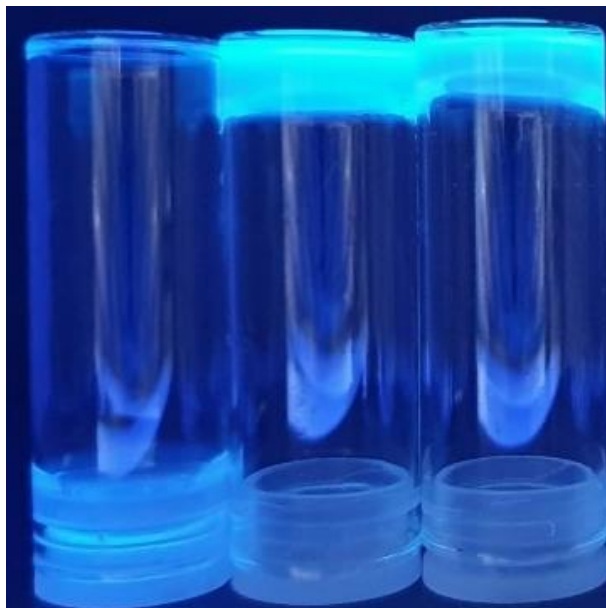


Figure S6 – Compound **1** (5 mg) in 1 mL of H₂O (left) hydrogel of compound **1** (5 mg) in 1 mL NaCl (0.505 M) (centre), hydrogel of compound **1** (5 mg) in 1 mL of NaH₂PO₄ (0.505 M) (right).

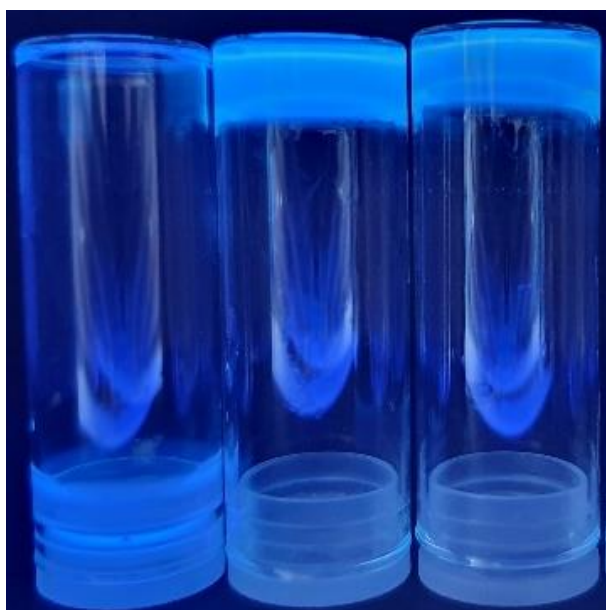


Figure S7 – Compound **1** (1.5 mg) in 1 mL of H₂O (left), hydrogel of compound **1** at MGC (1.5 mg) in 1 mL NaCl (0.505 M) (centre), hydrogel of compound **1** at MGC (1.5 mg) in 1 mL of NaH₂PO₄ (0.505 M) (right).

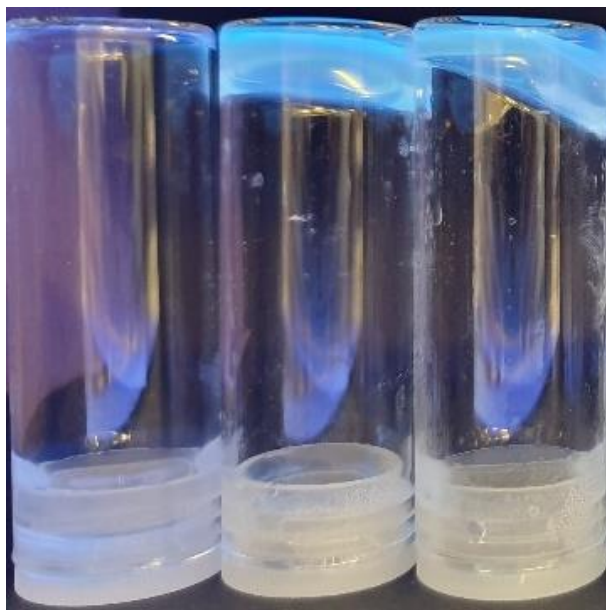


Figure S8 – Compound **1** (1.5 mg) in 1 mL of H₂O (left), partial hydrogel of compound **1** (1 mg) in 1 mL NaCl (0.505 M) (centre), partial hydrogel of compound **1** (1 mg) in 1 mL of NaH₂PO₄ (0.505 M) (right).

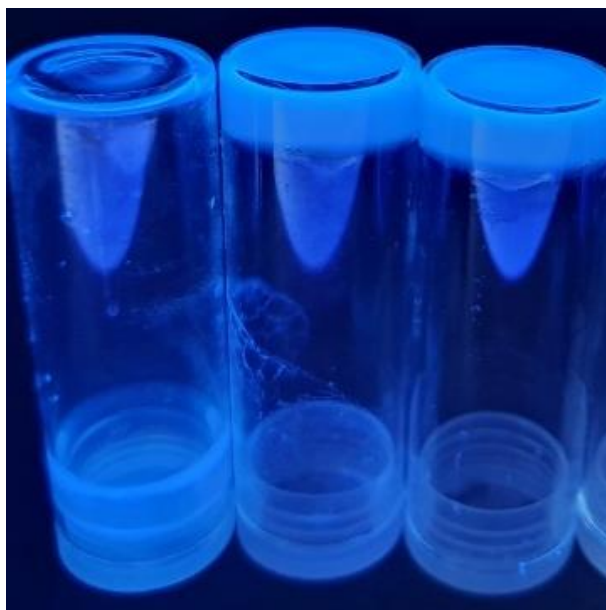


Figure S9 - Compound **1** (5 mg) in 1 mL of H₂O (left) hydrogel of compound **1** (5 mg) in 1 mL NaCl (0.505 M) (centre), hydrogel of compound **1** (5 mg) in 1 mL of Na₂CO₃ (0.505 M) (right).

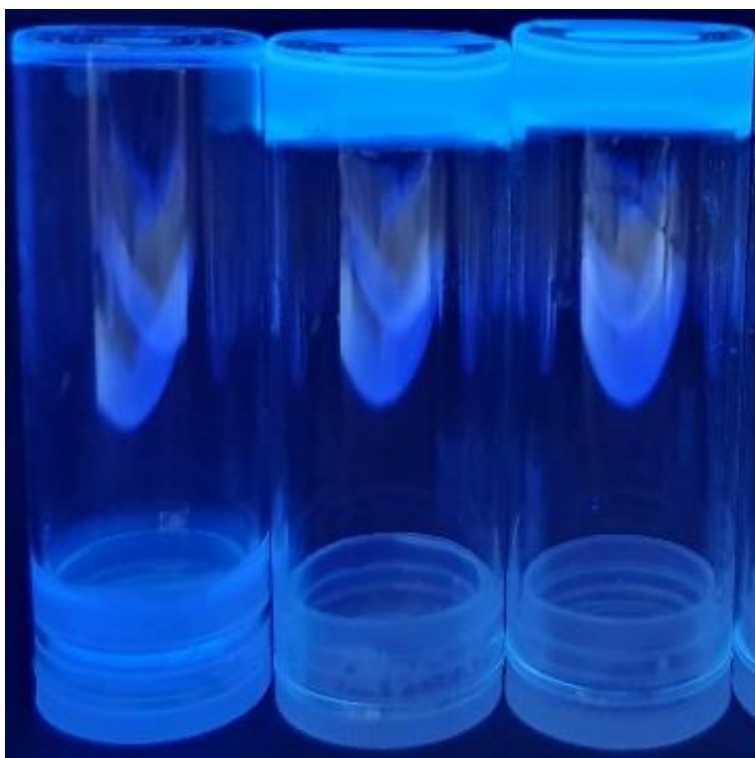


Figure S10 - Compound **1** (3 mg) in 1 mL of H₂O (left), hydrogel of compound **1** (3 mg) in 1 mL NaCl (0.505 M) (centre), hydrogel of compound **1** at MGC (3 mg) in 1 mL of Na₂CO₃ (0.505 M) (right).

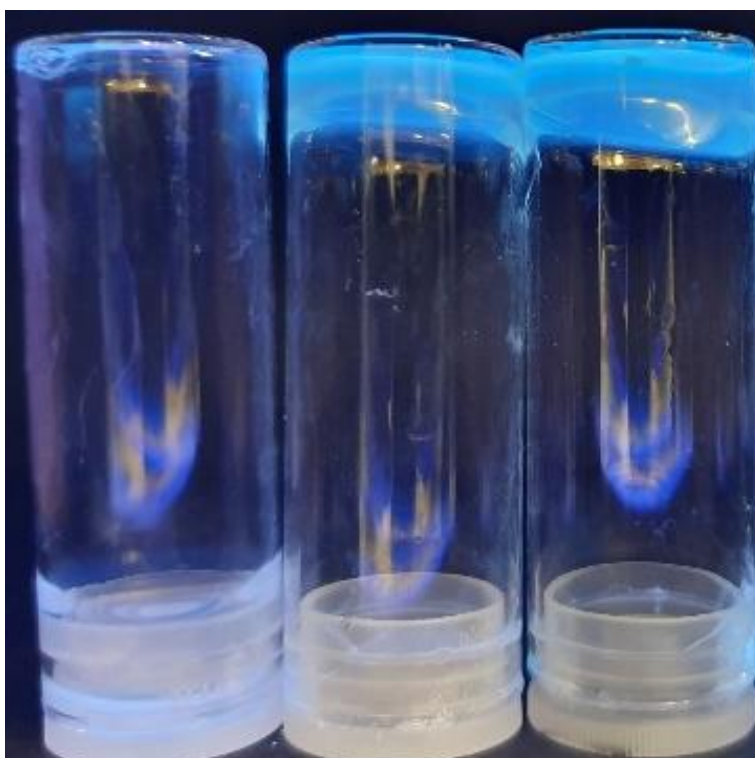


Figure S11 - Compound **1** (2.5 mg) in 1 mL of H₂O (left), hydrogel of compound **1** (2.5 mg) in 1 mL NaCl (0.505 M) (centre), partial hydrogel of compound **1** (2.5 mg) in 1 mL of Na₂CO₃ (0.505 M) (right).

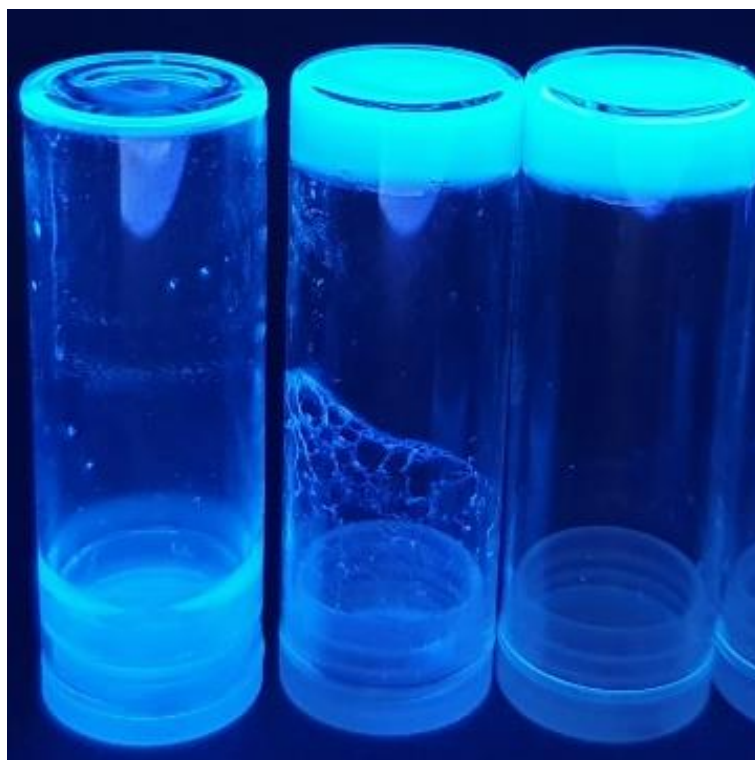


Figure S12 - Compound **1** (5 mg) in 1 mL of H₂O (left) hydrogel of compound **1** (5 mg) in 1 mL NaCl (0.505 M) (centre), hydrogel of compound **1** (5 mg) in 1 mL of NaNO₃ (0.505 M) (right).

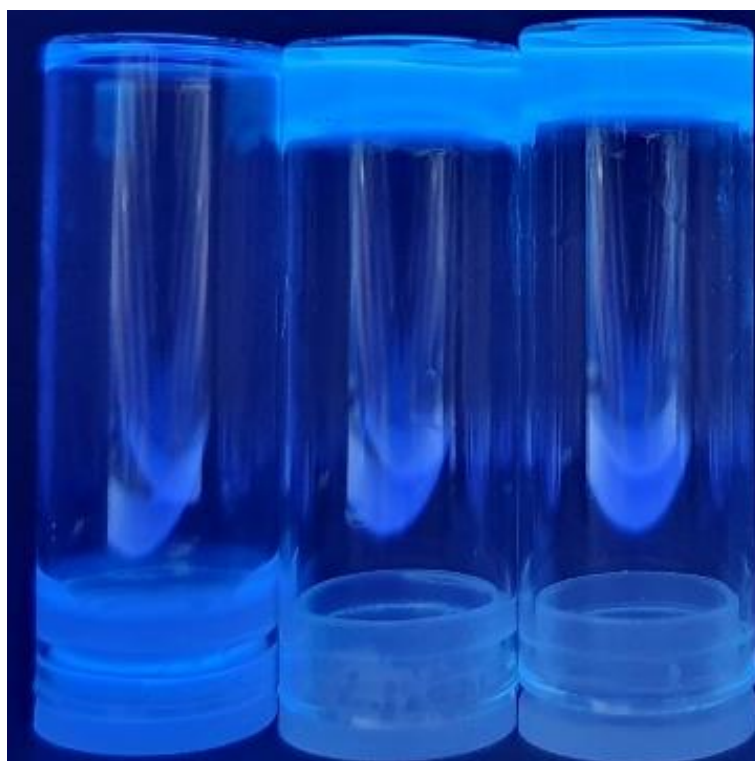


Figure S13 - Compound **1** (1.5 mg) in 1 mL of H₂O (left), hydrogel of compound **1** at MGC (1.5 mg) in 1 mL NaCl (0.505 M) (centre), hydrogel of compound **1** at MGC (1.5 mg) in 1 mL of NaNO₃ (0.505 M) (right).

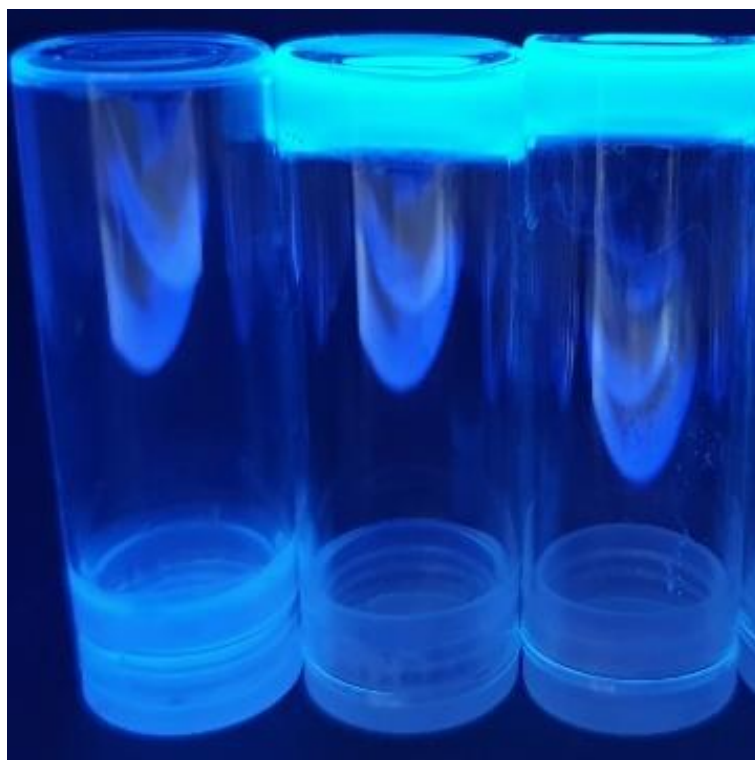


Figure S14 - Compound **1** (1 mg) in 1 mL of H₂O (left), partial hydrogel of compound **1** (1 mg) in 1 mL NaCl (0.505 M) (centre), partial hydrogel of compound **1** (1 mg) in 1 mL of NaNO₃ (0.505 M) (right).

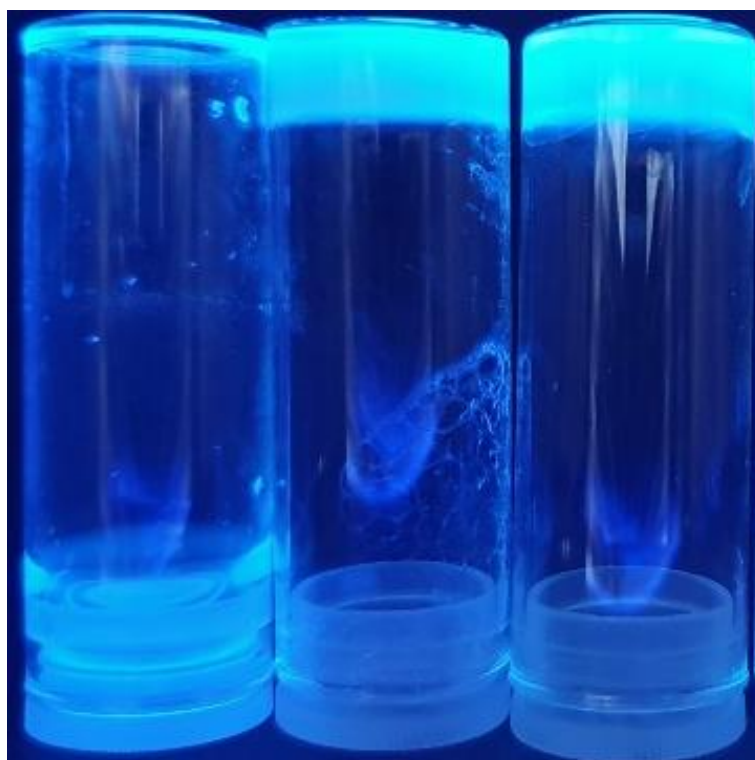


Figure S15 - Compound **1** (5 mg) in 1 mL of H₂O (left) hydrogel of compound **1** (5 mg) in 1 mL NaCl (0.505 M) (centre), hydrogel of compound **1** (5 mg) in 1 mL of NaC₇H₅O₂ (0.505 M) (right).

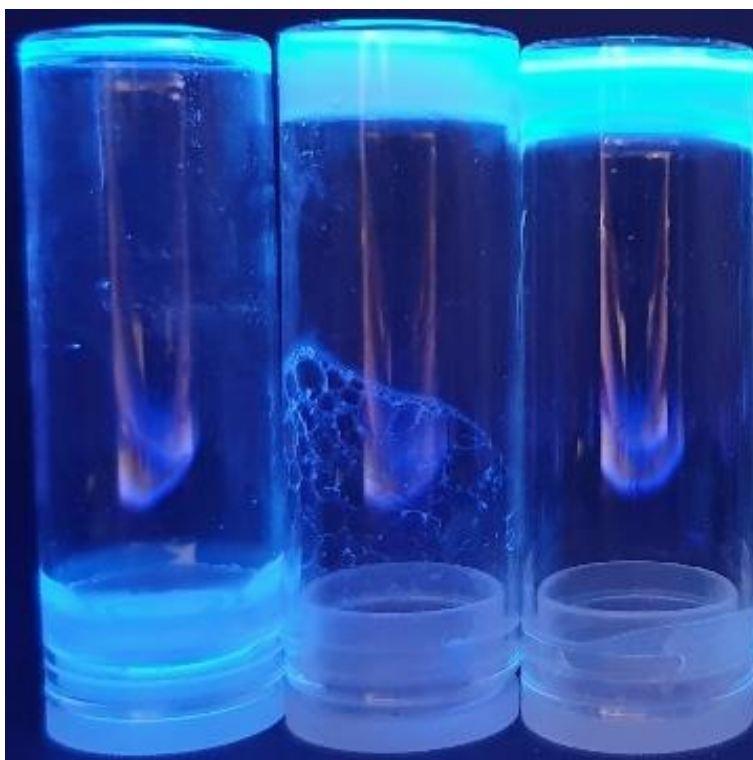


Figure S16 - Compound **1** (1.5 mg) in 1 mL of H₂O (left), hydrogel of compound **1** at MGC (1.5 mg) in 1 mL NaCl (0.505 M) (centre), hydrogel of compound **1** at MGC (1.5 mg) in 1 mL of NaC₇H₅O₂ (0.505 M) (right).

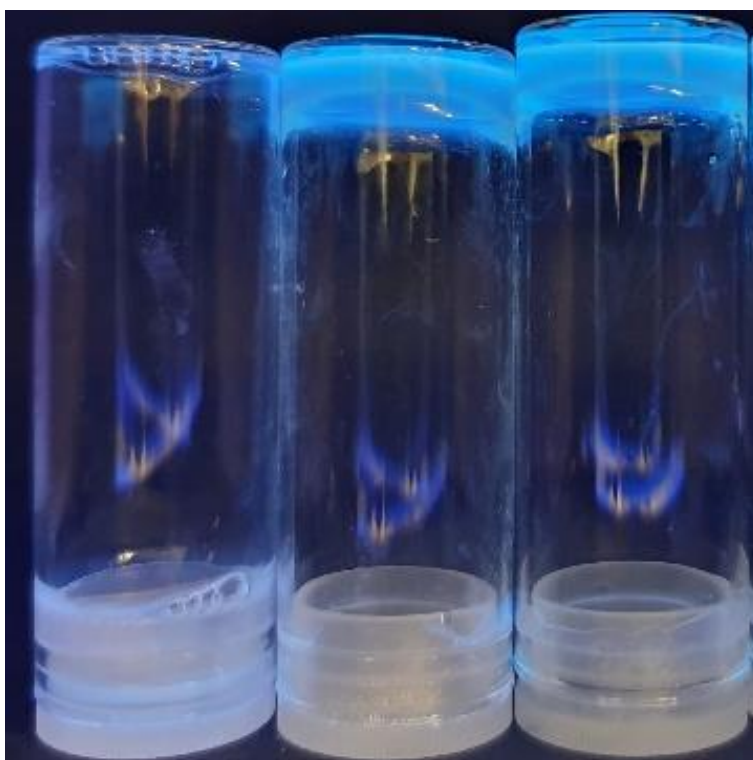


Figure S17 - Compound **1** (1 mg) in 1 mL of H₂O (left), partial hydrogel of compound **1** (1 mg) in 1 mL NaCl (0.505 M) (centre), partial hydrogel of compound **1** (1 mg) in 1 mL of NaC₇H₅O₂ (0.505 M) (right).

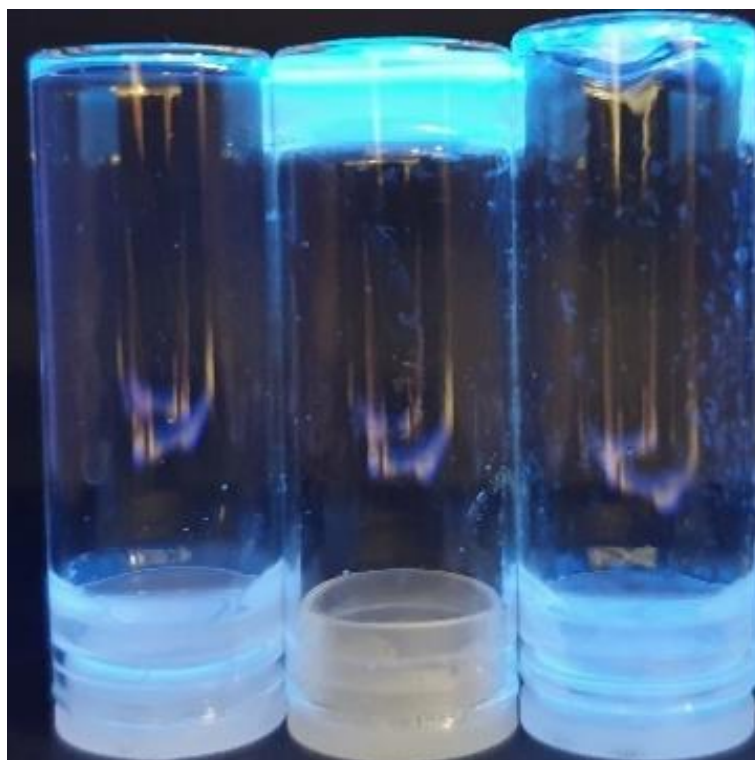


Figure S18 - Compound **1** (5 mg) in 1 mL of H₂O (left) hydrogel of compound **1** (5 mg) in 1 mL NaCl (0.505 M) (centre), partial hydrogel of compound **1** (5 mg) in 1 mL of Na₂HPO₄ (0.505 M) (right).

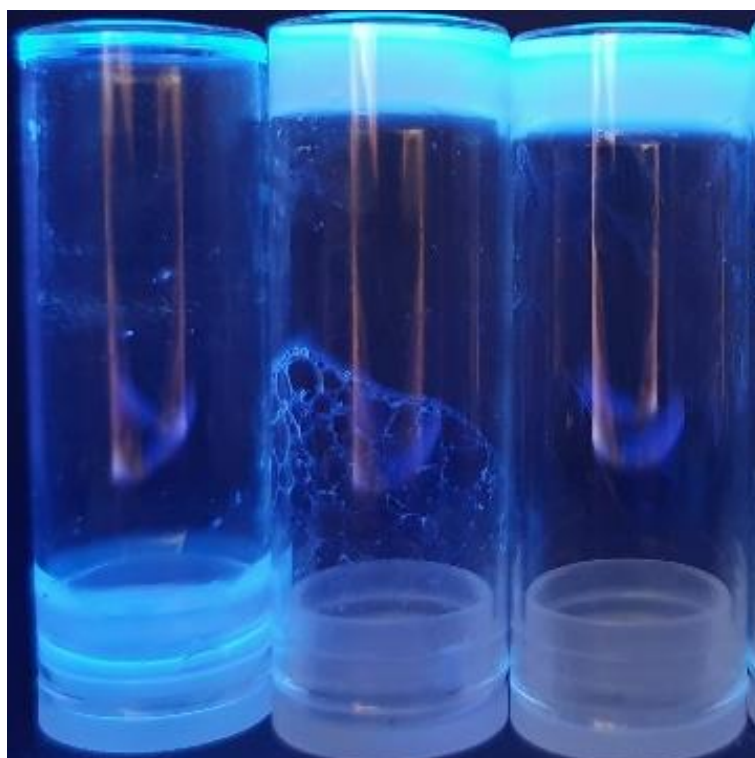


Figure S19 - Compound **1** (5 mg) in 1 mL of H₂O (left) hydrogel of compound **1** (5 mg) in 1 mL NaCl (0.505 M) (centre), hydrogel of compound **1** (5 mg) in 1 mL of Na₂SO₄ (0.505 M) (right).

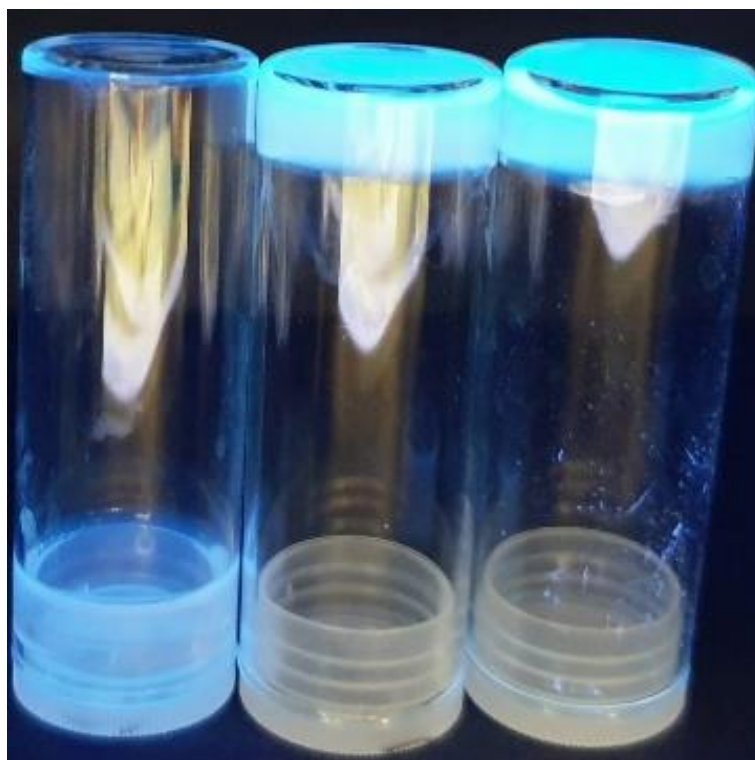


Figure S20 - Compound **1** (3.5 mg) in 1 mL of H₂O (left), hydrogel of compound **1** (3.5 mg) in 1 mL NaCl (0.505 M) (centre), hydrogel of compound **1** at MGC (3.5 mg) in 1 mL of Na₂SO₄ (0.505 M) (right).

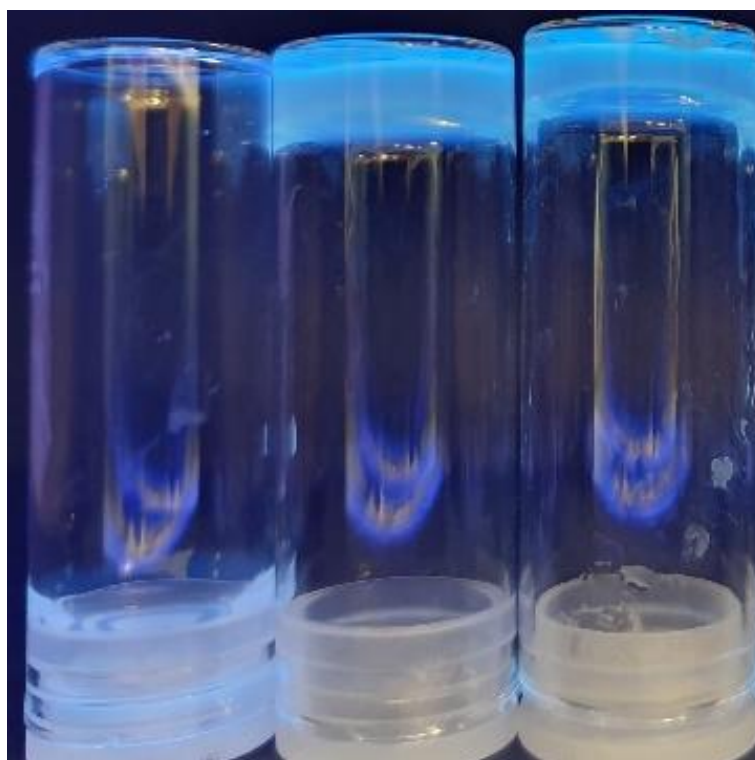


Figure S21 - Compound **1** (3 mg) in 1 mL of H₂O (left), hydrogel of compound **1** (3 mg) in 1 mL NaCl (0.505 M) (centre), partial hydrogel of compound **1** (3 mg) in 1 mL of Na₂SO₄ (0.505 M) (right).

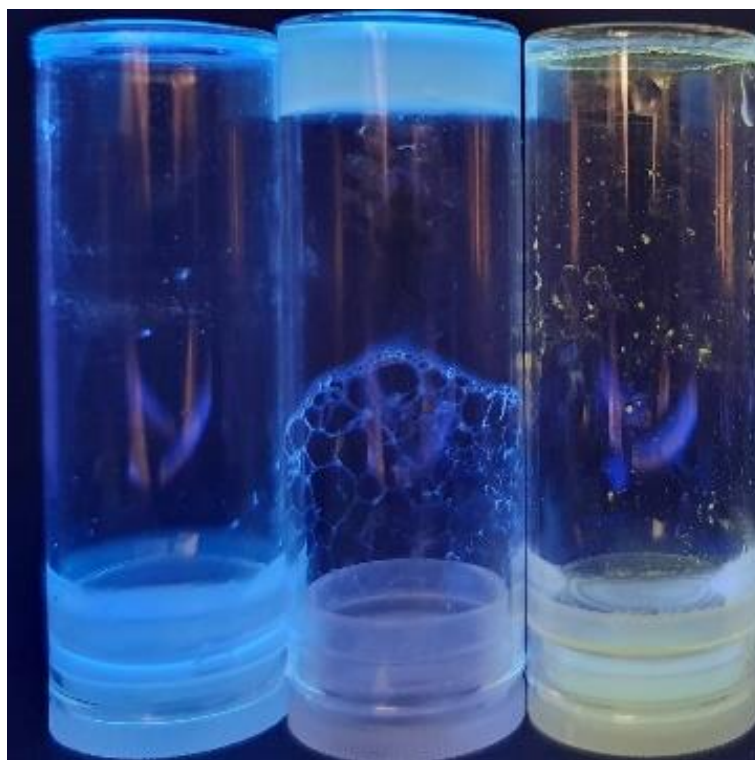


Figure S22 - Compound **1** (5 mg) in 1 mL of H₂O (left) hydrogel of compound **1** (5 mg) in 1 mL NaCl (0.505 M) (centre), compound **1** (5 mg) in 1 mL of NaHSO₄ (0.505 M) (right).

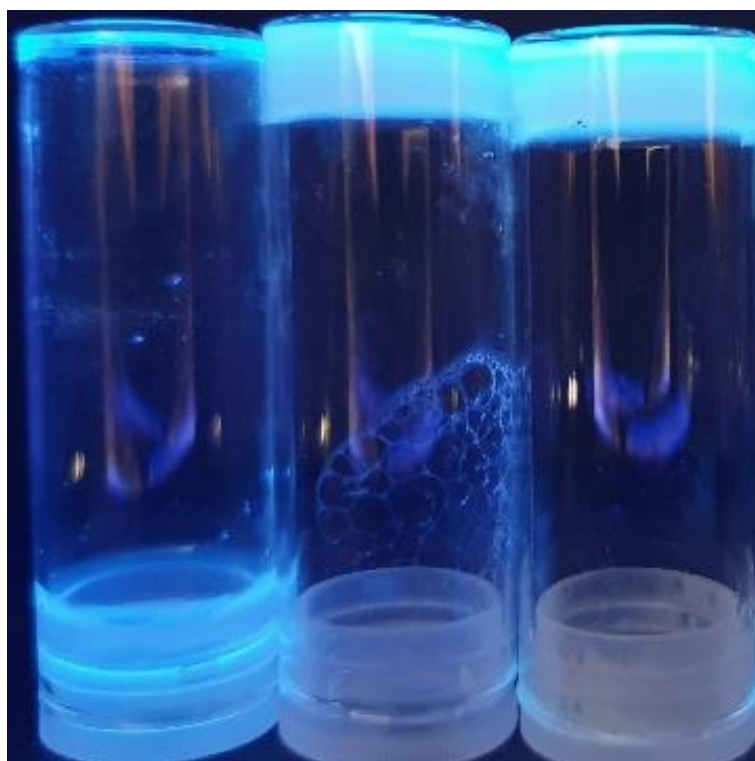


Figure S23 - Compound **1** (5 mg) in 1 mL of H₂O (left) hydrogel of compound **1** (5 mg) in 1 mL NaCl (0.505 M) (centre), hydrogel of compound **1** (5 mg) in 1 mL of NaHCO₃ (0.505 M) (right).

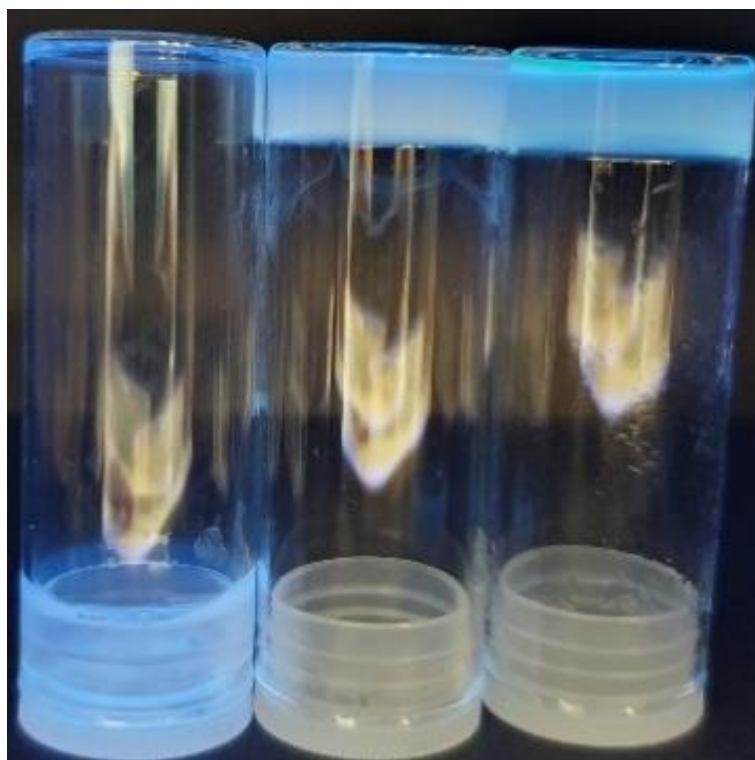


Figure S24 - Compound **1** (4 mg) in 1 mL of H₂O (left), hydrogel of compound **1** (4 mg) in 1 mL NaCl (0.505 M) (centre), hydrogel of compound **1** at MGC (4 mg) in 1 mL of NaHCO₃ (0.505 M) (right).

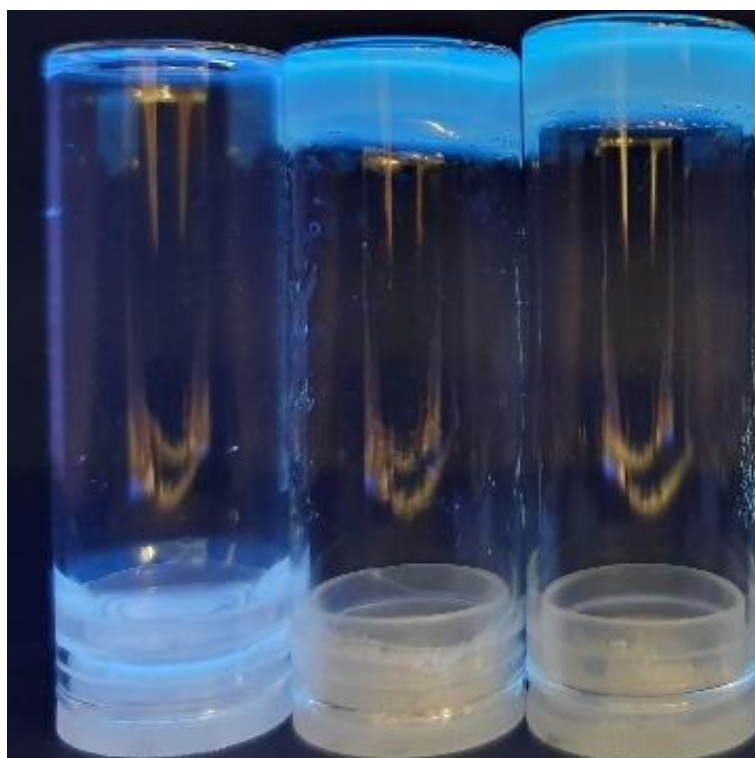


Figure S25 - Compound **1** (3.5 mg) in 1 mL of H₂O (left), hydrogel of compound **1** (3.5 mg) in 1 mL NaCl (0.505 M) (centre), partial hydrogel of compound **1** (3.5 mg) in 1 mL of NaHCO₃ (0.505 M) (right).

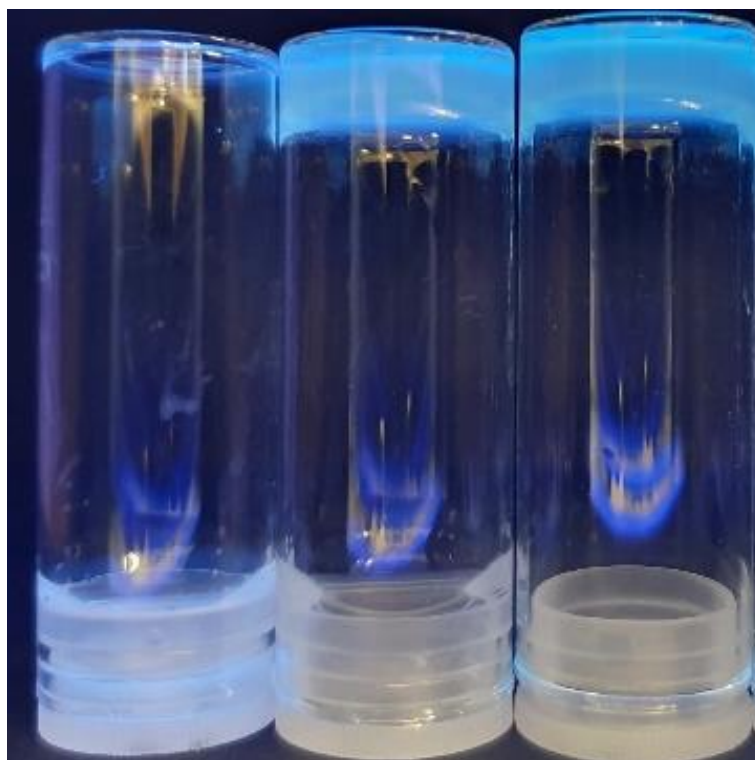


Figure S26 - Compound **1** (5 mg) in 1 mL of H₂O (left) hydrogel of compound **1** (5 mg) in 1 mL NaCl (0.505 M) (centre), hydrogel of compound **1** (5 mg) in 1 mL of NaC₂H₃O₂ (0.505 M) (right).

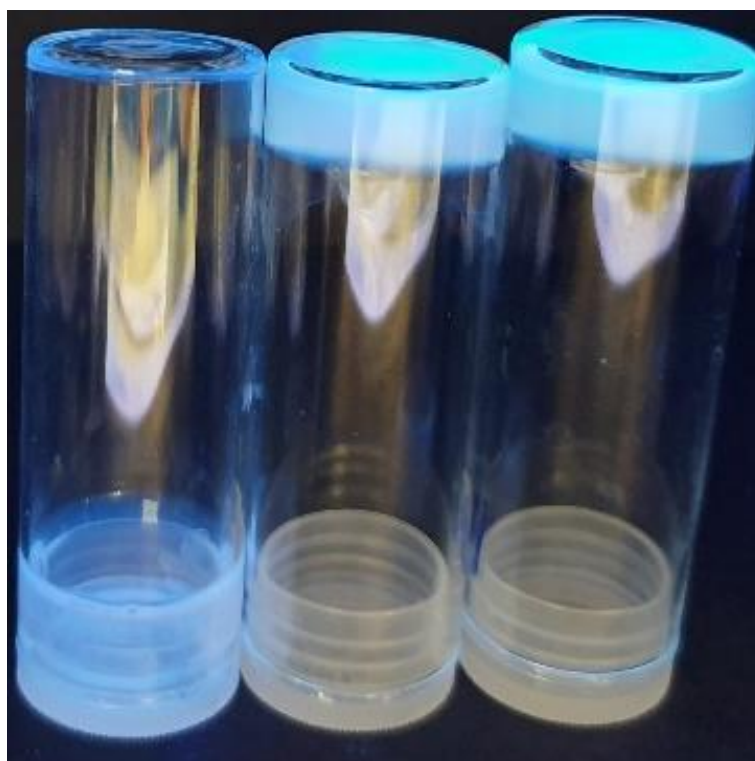


Figure S27 - Compound **1** (3.5 mg) in 1 mL of H₂O (left), hydrogel of compound **1** (3.5 mg) in 1 mL NaCl (0.505 M) (centre), hydrogel of compound **1** at MGC (3.5 mg) in 1 mL of NaC₂H₃O₂ (0.505 M) (right).

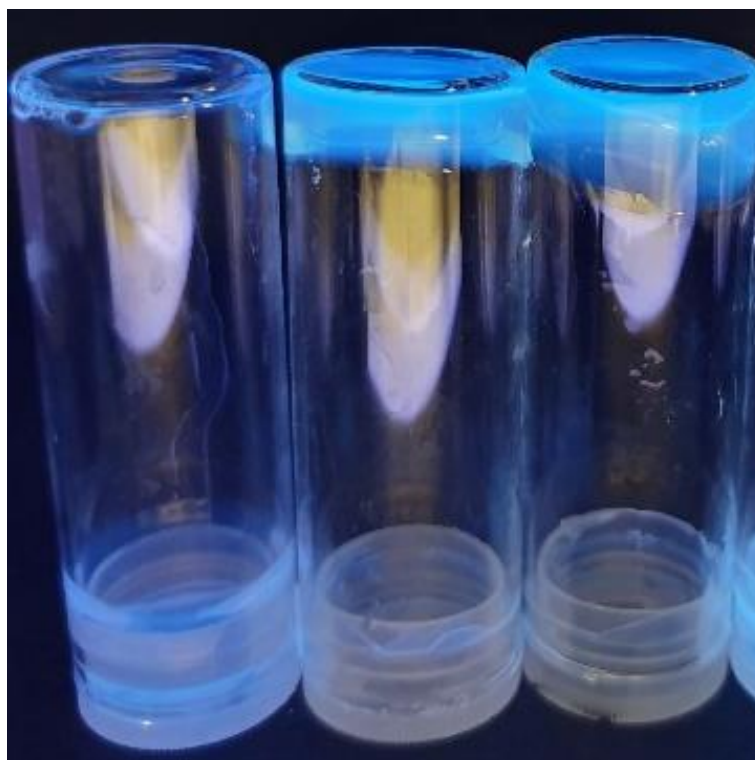


Figure S28 - Compound **1** (3 mg) in 1 mL of H₂O (left), hydrogel of compound **1** (3 mg) in 1 mL NaCl (0.505 M) (centre), partial hydrogel of compound **1** (3 mg) in 1 mL of NaC₂H₃O₂ (0.505 M) (right).

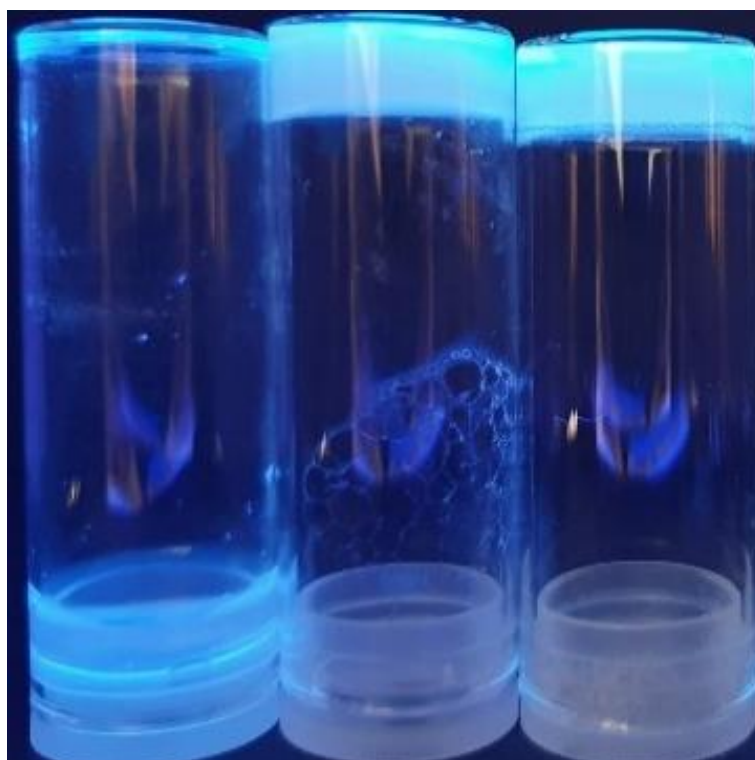


Figure S29 - Compound **1** (5 mg) in 1 mL of H₂O (left) hydrogel of compound **1** (5 mg) in 1 mL NaCl (0.505 M) (centre), hydrogel of compound **1** (5 mg) in 1 mL of NaF (0.505 M) (right).

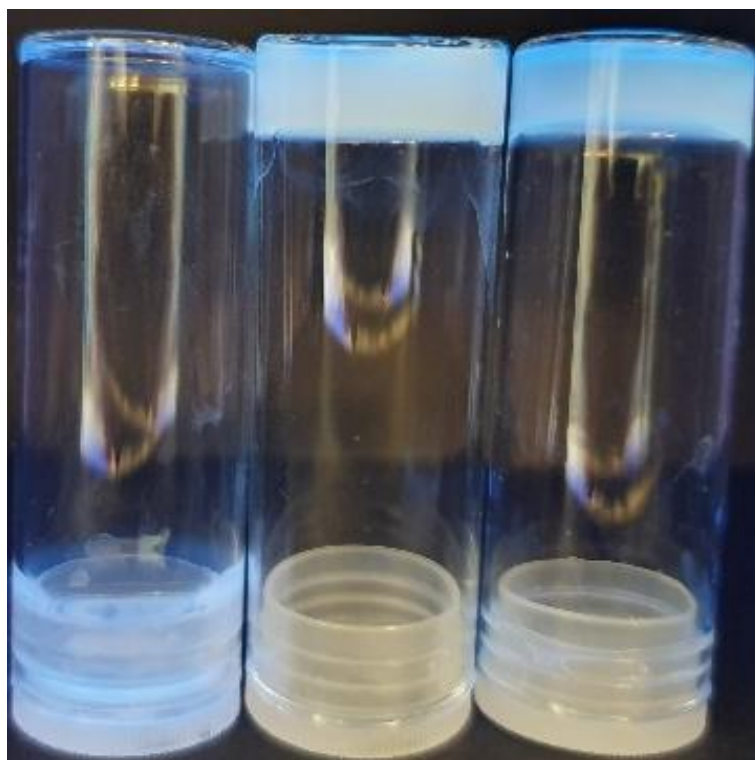


Figure S30 - Compound **1** (2 mg) in 1 mL of H₂O (left), hydrogel of compound **1** (2 mg) in 1 mL NaCl (0.505 M) (centre), hydrogel of compound **1** at MGC (2 mg) in 1 mL of NaF (0.505 M) (right).

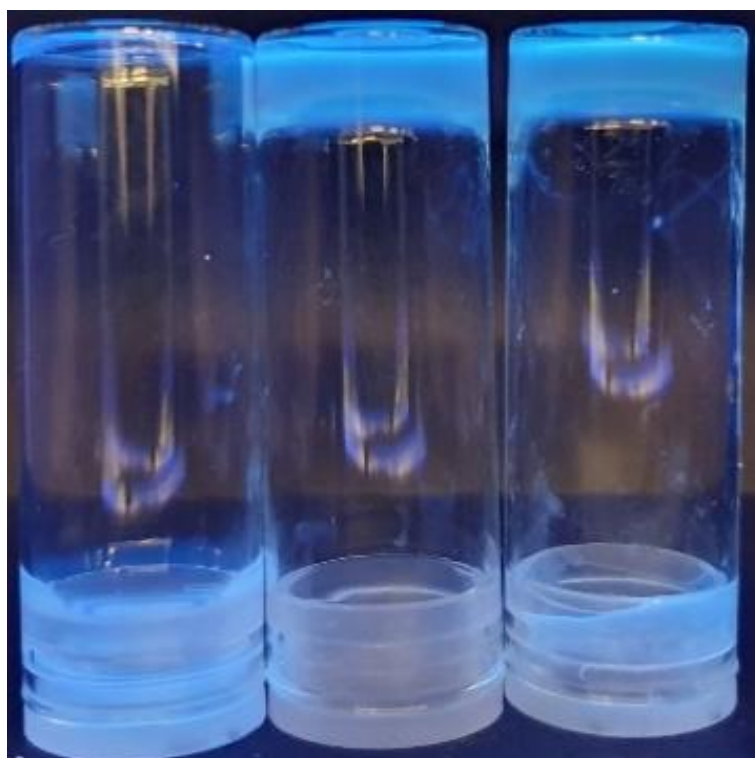


Figure S31 - Compound **1** (1.5 mg) in 1 mL of H₂O (left), hydrogel of compound **1** (1.5 mg) in 1 mL NaCl (0.505 M) (centre), partial hydrogel of compound **1** (1.5 mg) in 1 mL of NaF (0.505 M) (right).

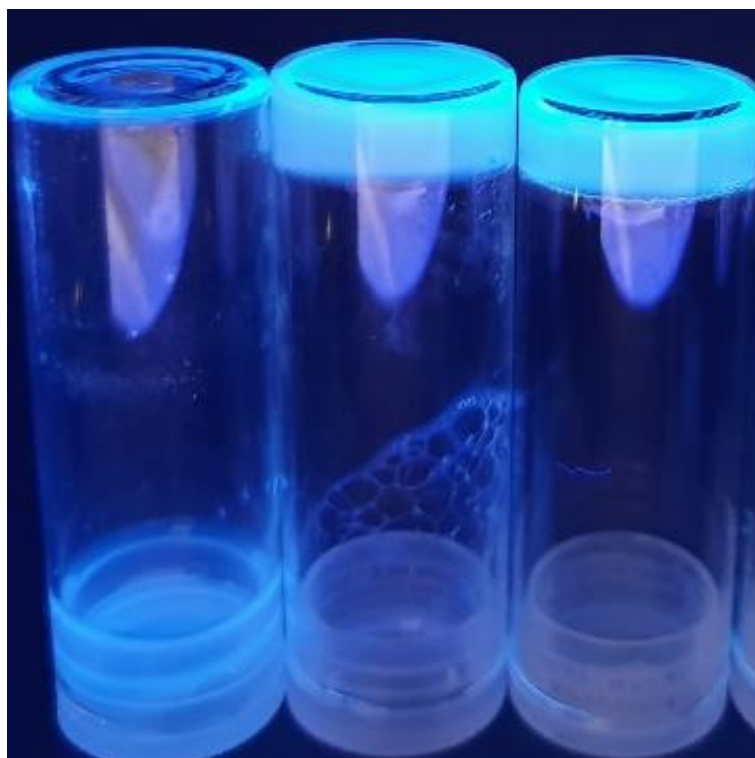


Figure S32 - Compound **1** (5 mg) in 1 mL of H₂O (left) hydrogel of compound **1** (5 mg) in 1 mL NaCl (0.505 M) (centre), hydrogel of compound **1** (5 mg) in 1 mL of KCl (0.505 M) (right).

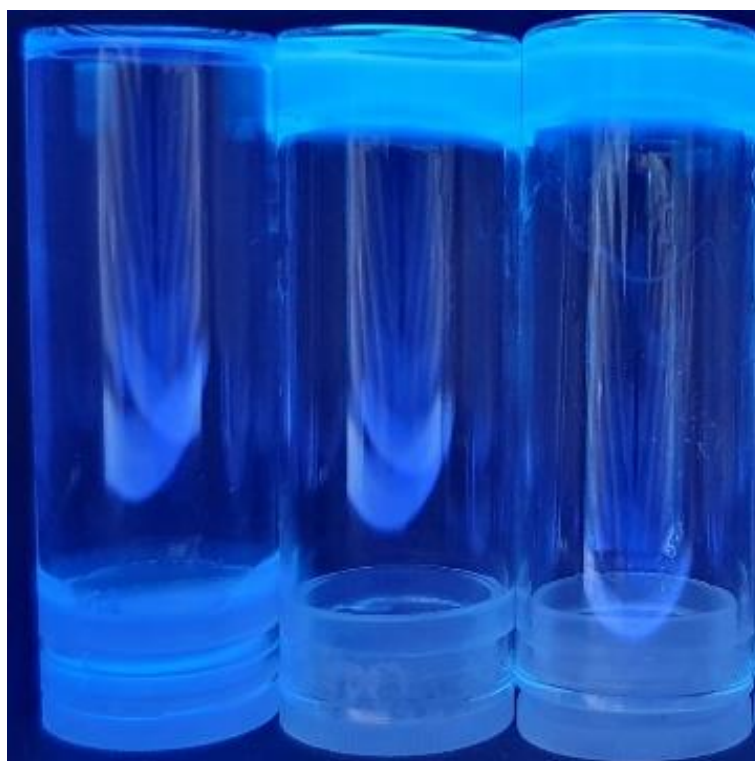


Figure S33 - Compound **1** (2.5 mg) in 1 mL of H₂O (left), hydrogel of compound **1** (2.5 mg) in 1 mL NaCl (0.505 M) (centre), hydrogel of compound **1** at MGC (2.5 mg) in 1 mL of KCl (0.505 M) (right).

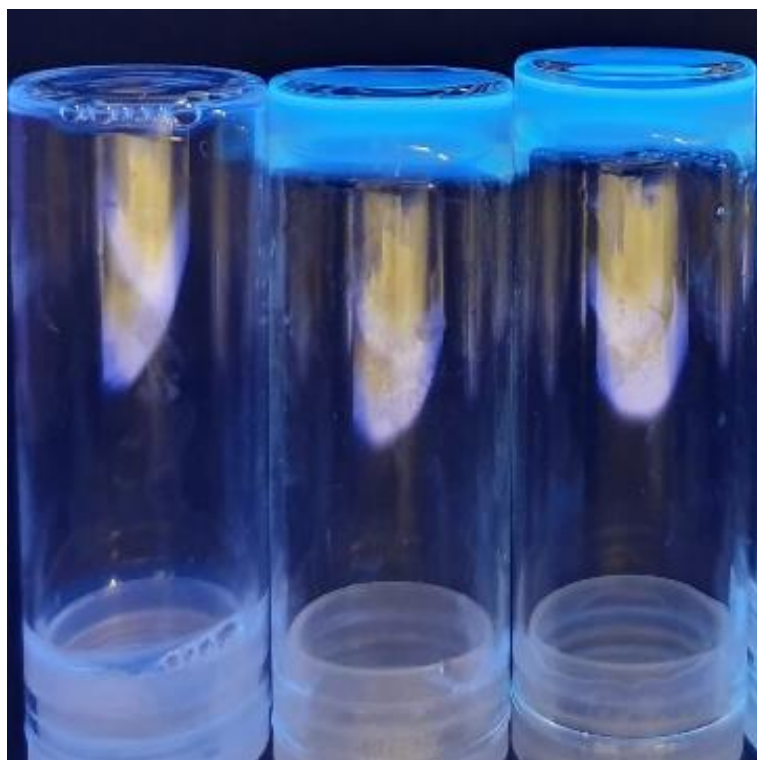


Figure S34 - Compound **1** (2 mg) in 1 mL of H₂O (left), hydrogel of compound **1** (2 mg) in 1 mL NaCl (0.505 M) (centre), partial hydrogel of compound **1** (2 mg) in 1 mL of KCl (0.505 M) (right).

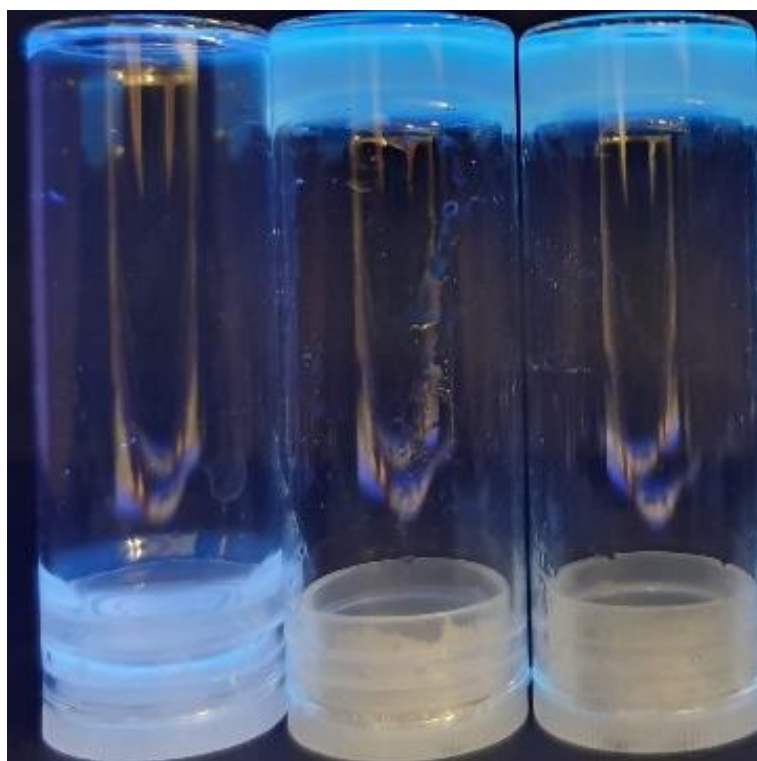


Figure S35 - Compound **1** (5 mg) in 1 mL of H₂O (left) hydrogel of compound **1** (5 mg) in 1 mL NaCl (0.505 M) (centre), hydrogel of compound **1** (5 mg) in 1 mL of RbCl (0.505 M) (right).

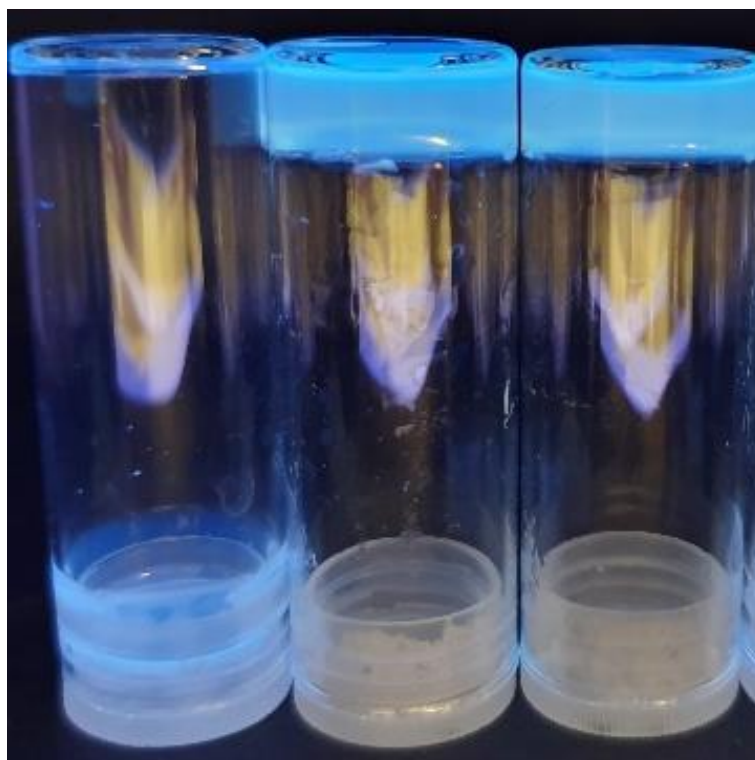


Figure S36 - Compound **1** (3.5 mg) in 1 mL of H₂O (left), hydrogel of compound **1** (3.5 mg) in 1 mL NaCl (0.505 M) (centre), hydrogel of compound **1** at MGC (3.5 mg) in 1 mL of RbCl (0.505 M) (right).

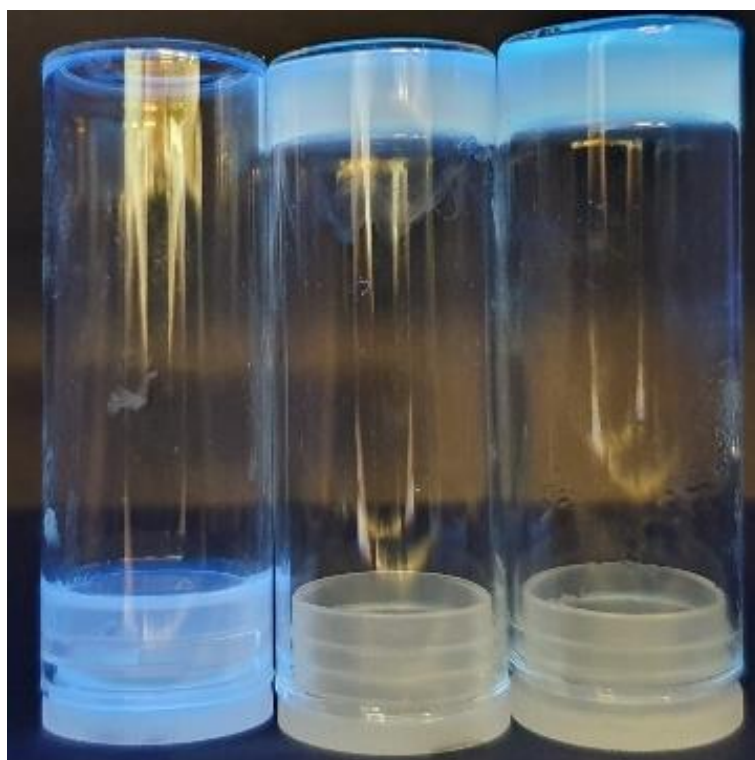


Figure S37 - Compound **1** (3 mg) in 1 mL of H₂O (left), hydrogel of compound **1** (3 mg) in 1 mL NaCl (0.505 M) (centre), partial hydrogel of compound **1** (3 mg) in 1 mL of RbCl (0.505 M) (right).

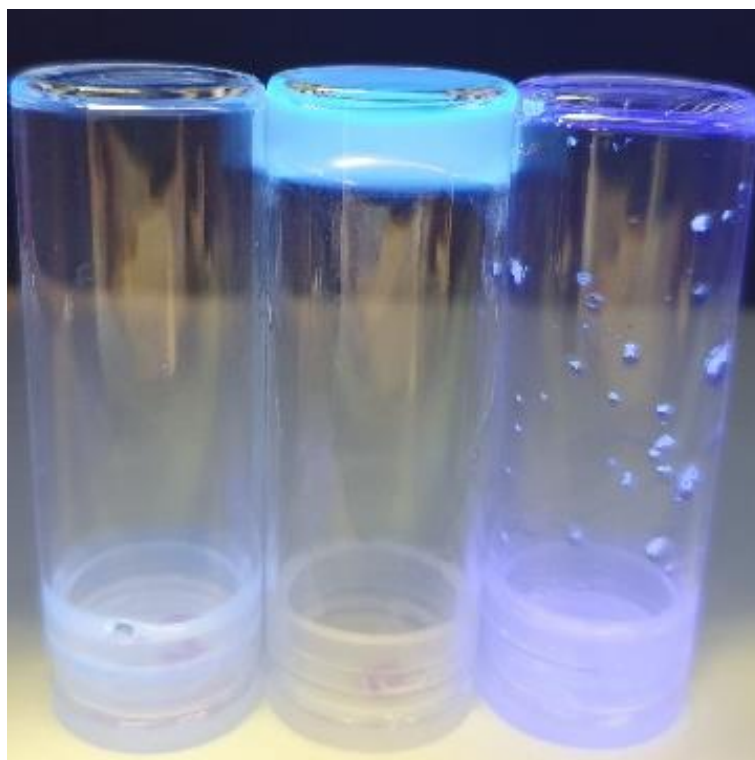


Figure S38 - Compound **1** (5 mg) in 1 mL of H₂O (left) hydrogel of compound **1** (5 mg) in 1 mL NaCl (0.505 M) (centre), compound **1** (5 mg) in 1 mL of TBACl (0.505 M) (right).



Figure S39 - Compound **1** (5 mg) in 1 mL of NaCl on a 1:1 molar ratio with ampicillin

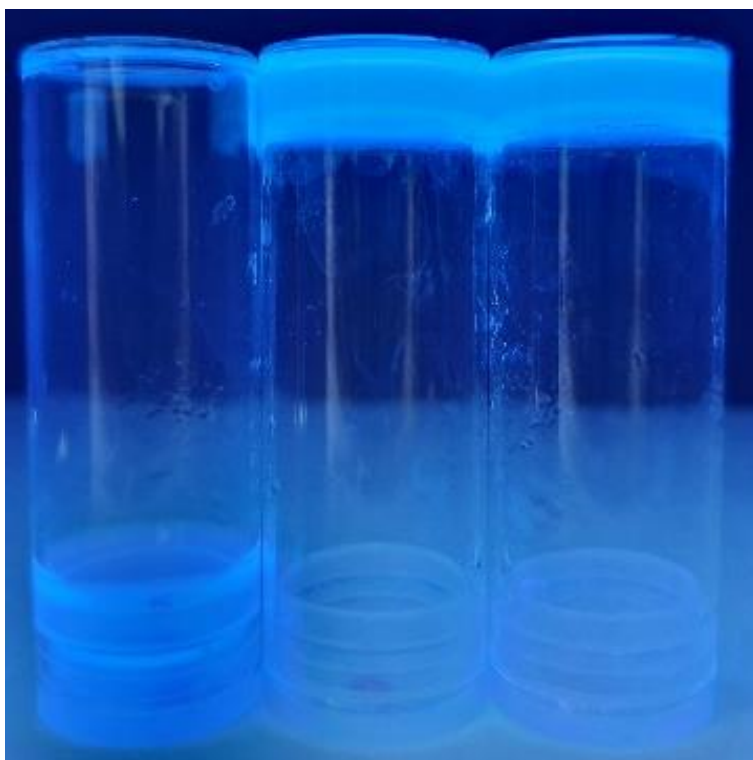


Figure S40 - Compound **1** (1.5 mg) in 1 mL of H₂O (left), hydrogel of compound **1** at MGC (1.5 mg) in 1 mL NaCl (0.505 M) (centre), hydrogel of compound **1** (1.5 mg) on a 1:1 molar ratio with ampicillin in 1 mL of NaCl (0.505 M) (right).

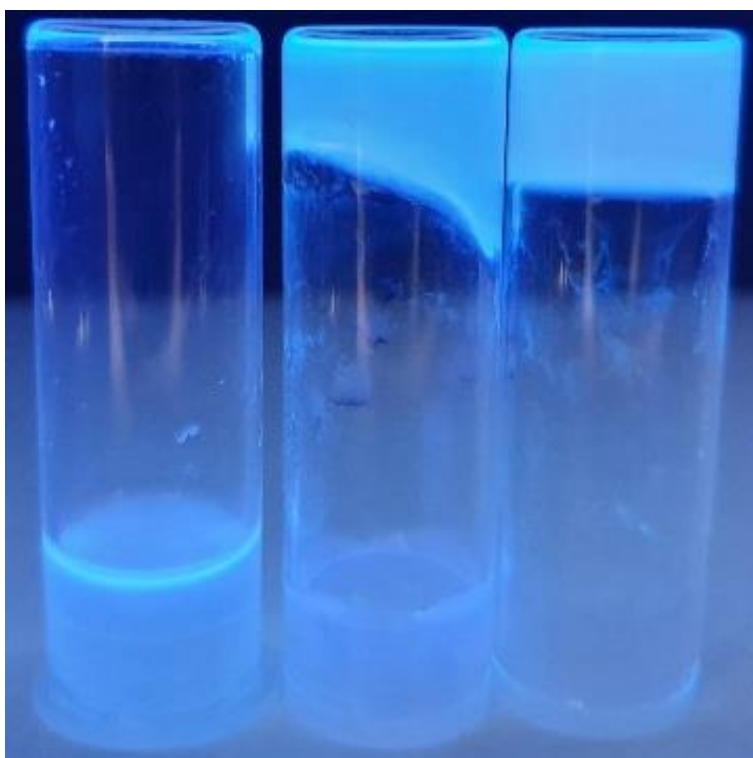


Figure S41 - Compound **1** (1 mg) in 1 mL of H₂O (left), partial hydrogel of compound **1** (1 mg) in 1 mL NaCl (0.505 M) (centre), hydrogel of compound **1** (1 mg) on a 1:1 molar ratio with ampicillin in 1 mL of NaCl (0.505 M) (right).

Dynamic light scattering data

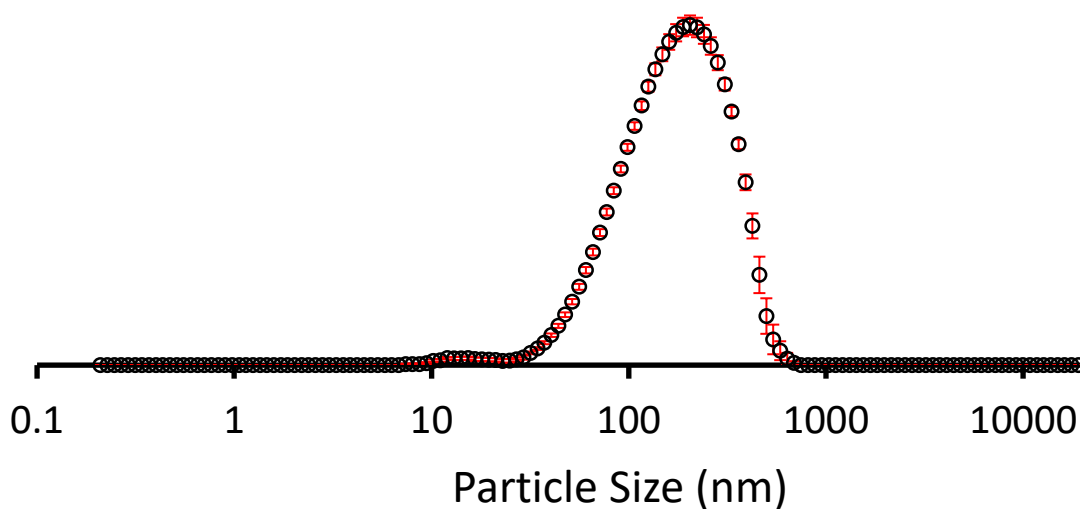


Figure S42 - The average intensity particle size distribution calculated using 9 DLS runs for compound **1** (5 mg/mL) in an EtOH:H₂O (1:19) solution at 298 K.

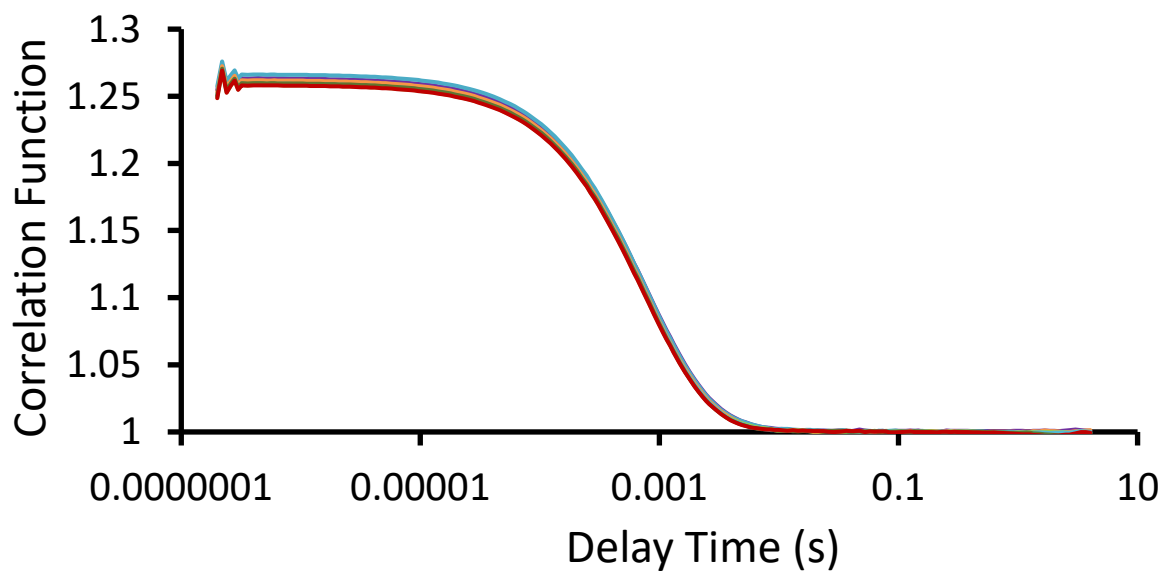


Figure S43 - Correlation function data for 9 DLS runs of compound **1** (5 mg/mL) in an EtOH:H₂O (1:19) solution at 298 K.

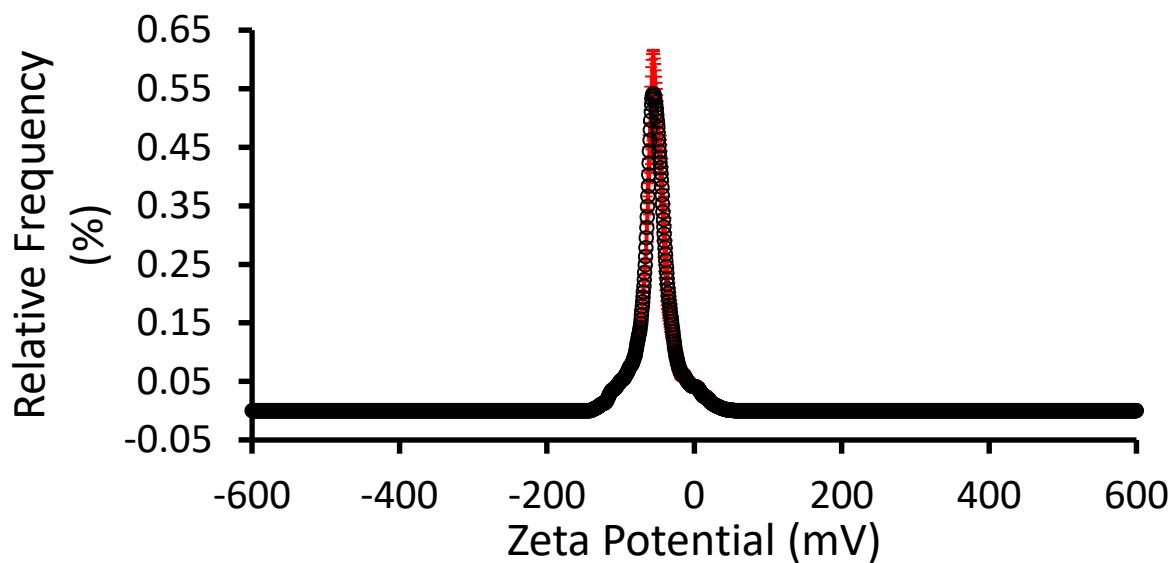


Figure S44 - The average zeta potential distribution calculated using 10 runs for compound **1** (5 mg/mL) in an EtOH:H₂O (1:19) solution at 298 K. Average measurement value -59.0 mV.

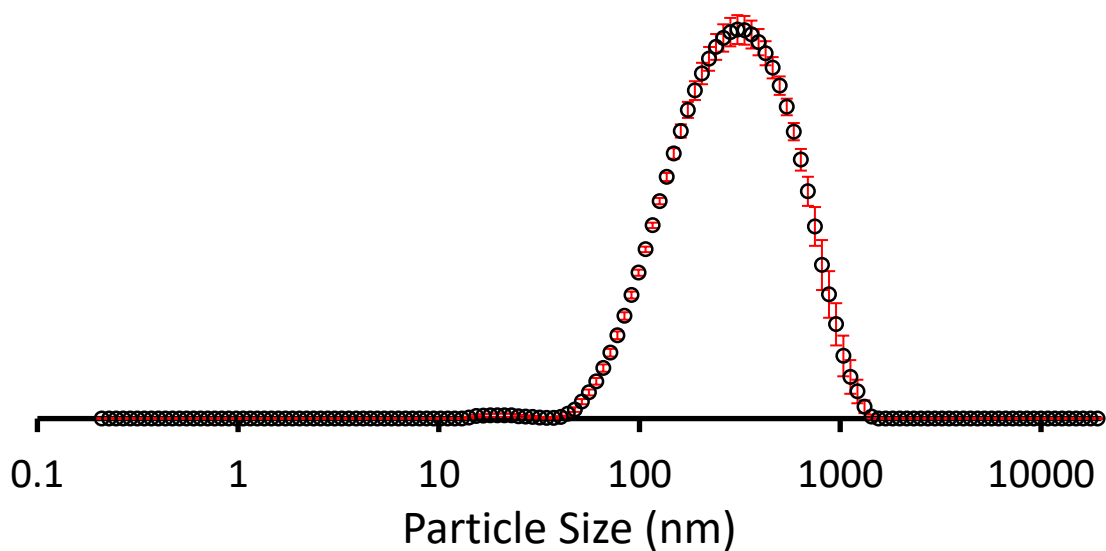


Figure S45 - The average intensity particle size distribution calculated using 10 DLS runs for compound **1** (5 mg/mL) in a H₂O solution at 298 K.

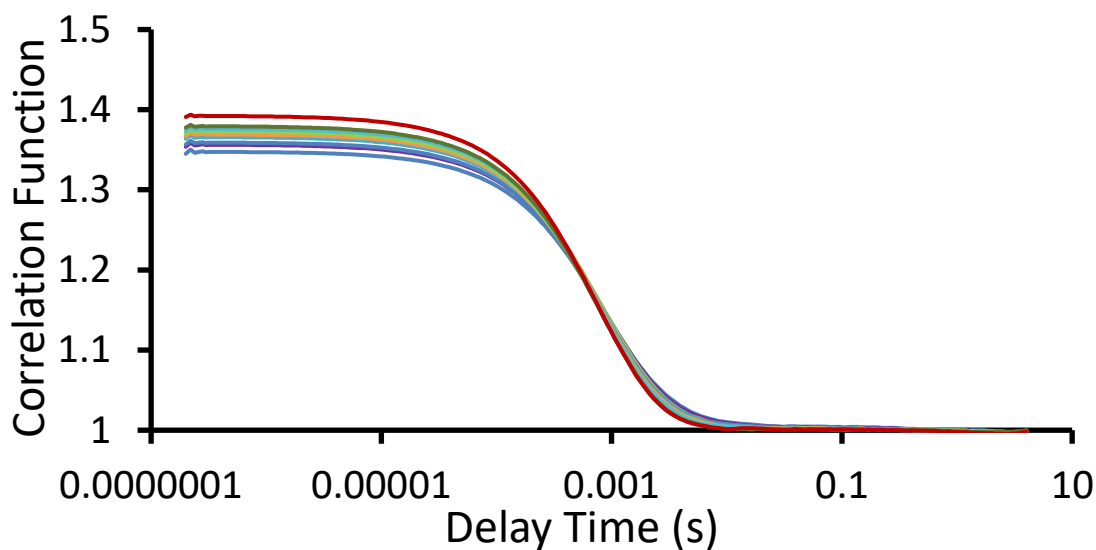


Figure S46 - Correlation function data for 10 DLS runs of compound **1** (5 mg/mL) in a H₂O solution at 298 K.

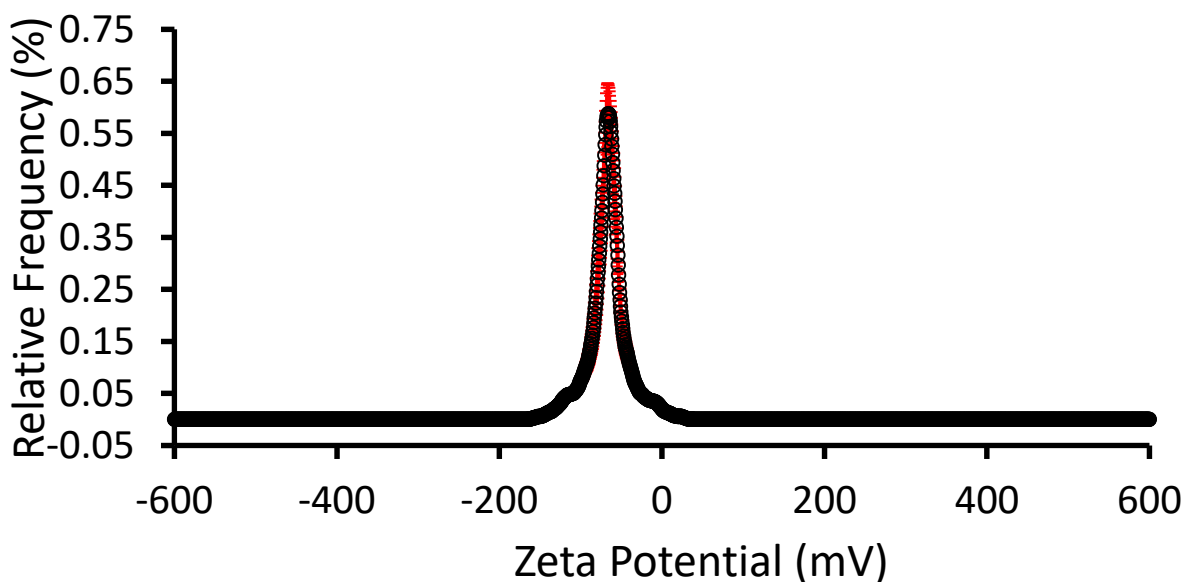


Figure S47 - The average zeta potential distribution calculated using 10 runs for compound **1** (5 mg/mL) in a H₂O solution at 298 K. Average measurement value -71.4 mV.

Table S1 - Summary of average intensity particle size distribution and zeta potential data for compound **1** at 5 mg/ mL. Error = standard error of the mean.

Solution	Peak maxima (nm)	Polydispersity (%)	Zeta potential (mV)
H ₂ O:EtOH 19:1	197	26 (± 0.3708)	-59.0
H ₂ O	349	22 (± 1.1579)	-71.4

Rheological data

Amplitude sweep

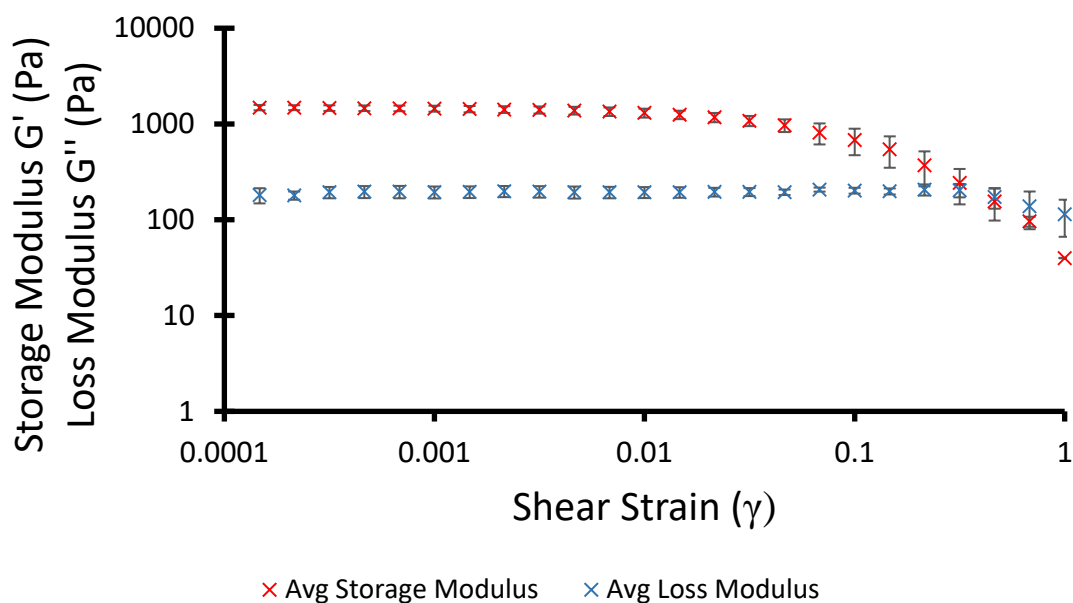


Figure S48 – Graph showing average results (n=3) from amplitude sweep experiments used to define the linear viscoelastic region of the sample at 298 K. Compound **1** (5 mg) in 1 mL NaCl (0.505 M) (1 = 100%).

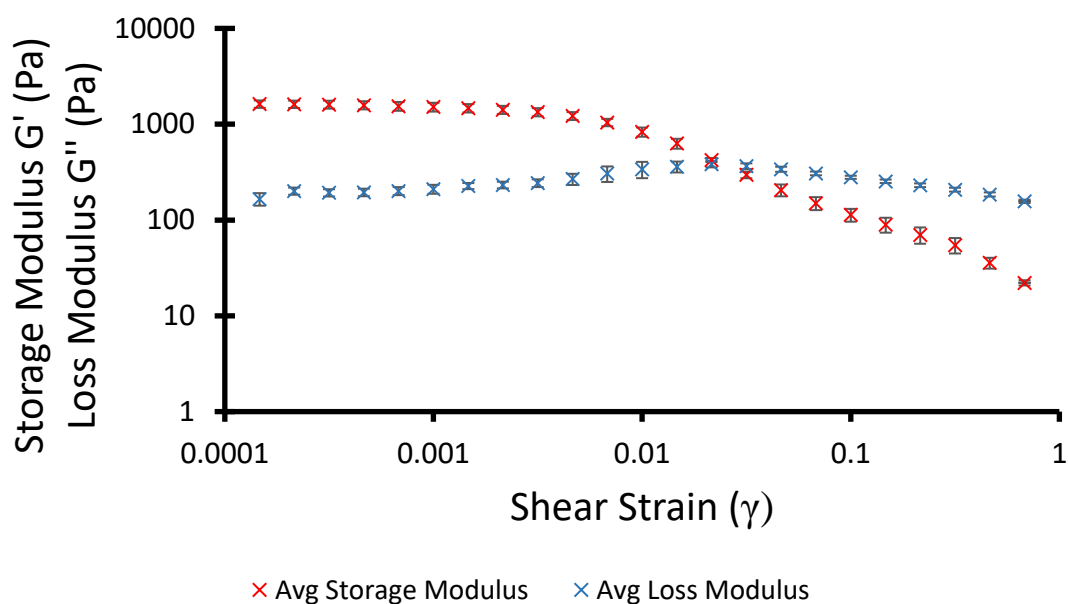


Figure S49 – Graph showing average results (n=3) from amplitude sweep experiments used to define the linear viscoelastic region of the sample at 298 K. Compound **1** (5 mg) in 1 mL NaH_2PO_4 (0.505 M) (1 = 100%).

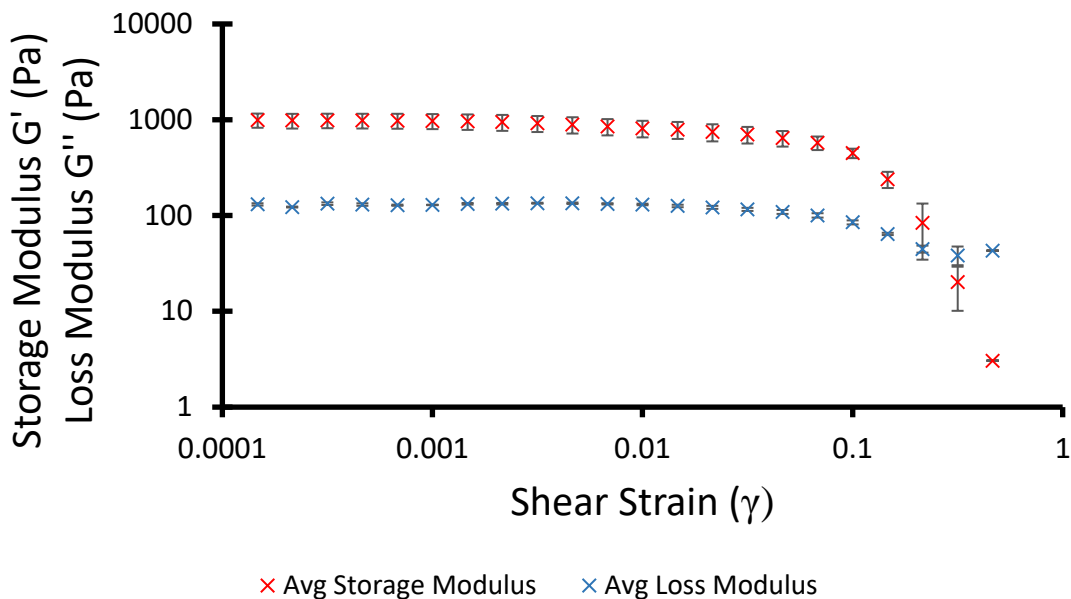


Figure S50 – Graph showing average results (n=3) from amplitude sweep experiments used to define the linear viscoelastic region of the sample at 298 K. Compound **1** (5 mg) in 1 mL Na_2CO_3 (0.505 M) (1 = 100%).

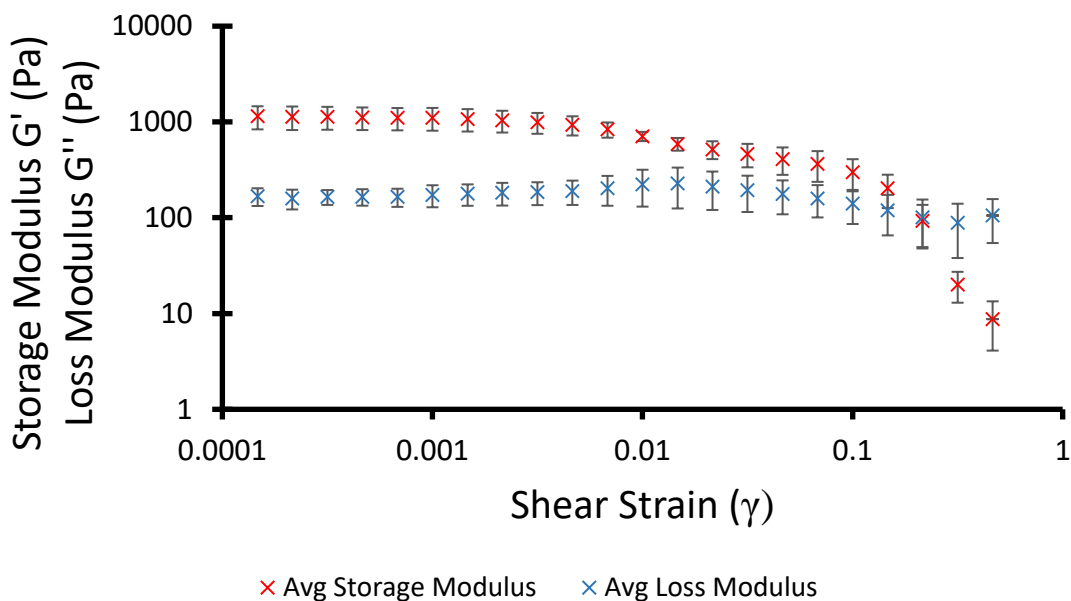


Figure S51 – Graph showing average results (n=3) from amplitude sweep experiments used to define the linear viscoelastic region of the sample at 298 K. Compound **1** (5 mg) in 1 mL NaNO_3 (0.505 M) (1 = 100%).

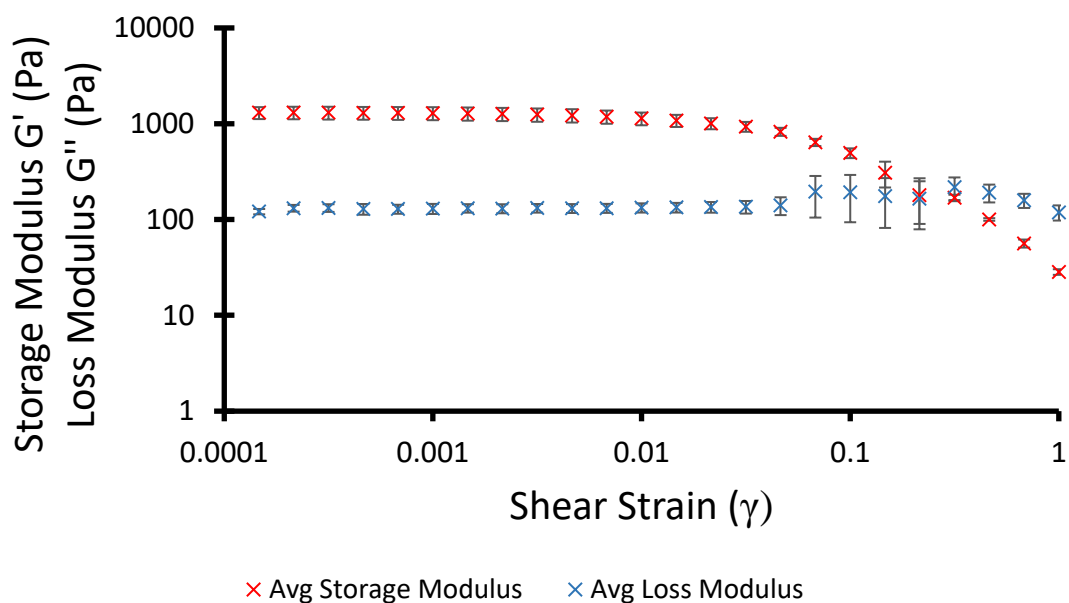


Figure S52 – Graph showing average results (n=3) from amplitude sweep experiments used to define the linear viscoelastic region of the sample at 298 K. Compound **1** (5 mg) in 1 mL $\text{NaC}_7\text{H}_5\text{O}_2$ (0.505 M) (1 = 100%).

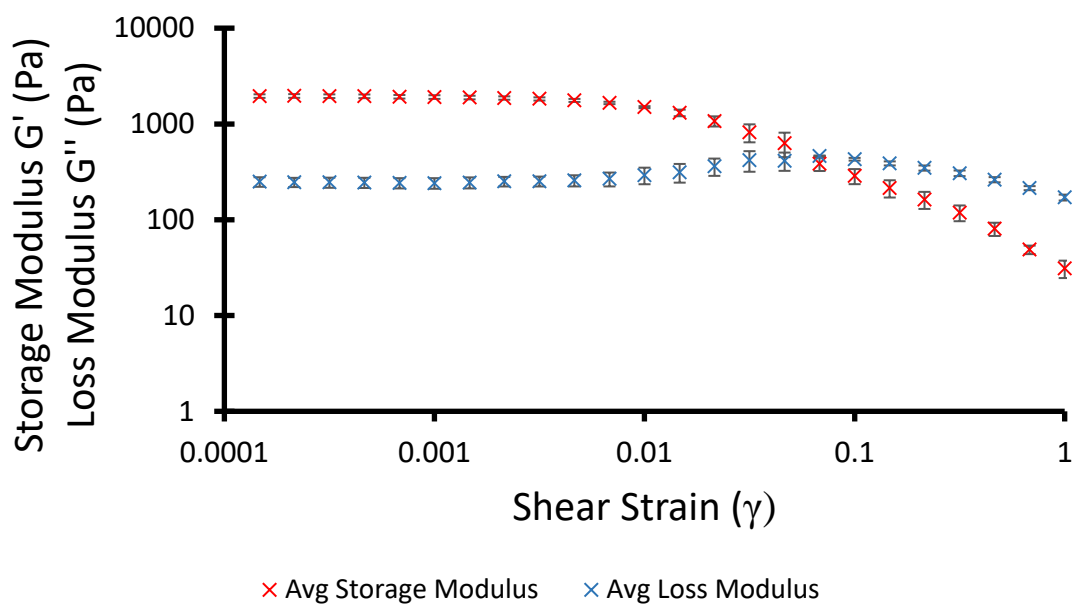


Figure S53 – Graph showing average results (n=3) from amplitude sweep experiments used to define the linear viscoelastic region of the sample at 298 K. Compound **1** (5 mg) in 1 mL Na_2SO_4 (0.505 M) (1 = 100%).

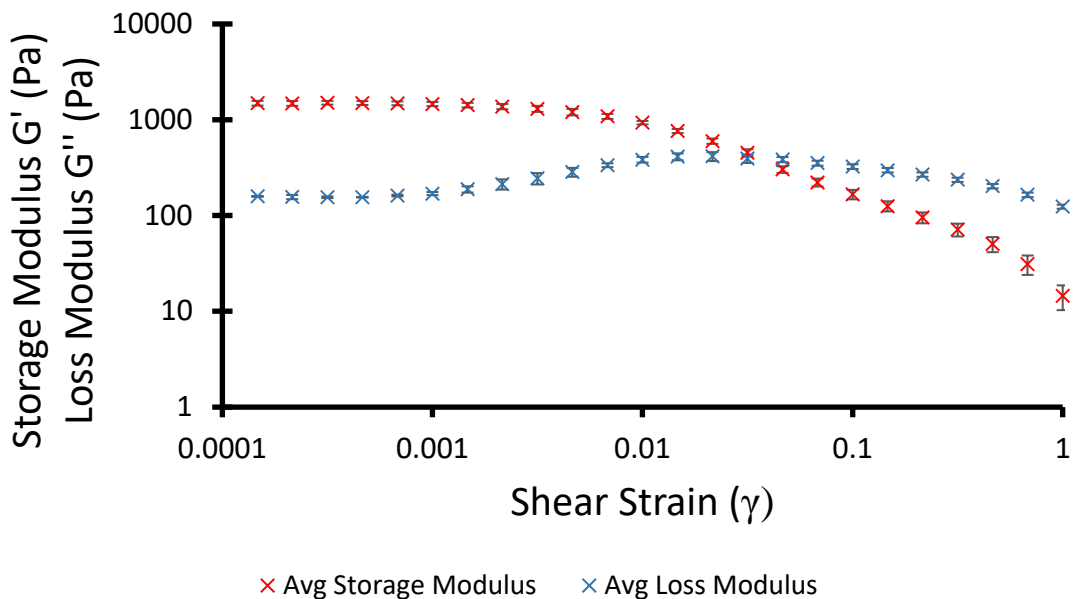


Figure S54 – Graph showing average results (n=3) from amplitude sweep experiments used to define the linear viscoelastic region of the sample at 298 K. Compound **1** (5 mg) in 1 mL NaHCO_3 (0.505 M) (1 = 100%).

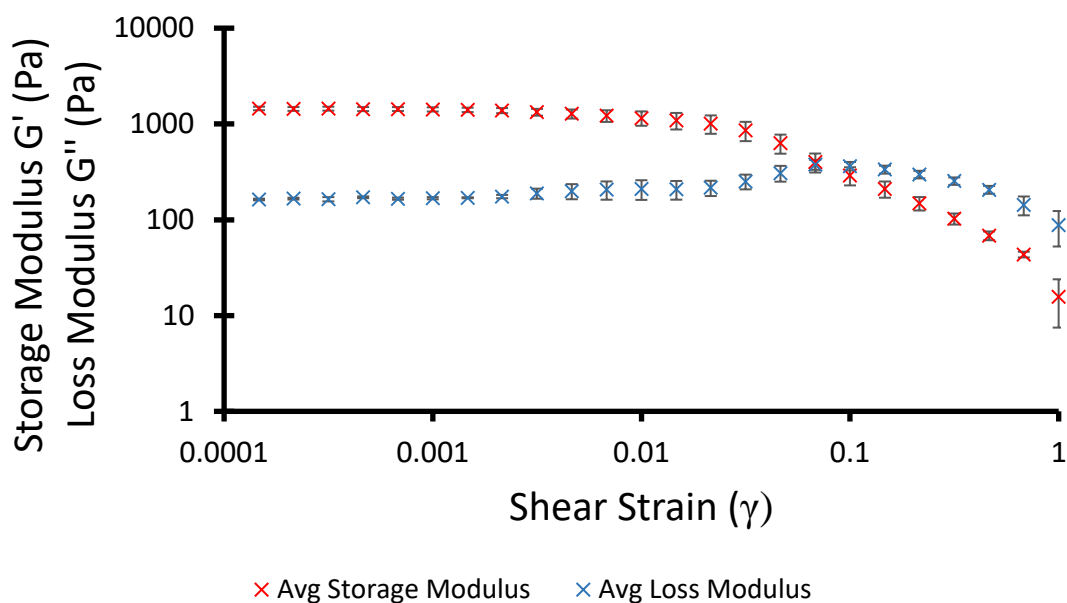


Figure S55 – Graph showing average results (n=3) from amplitude sweep experiments used to define the linear viscoelastic region of the sample at 298 K. Compound **1** (5 mg) in 1 mL $\text{NaC}_2\text{H}_3\text{O}_2$ (0.505 M) (1 = 100%).

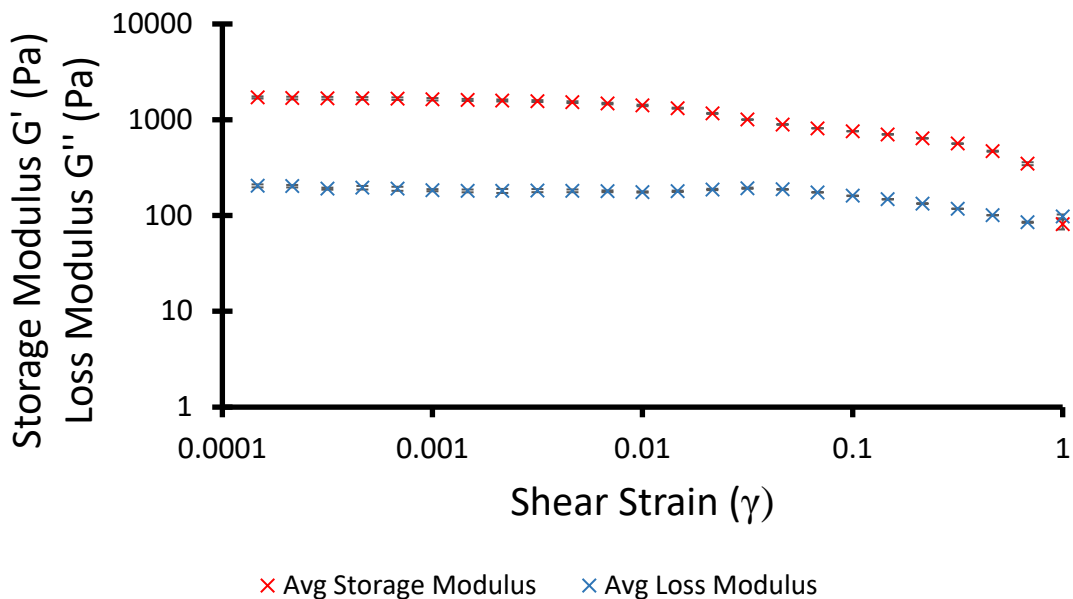


Figure S56 – Graph showing average results (n=3) from amplitude sweep experiments used to define the linear viscoelastic region of the sample at 298 K. Compound **1** (5 mg) in 1 mL NaF (0.505 M) (1 = 100%).

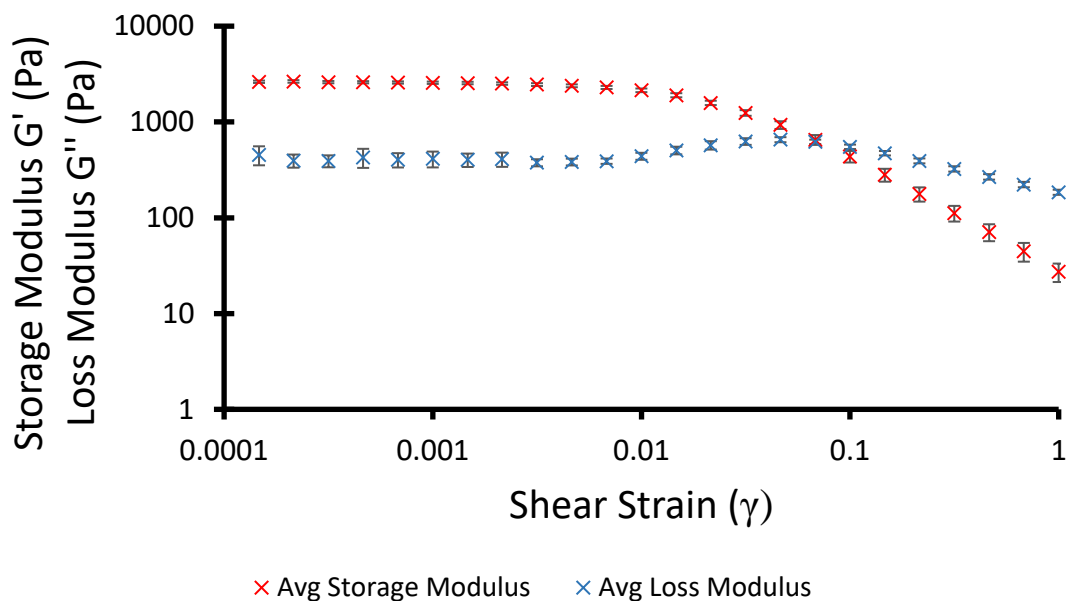


Figure S57 – Graph showing average results (n=3) from amplitude sweep experiments used to define the linear viscoelastic region of the sample at 298 K. Compound **1** (5 mg) in 1 mL KCl (0.505 M) (1 = 100%).

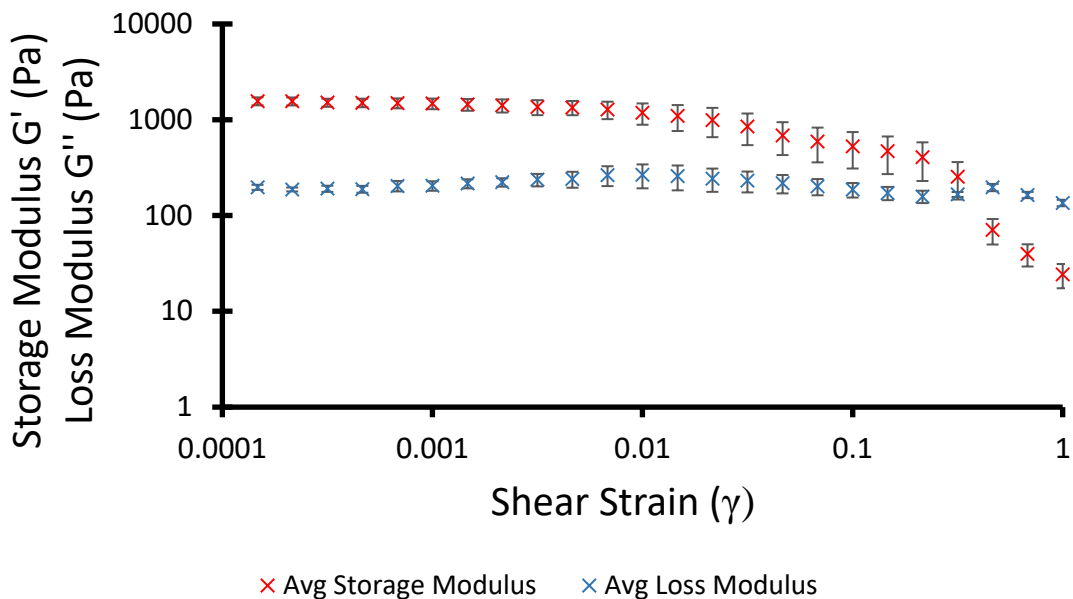


Figure S58 – Graph showing average results (n=3) from amplitude sweep experiments used to define the linear viscoelastic region of the sample at 298 K. Compound **1** (5 mg) in 1 mL RbCl (0.505 M) ($\phi = 100\%$).

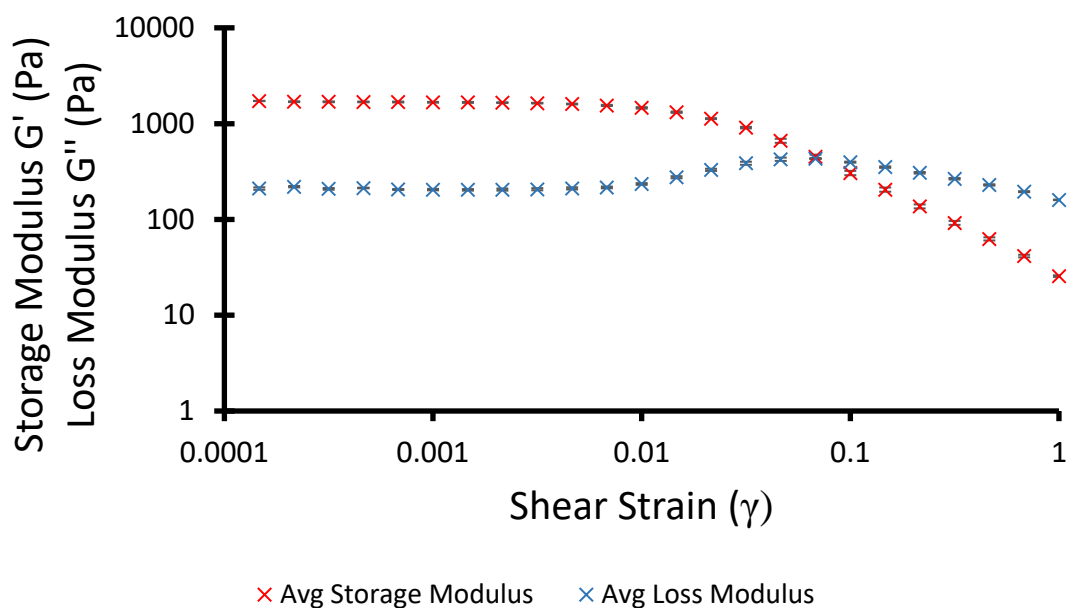


Figure S59 – Graph showing average results (n=3) from amplitude sweep experiments used to define the linear viscoelastic region of the sample at 298 K. Compound **1** (5 mg) and ampicillin (3 mg) in 1 mL NaCl (0.505 M) ($\phi = 100\%$).

Frequency sweep

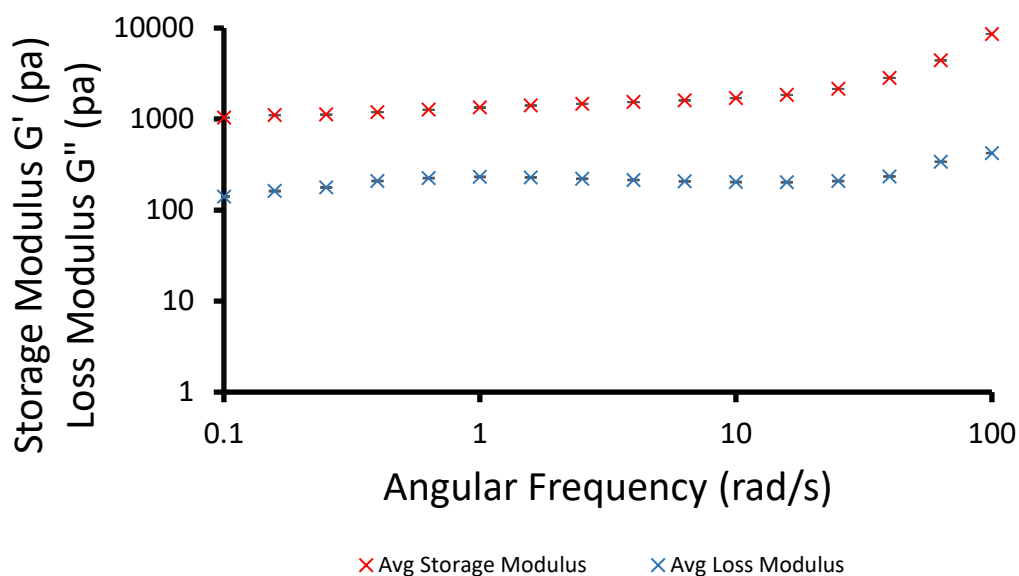


Figure S60 – Graph showing average results (n=3) from frequency sweep experiments obtained from the linear viscoelastic region under a constant shear strain (γ) of 0.925% (298 K). Compound 1 (5 mg) in 1 mL NaCl (0.505 M).

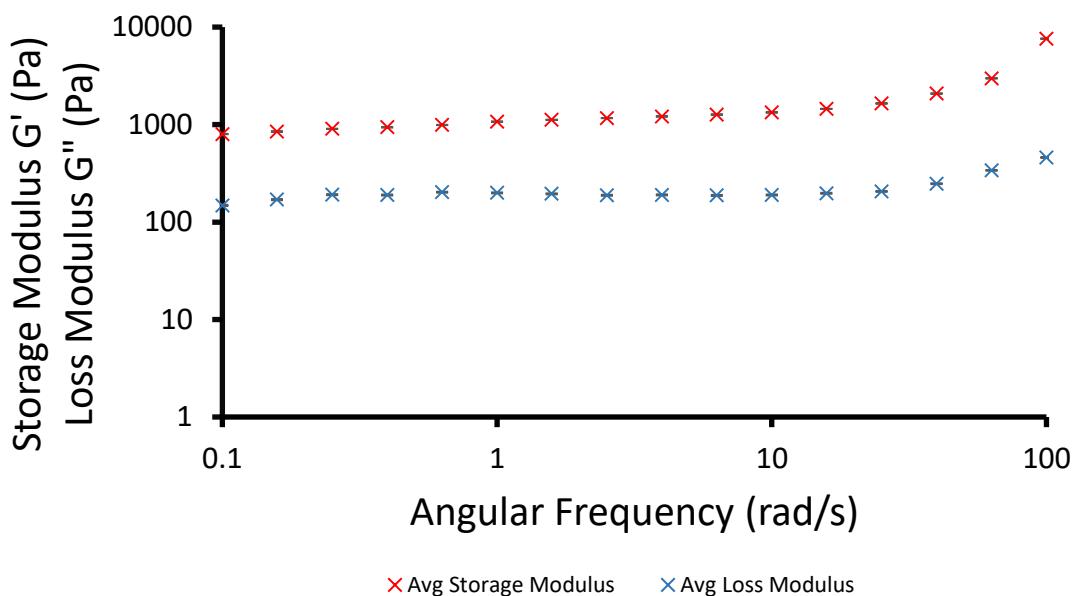


Figure S61 – Graph showing average results (n=3) from frequency sweep experiments obtained from the linear viscoelastic region under a constant shear strain (γ) of 0.925% (298 K). Compound 1 (5 mg) in 1 mL Na₂HPO₄ (0.505 M).

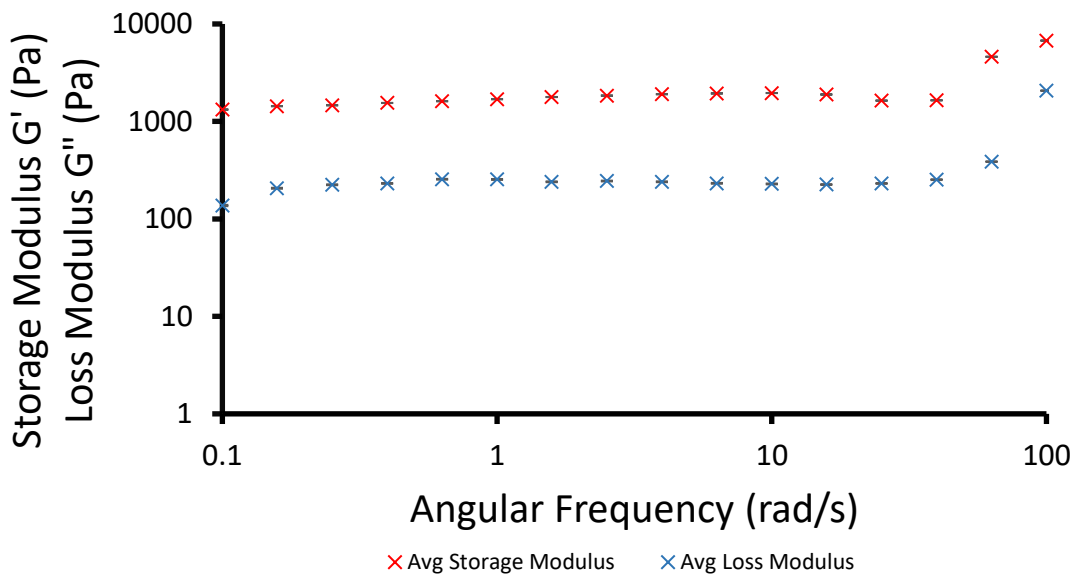


Figure S62 – Graph showing average results (n=3) from frequency sweep experiments obtained from the linear viscoelastic region under a constant shear strain (γ) of 0.925% (298 K). Compound **1** (5 mg) in 1 mL Na₂CO₃ (0.505 M).

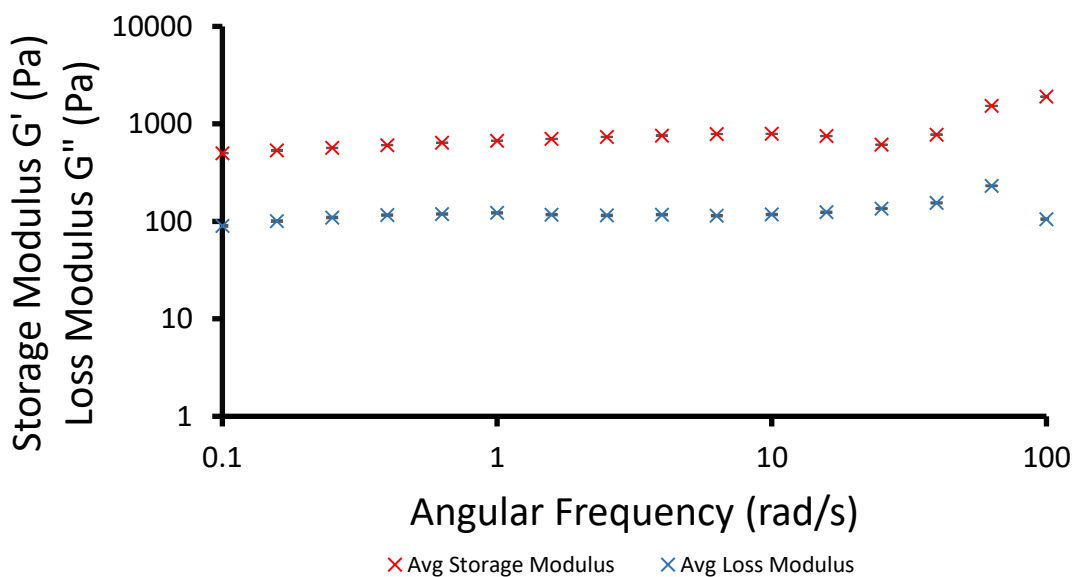


Figure S63 – Graph showing average results (n=3) from frequency sweep experiments obtained from the linear viscoelastic region under a constant shear strain (γ) of 0.925% (298 K). Compound **1** (5 mg) in 1 mL NaNO₃ (0.505 M).

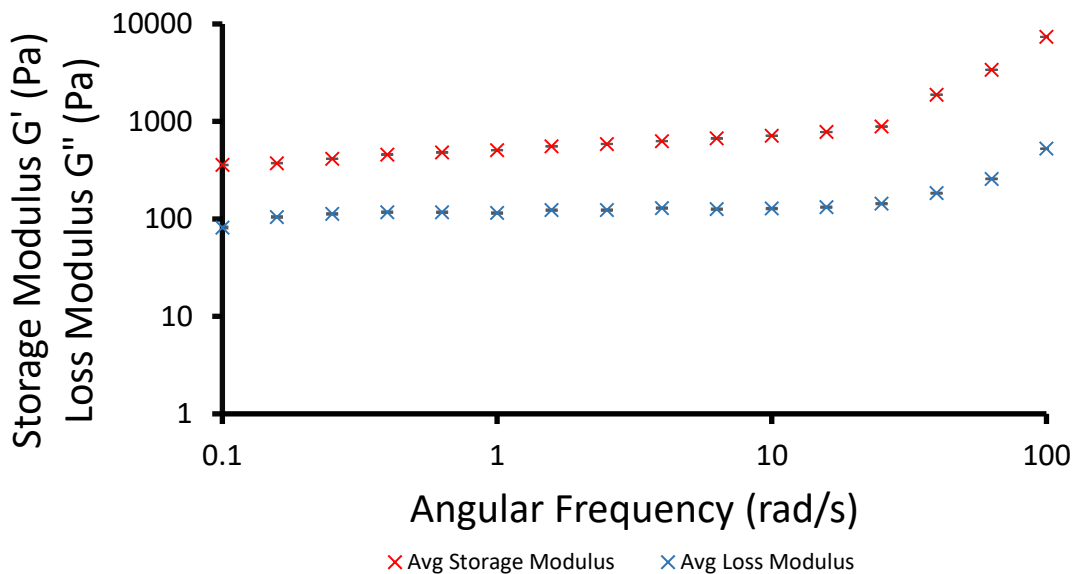


Figure S64 – Graph showing average results (n=3) from frequency sweep experiments obtained from the linear viscoelastic region under a constant shear strain (γ) of 0.925% (298 K). Compound 1 (5 mg) in 1 mL $\text{NaC}_7\text{H}_5\text{O}_2$ (0.505 M).

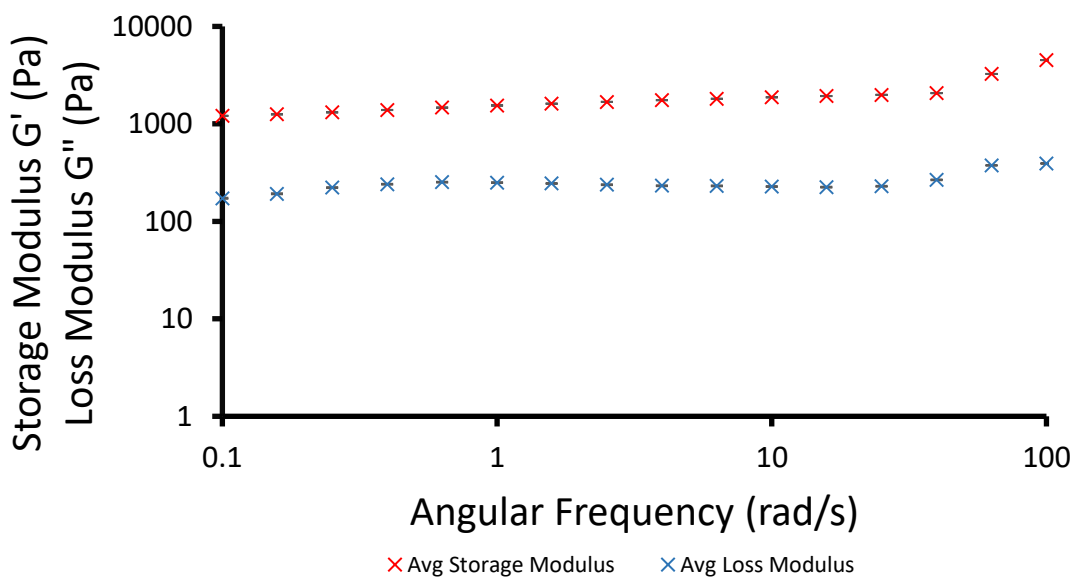


Figure S65 – Graph showing average results (n=3) from frequency sweep experiments obtained from the linear viscoelastic region under a constant shear strain (γ) of 0.925% (298 K). Compound 1 (5 mg) in 1 mL Na_2SO_4 (0.505 M).

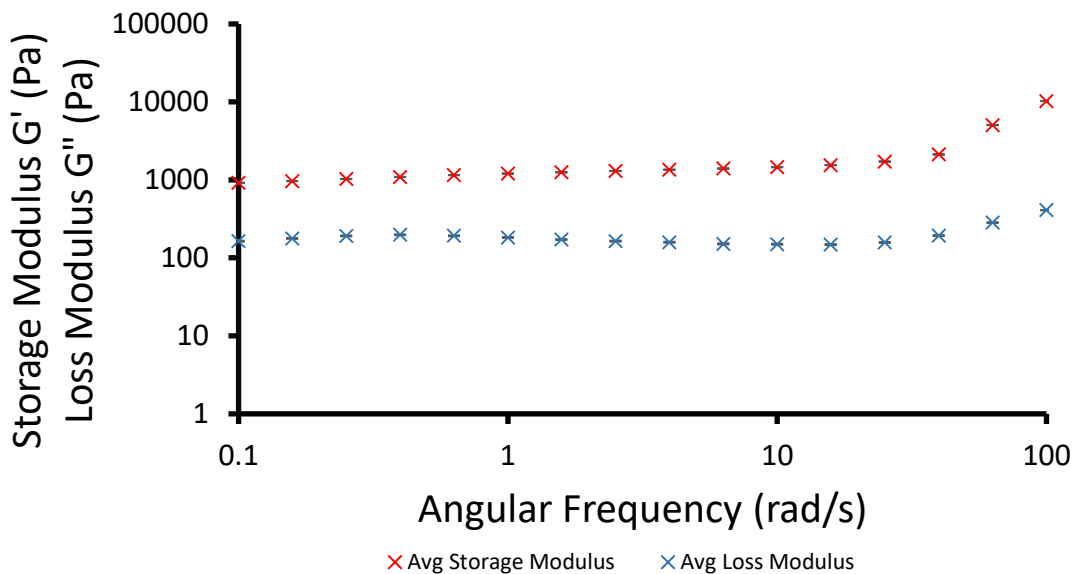


Figure S66 – Graph showing average results (n=3) from frequency sweep experiments obtained from the linear viscoelastic region under a constant shear strain (γ) of 0.925% (298 K). Compound **1** (5 mg) in 1 mL NaHCO₃ (0.505 M).

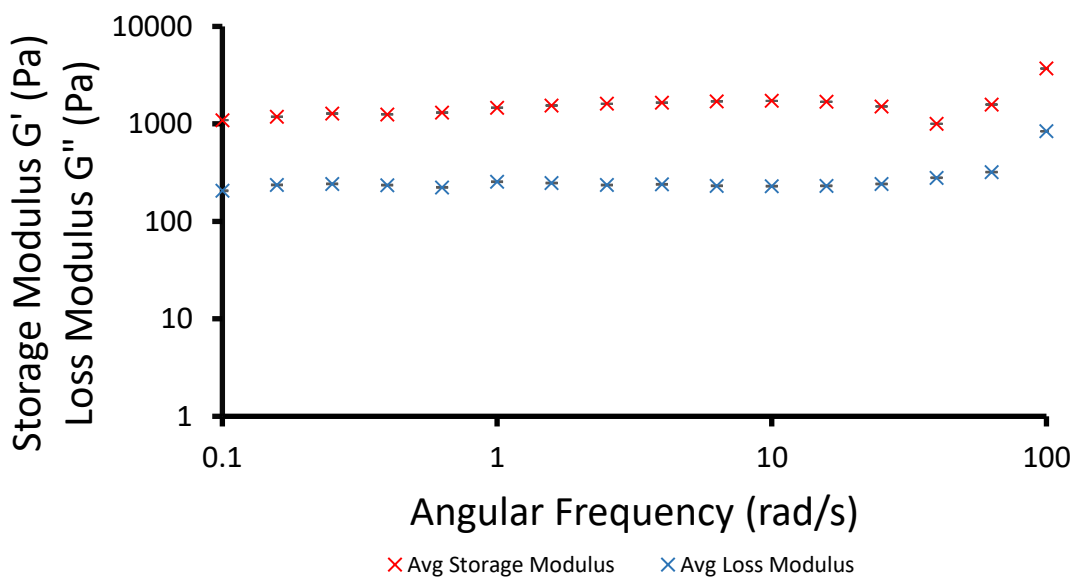


Figure S67 – Graph showing average results (n=3) from frequency sweep experiments obtained from the linear viscoelastic region under a constant shear strain (γ) of 0.925% (298 K). Compound **1** (5 mg) in 1 mL NaC₂H₃O₂ (0.505 M).

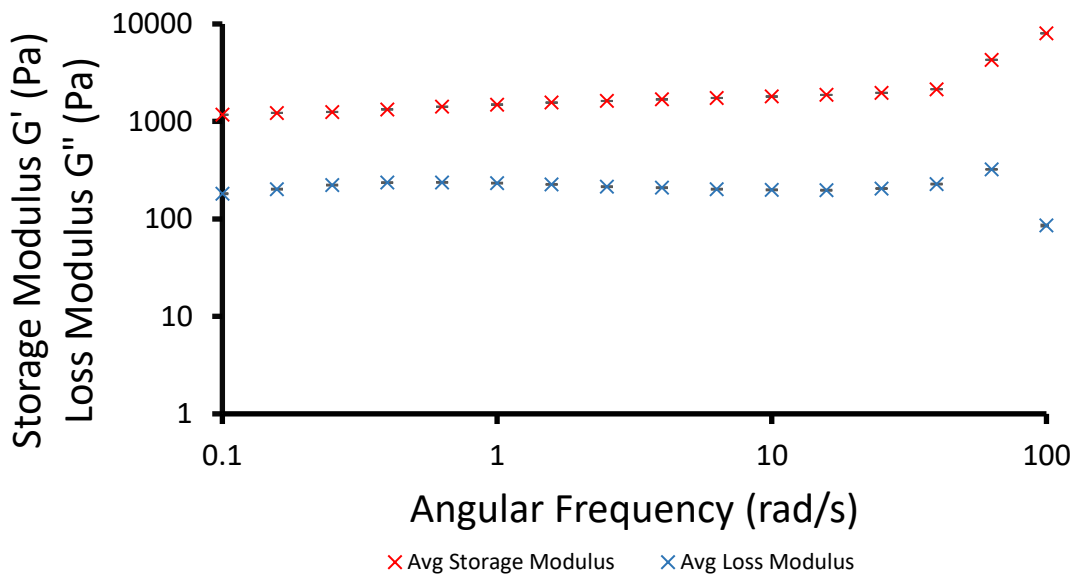


Figure S68 – Graph showing average results (n=3) from frequency sweep experiments obtained from the linear viscoelastic region under a constant shear strain (γ) of 0.925% (298 K). Compound 1 (5 mg) in 1 mL NaF (0.505 M).

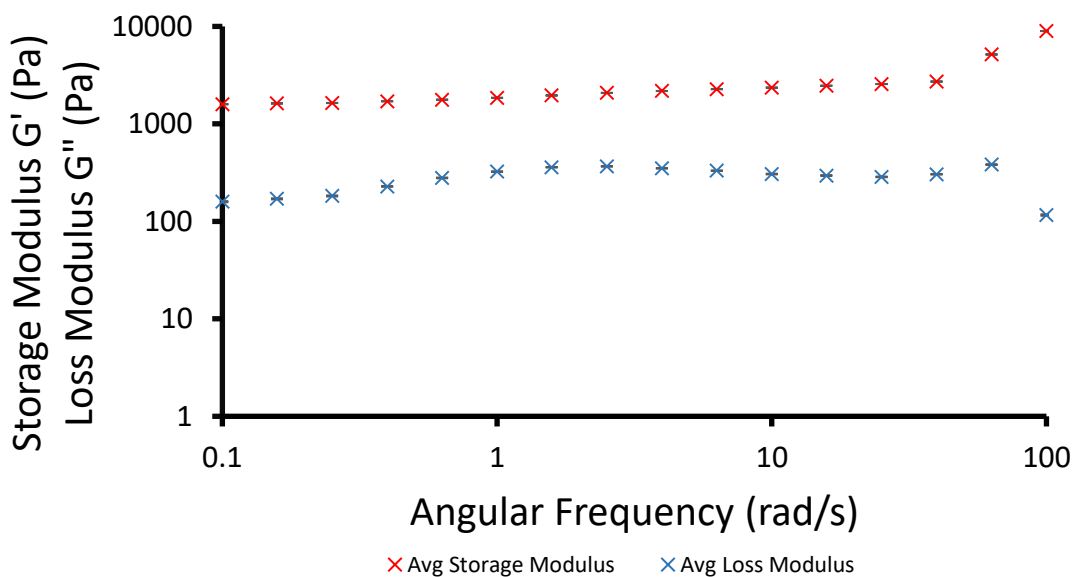


Figure S69 – Graph showing average results (n=3) from frequency sweep experiments obtained from the linear viscoelastic region under a constant shear strain (γ) of 0.925% (298 K). Compound 1 (5 mg) in 1 mL KCl (0.505 M).

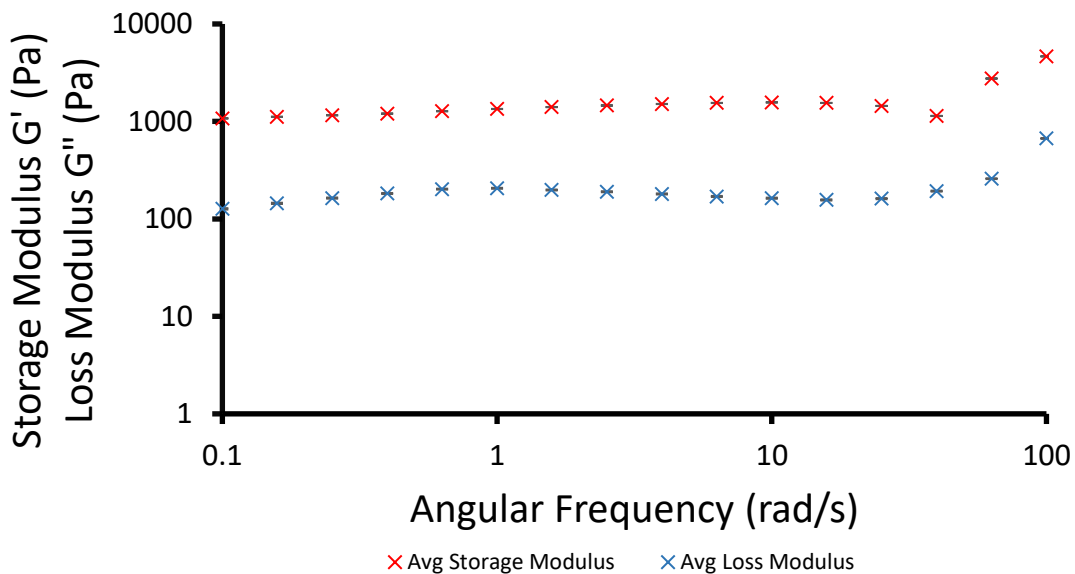


Figure S70 – Graph showing average results (n=3) from frequency sweep experiments obtained from the linear viscoelastic region under a constant shear strain (γ) of 0.925% (298 K). Compound 1 (5 mg) in 1 mL RbCl (0.505 M).

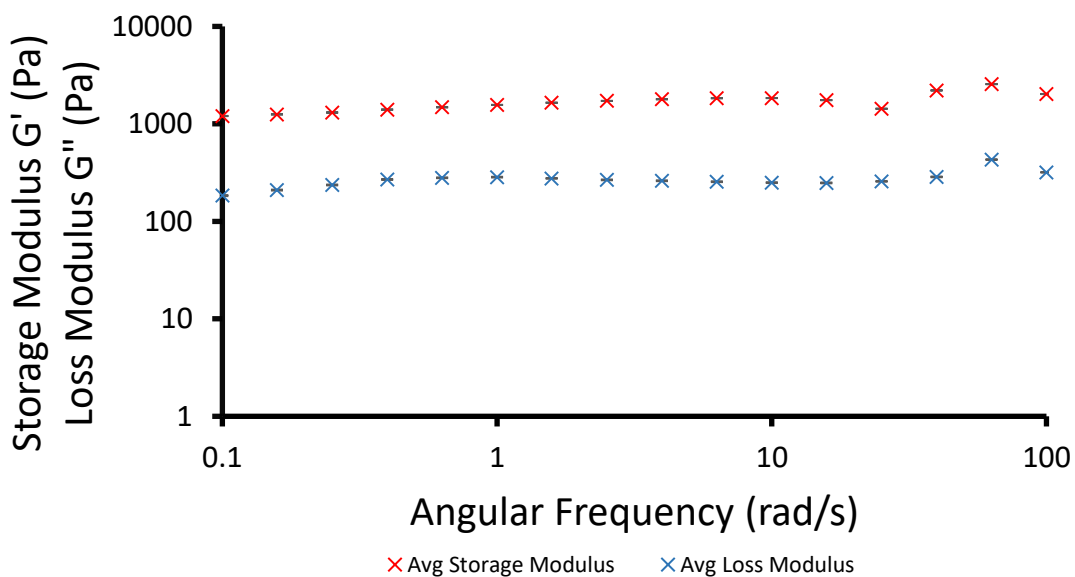


Figure S71 – Graph showing average results (n=3) from frequency sweep experiments obtained from the linear viscoelastic region under a constant shear strain (γ) of 0.925% (298 K). Compound 1 (5 mg) and ampicillin (3 mg) in 1 mL NaCl (0.505 M).

Fluorescence microscopy, scanning electron microscopy and energy dispersive X-ray analysis

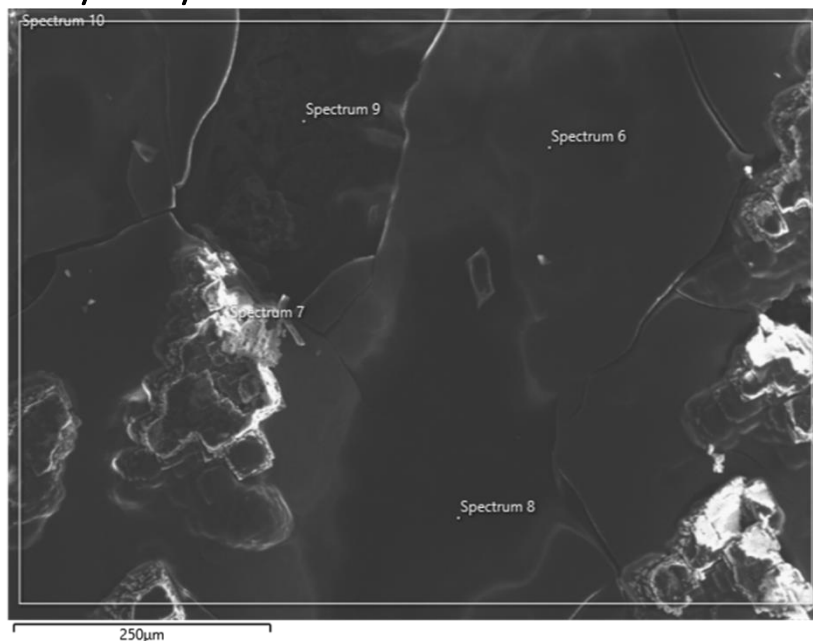


Figure S72 – Scanning electron microscopy image of a xerogel prepared from a dehydrated hydrogel containing compound **1** (5 mg/mL) in NaCl (0.505 M).

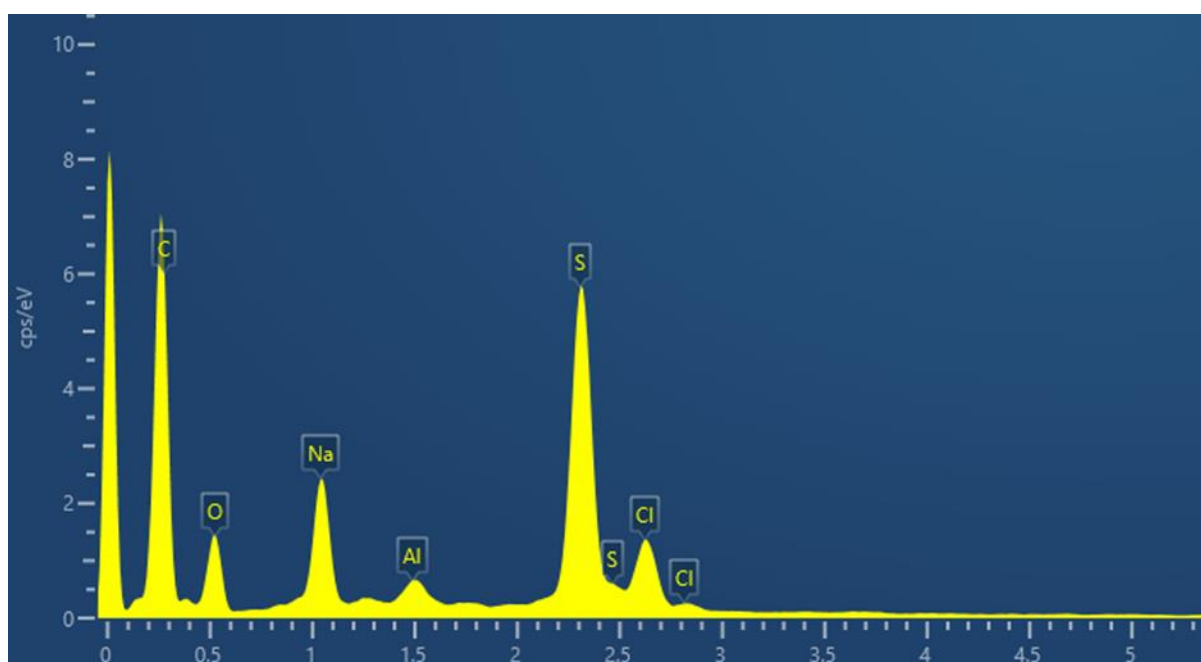


Figure S73 – Energy-dispersive X-ray spectrum showing elemental analysis of the xerogel imaged in Figure S69.

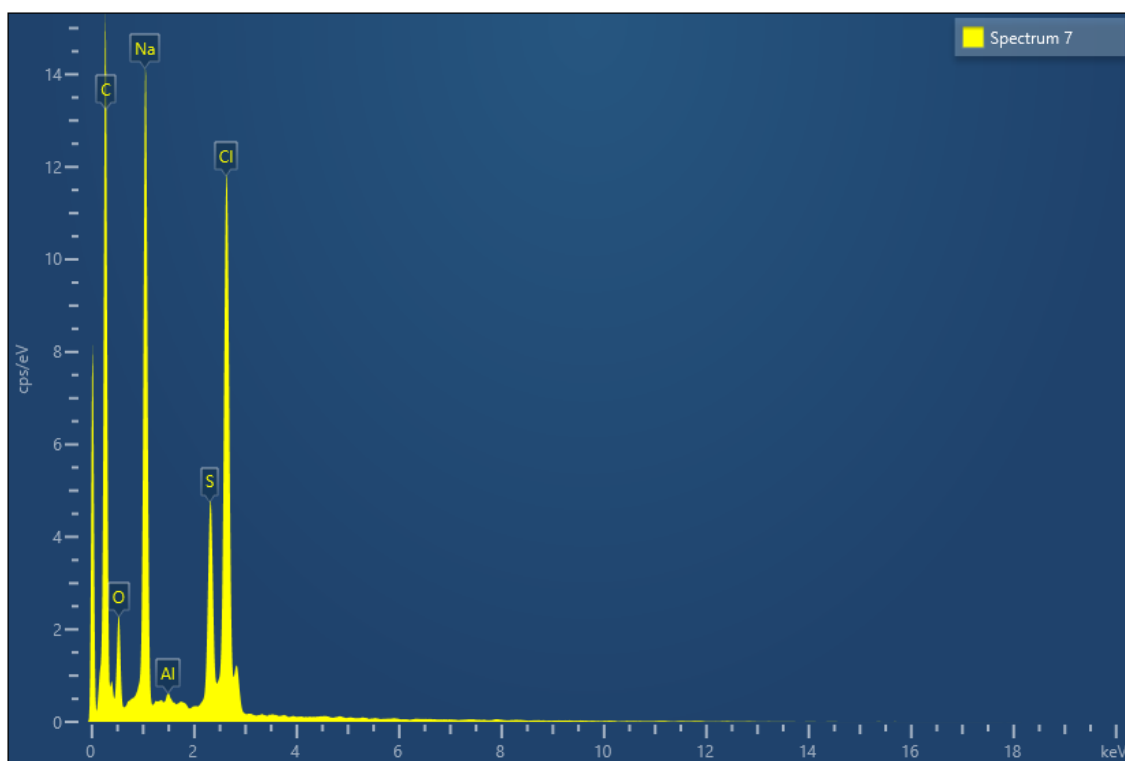


Figure S74 – Energy-dispersive X-ray spectrum showing elemental analysis of the xerogel imaged in Figure S69.

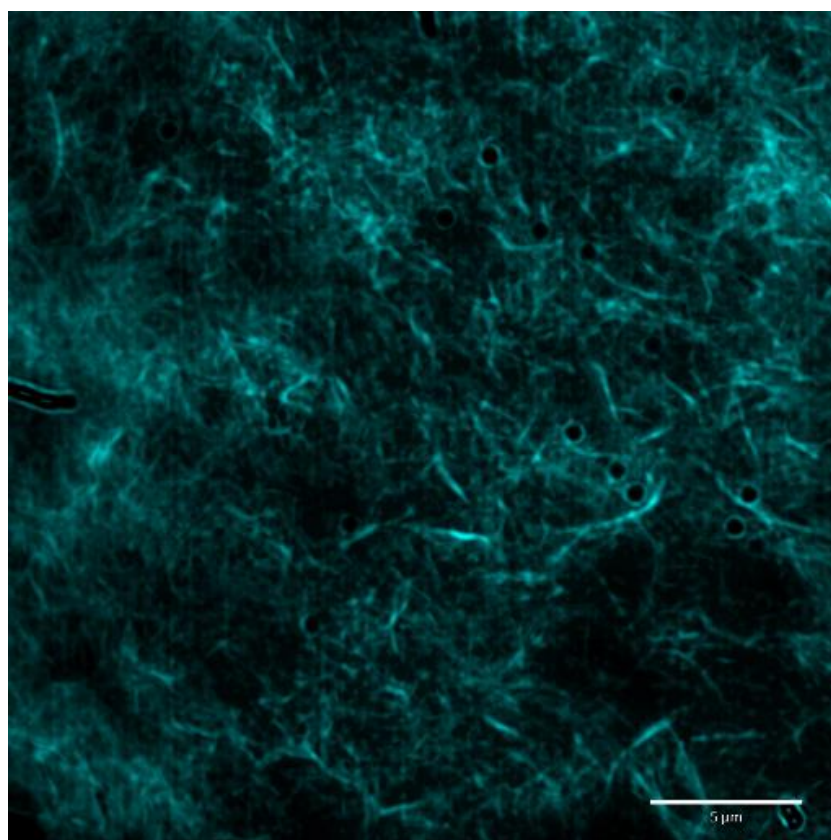


Figure S75 – Fluorescence microscopy image of a hydrogel containing compound **1** (5 mg/ mL) in NaCl (0.505 M).

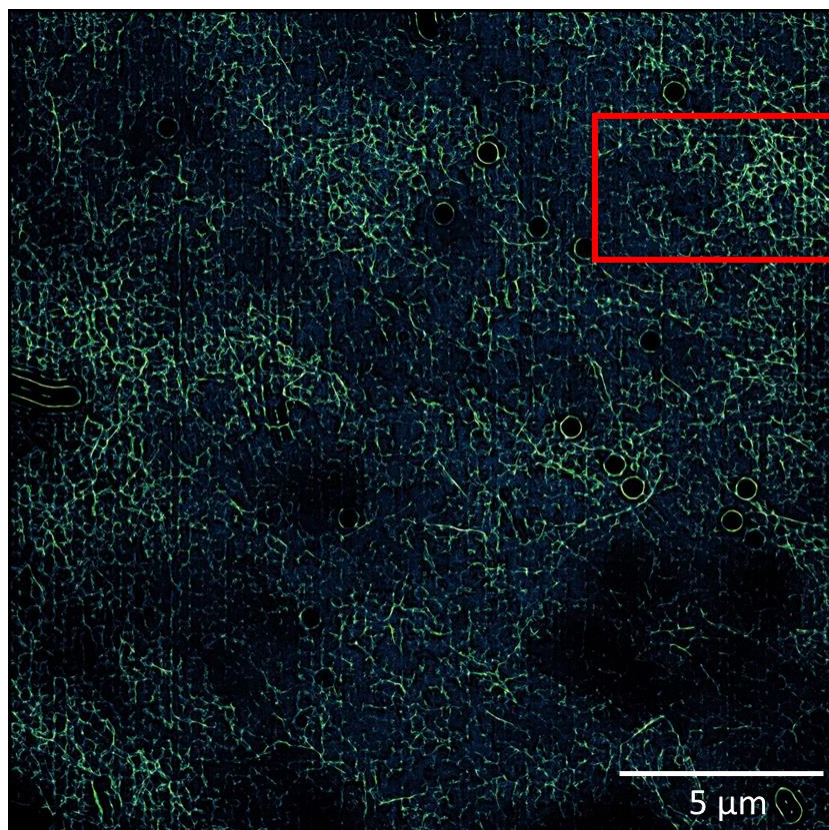


Figure S76 – Refined fluorescence microscopy image of the hydrogel observed in Figure S72.

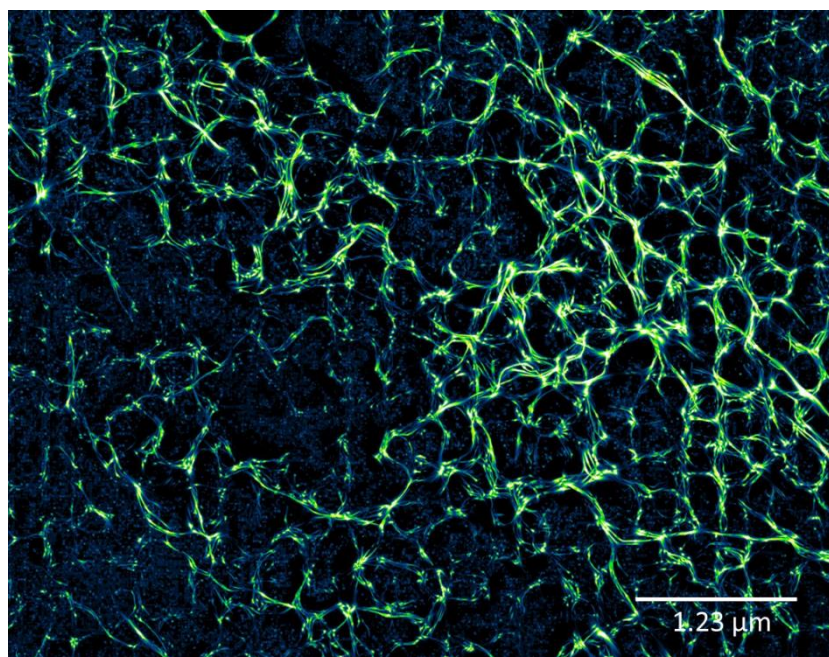


Figure S77 – Enlarged image of outlined red box observed for the hydrogel shown in Figure S73.

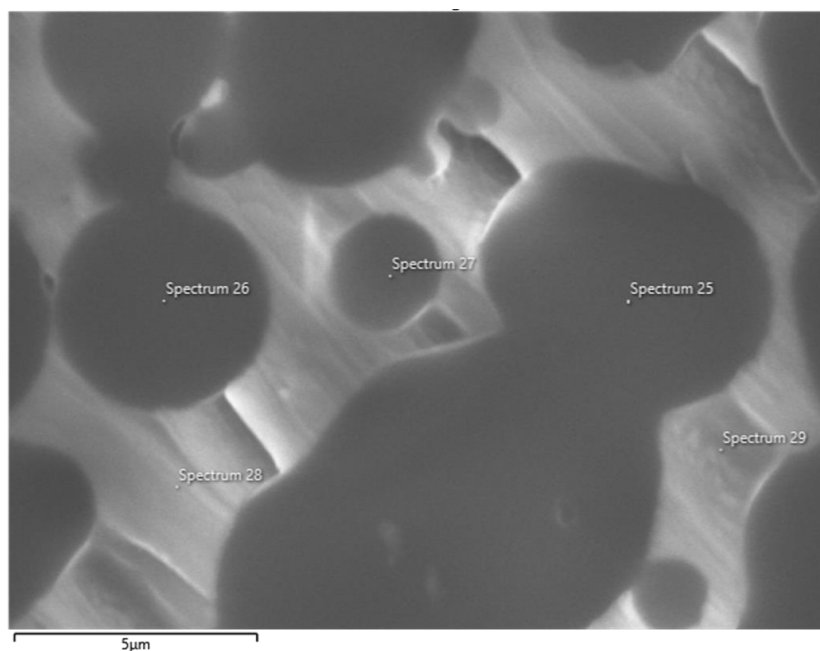


Figure S78 – Scanning electron microscopy image of a xerogel prepared from a dehydrated hydrogel containing compound **1** (5 mg/mL) in NaH_2PO_4 (0.505 M).

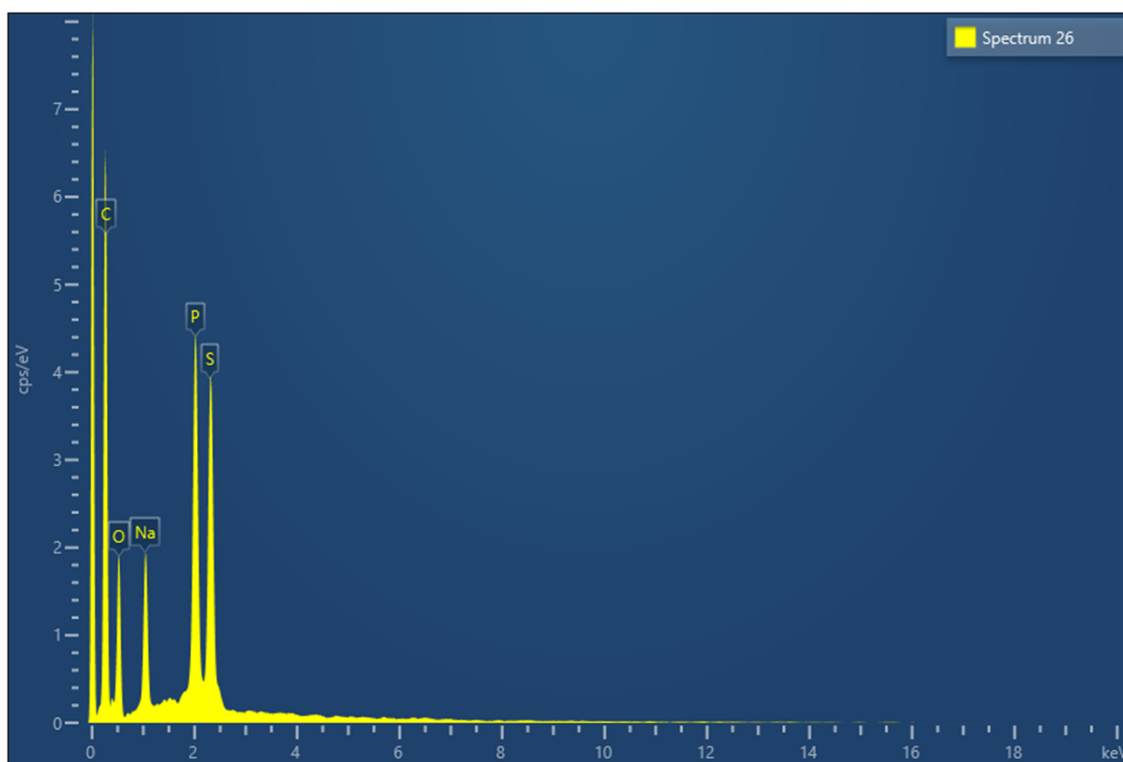


Figure S79 – Energy-dispersive X-ray spectrum showing elemental analysis of the xerogel imaged in Figure S75.

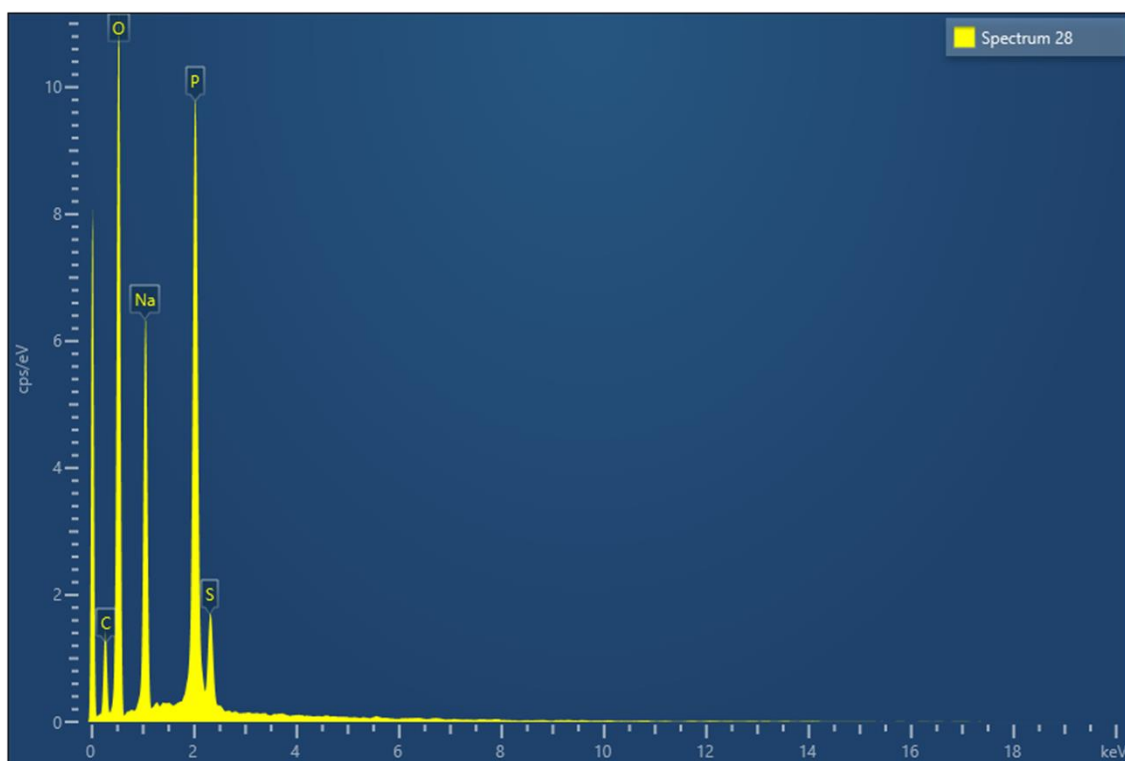


Figure S80 – Energy-dispersive X-ray spectrum showing elemental analysis of the xerogel imaged in Figure S75.

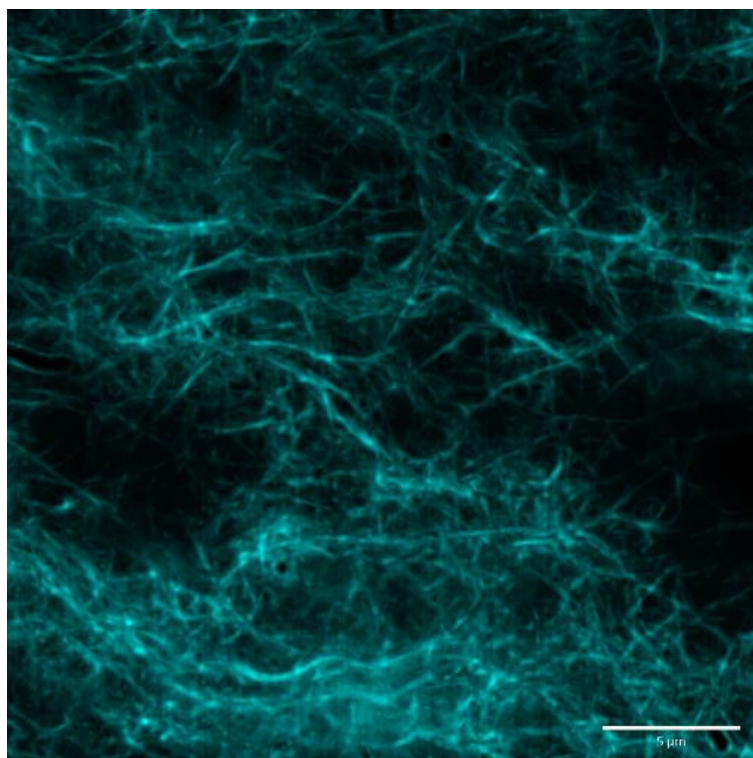


Figure S81 - Fluorescence microscopy image of a hydrogel containing compound **1** (5 mg/mL) in NaH_2PO_4 (0.505 M).

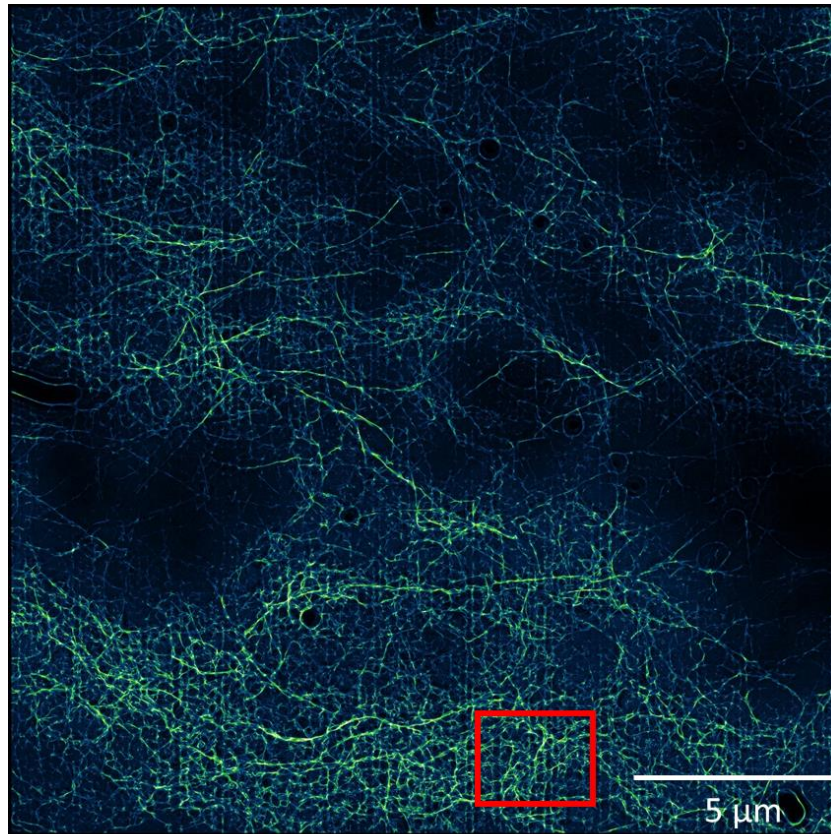


Figure S82 - Refined fluorescence microscopy image of the hydrogel observed in Figure S78.

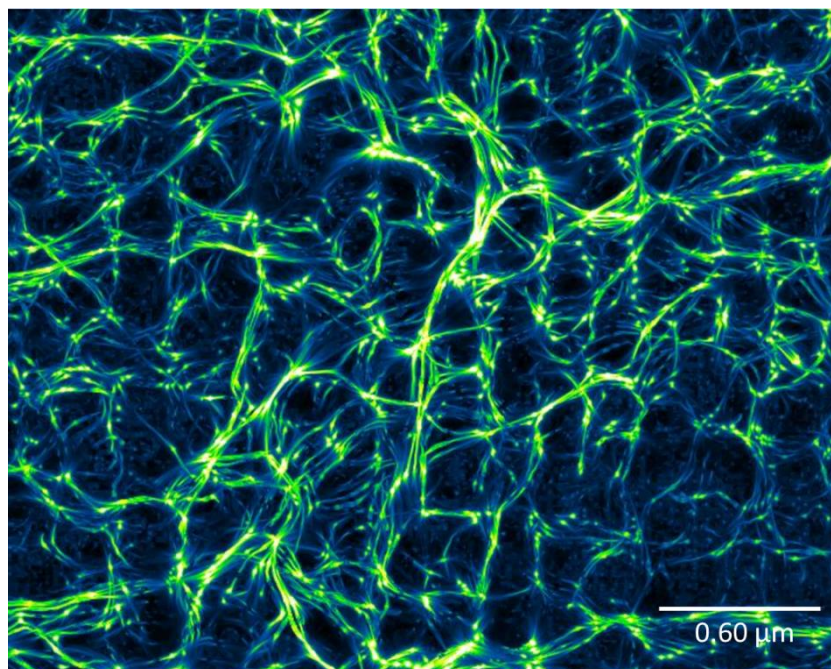


Figure S83 - Enlarged image of outlined red box observed for the hydrogel shown in Figure S79.

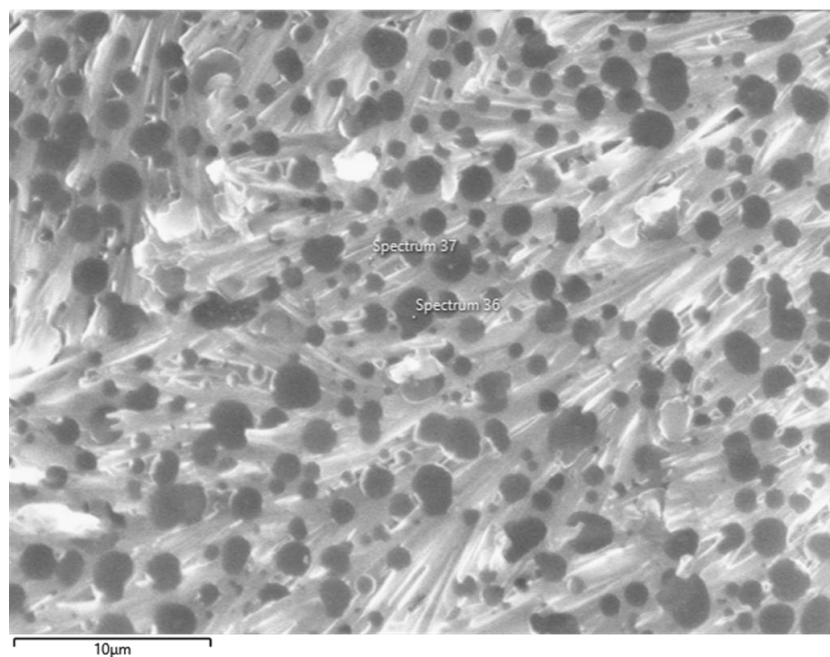


Figure S84 – Scanning electron microscopy image of a xerogel prepared from a dehydrated hydrogel containing compound **1** (5 mg/mL) in Na₂CO₃ (0.505 M).

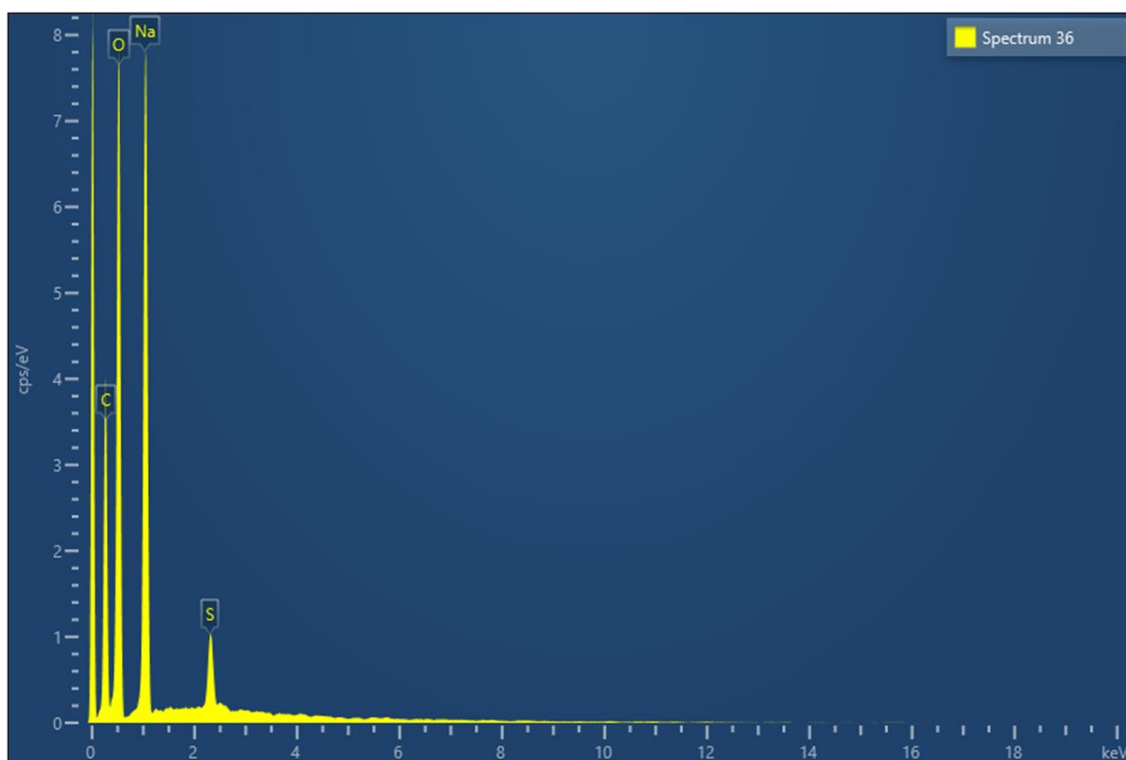


Figure S85 – Energy-dispersive X-ray spectrum showing elemental analysis of the xerogel imaged in Figure S81.

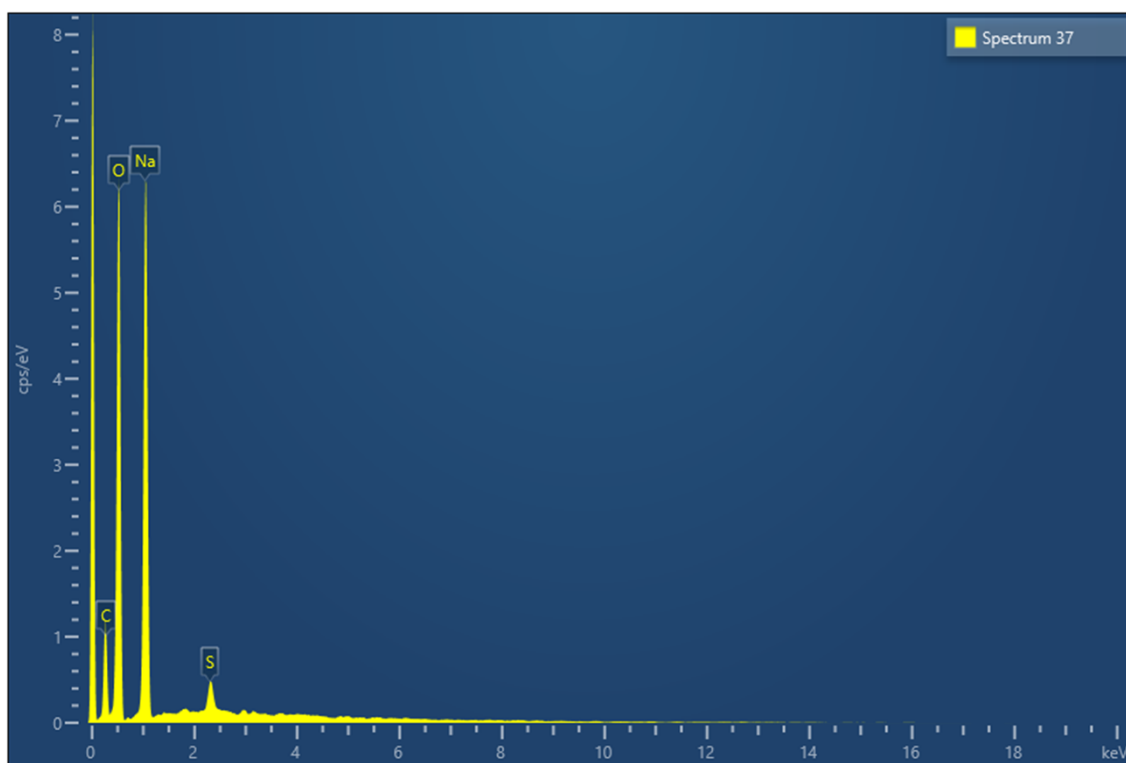


Figure S86 – Energy-dispersive X-ray spectrum showing elemental analysis of the xerogel imaged in Figure S81.

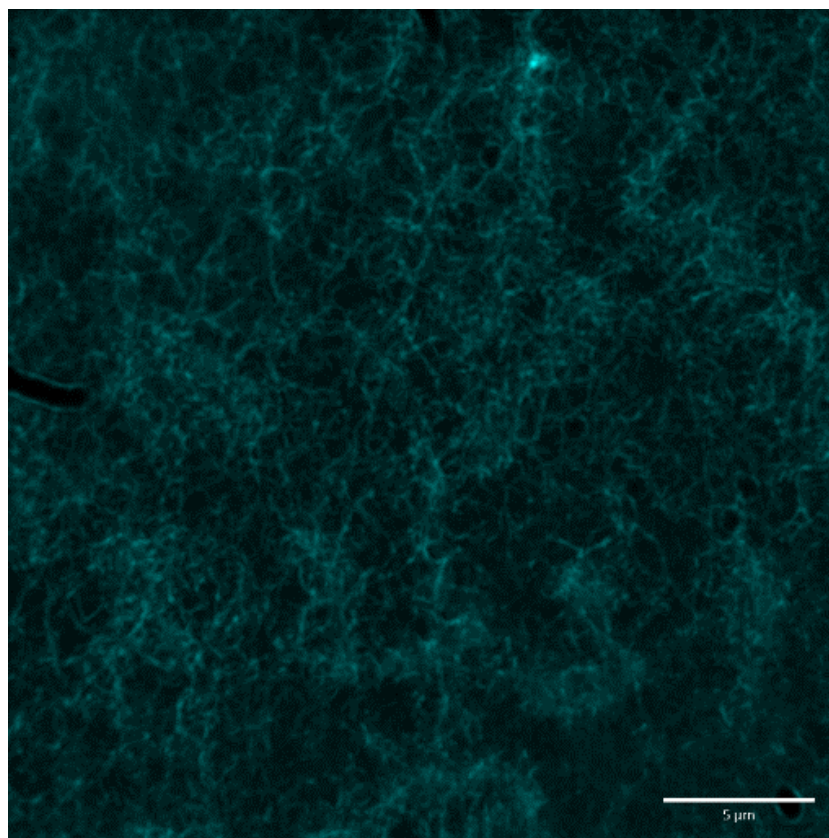


Figure S87 - Fluorescence microscopy image of a hydrogel containing compound **1** (5 mg/mL) in Na_2CO_3 (0.505 M).

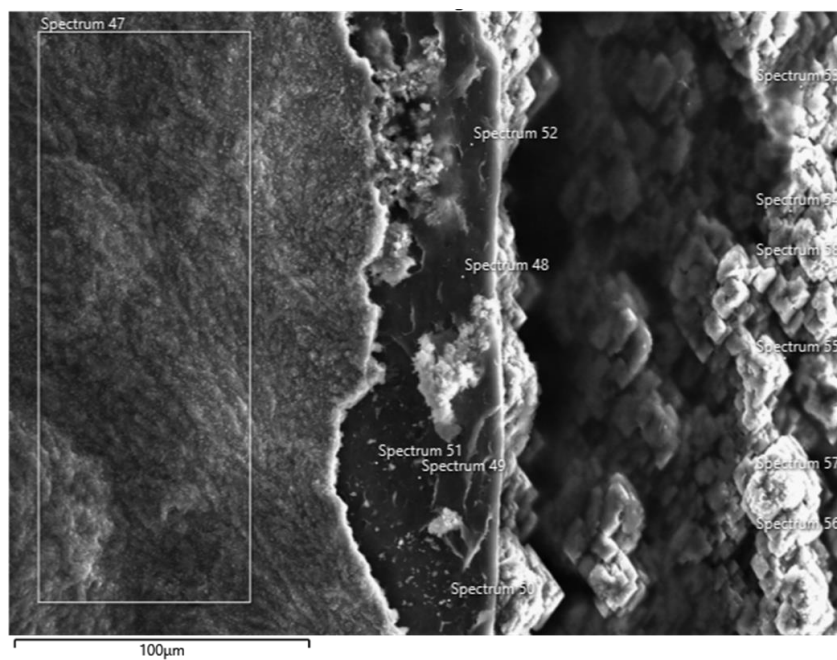


Figure S88 – Scanning electron microscopy image of a xerogel prepared from a dehydrated hydrogel containing compound **1** (5 mg/mL) in NaNO₃ (0.505 M).

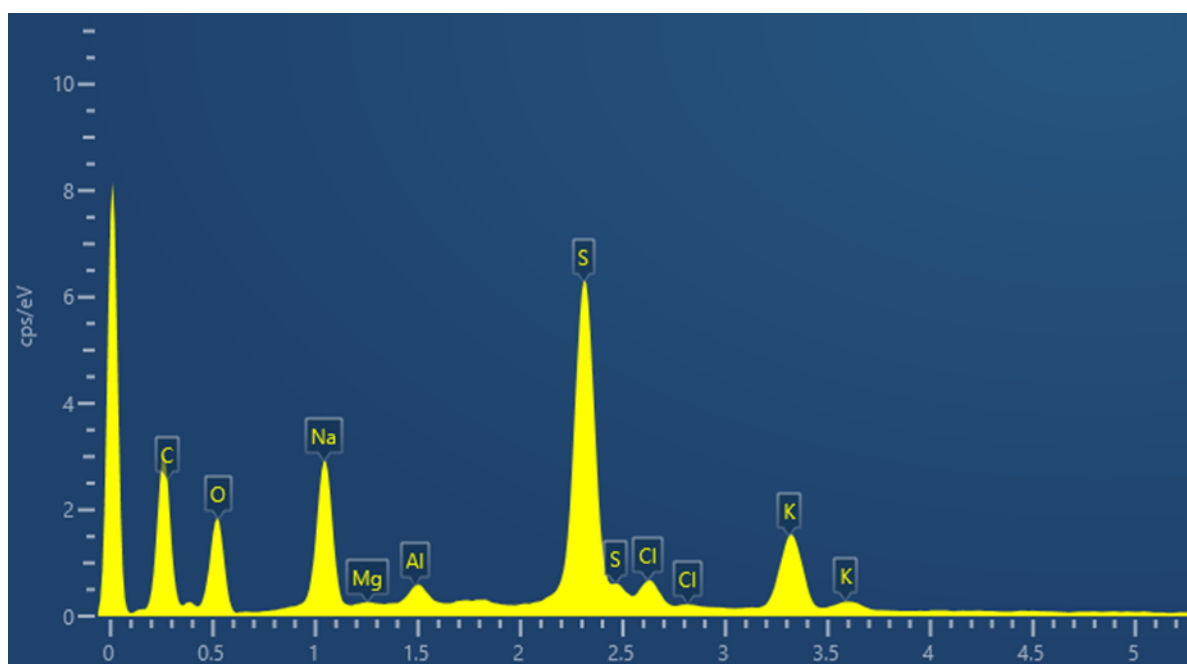


Figure S89 – Energy-dispersive X-ray spectrum showing elemental analysis of the xerogel imaged in Figure S85.

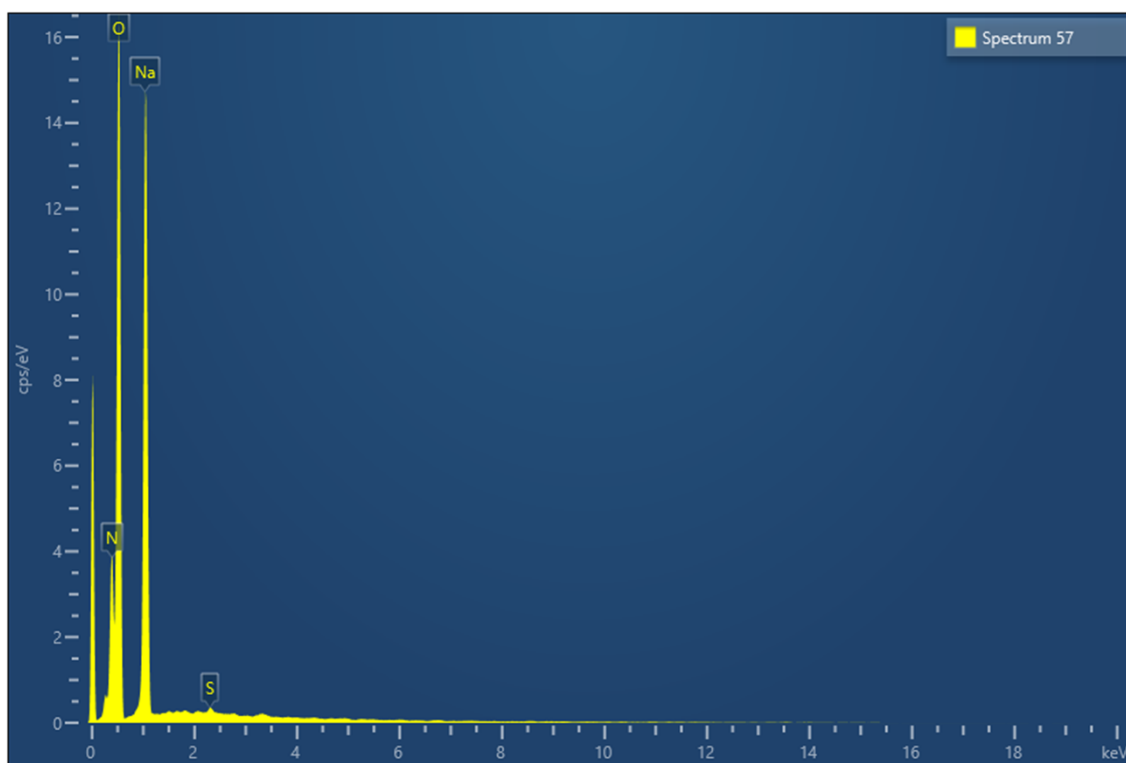


Figure S90 – Energy-dispersive X-ray spectrum showing elemental analysis of the xerogel imaged in Figure S85.

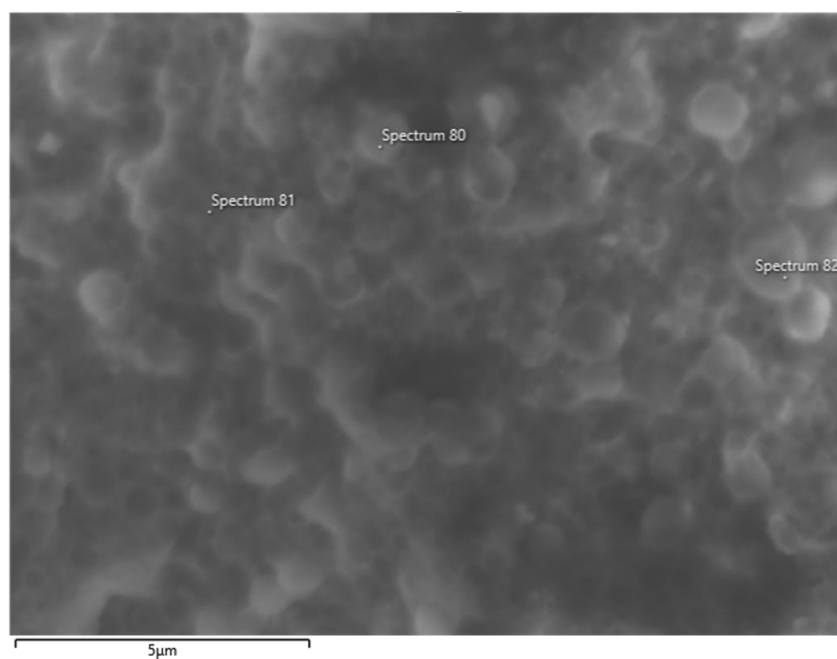


Figure S91 – Scanning electron microscopy image of a xerogel prepared from a dehydrated hydrogel containing compound **1** (5 mg/mL) in Na_2HPO_4 (0.505 M).

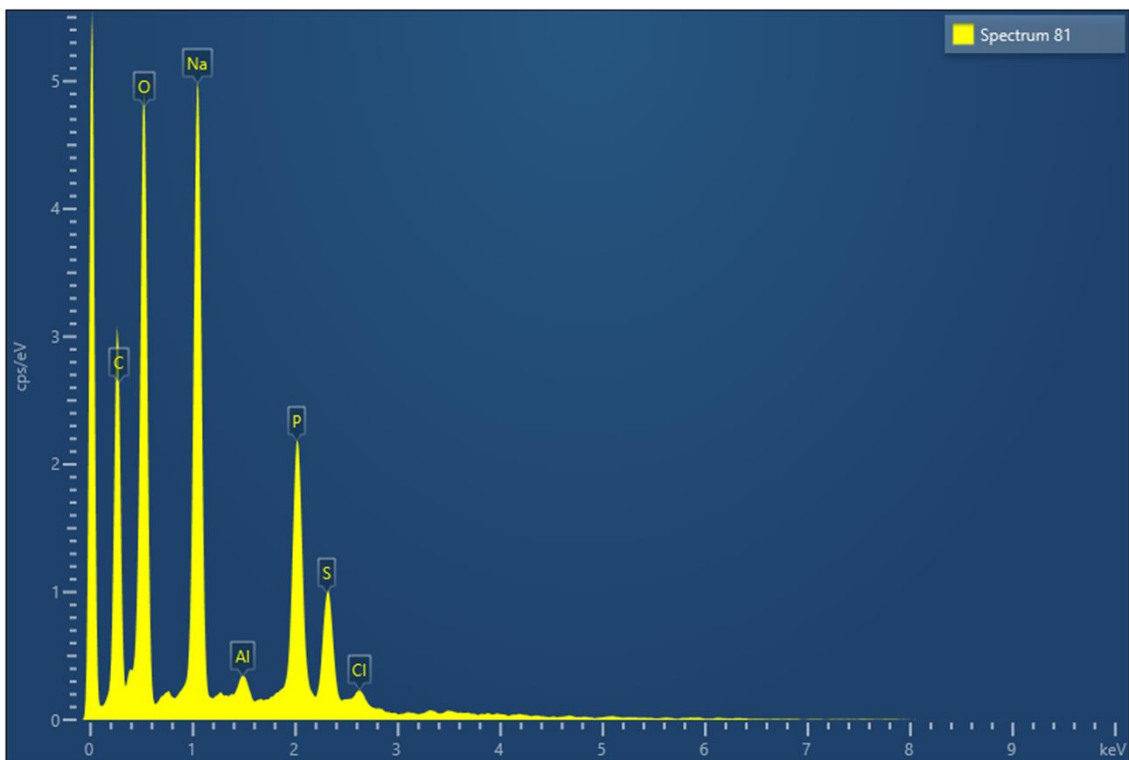


Figure S92 – Energy-dispersive X-ray spectrum showing elemental analysis of the xerogel imaged in Figure S88.

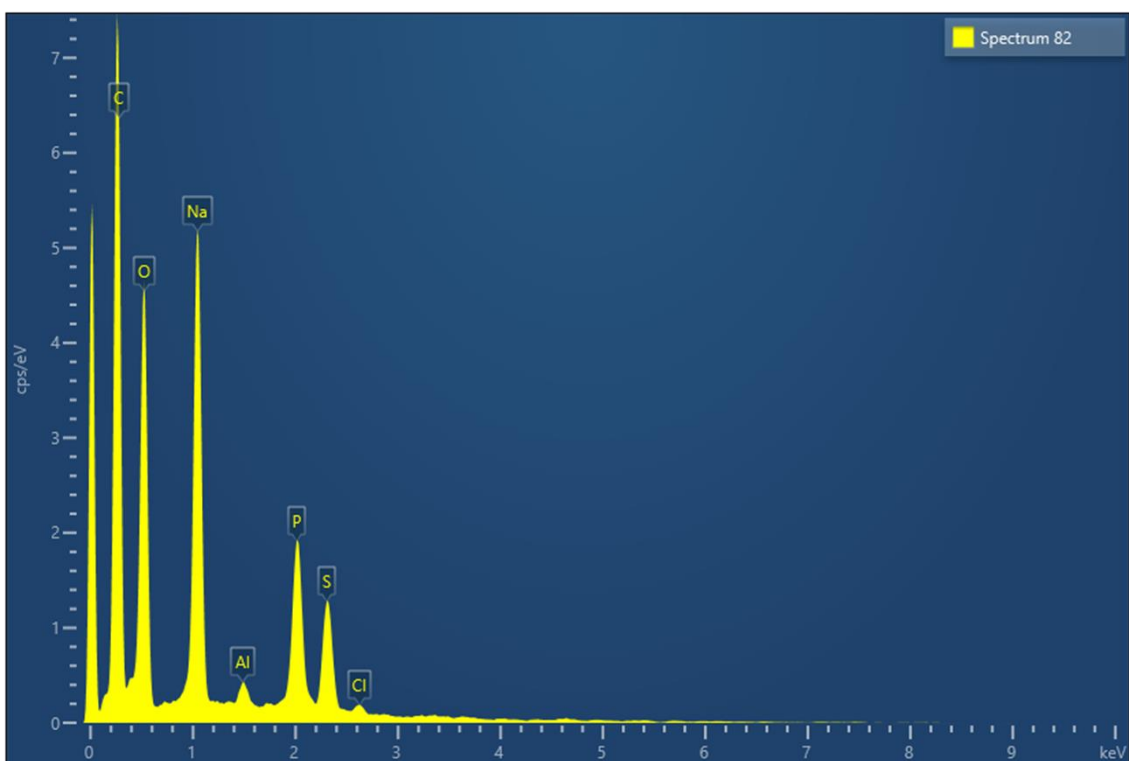


Figure S93 – Energy-dispersive X-ray spectrum showing elemental analysis of the xerogel imaged in Figure S88.

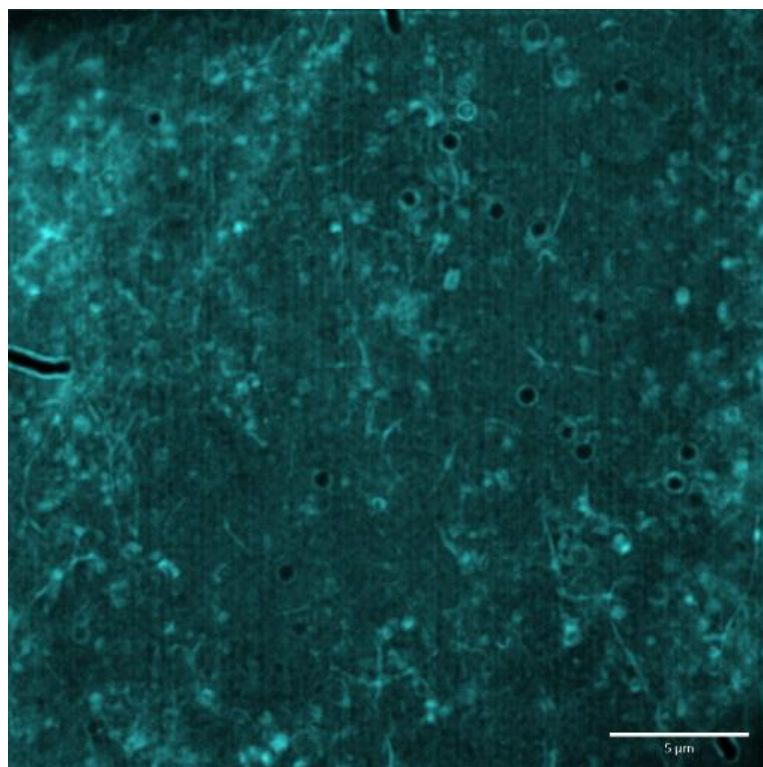


Figure S94 - Fluorescence microscopy image of a hydrogel containing compound **1** (5 mg/ mL) in Na_2HPO_4 (0.505 M).

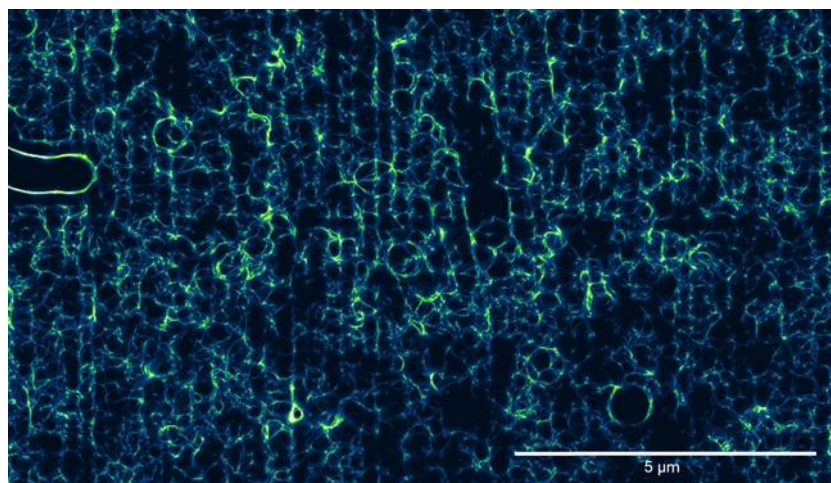


Figure S95 - Refined fluorescence microscopy image of the hydrogel observed in Figure S91.

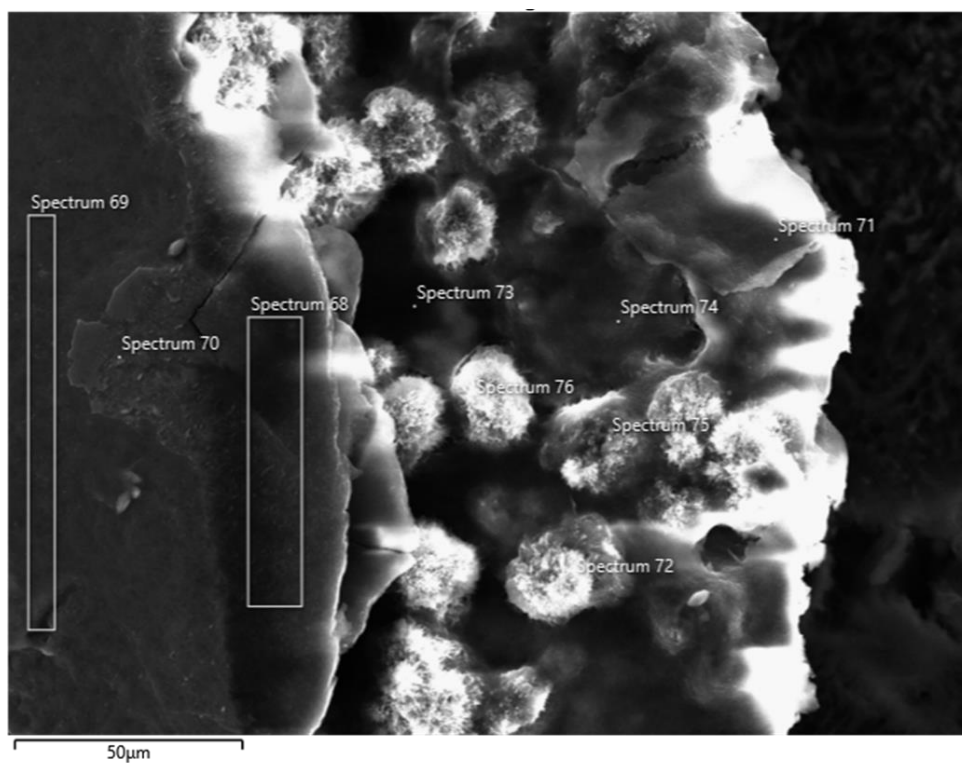


Figure S96 – Scanning electron microscopy image of a xerogel prepared from a dehydrated hydrogel containing compound **1** (5 mg/mL) in NaHCO₃ (0.505 M).

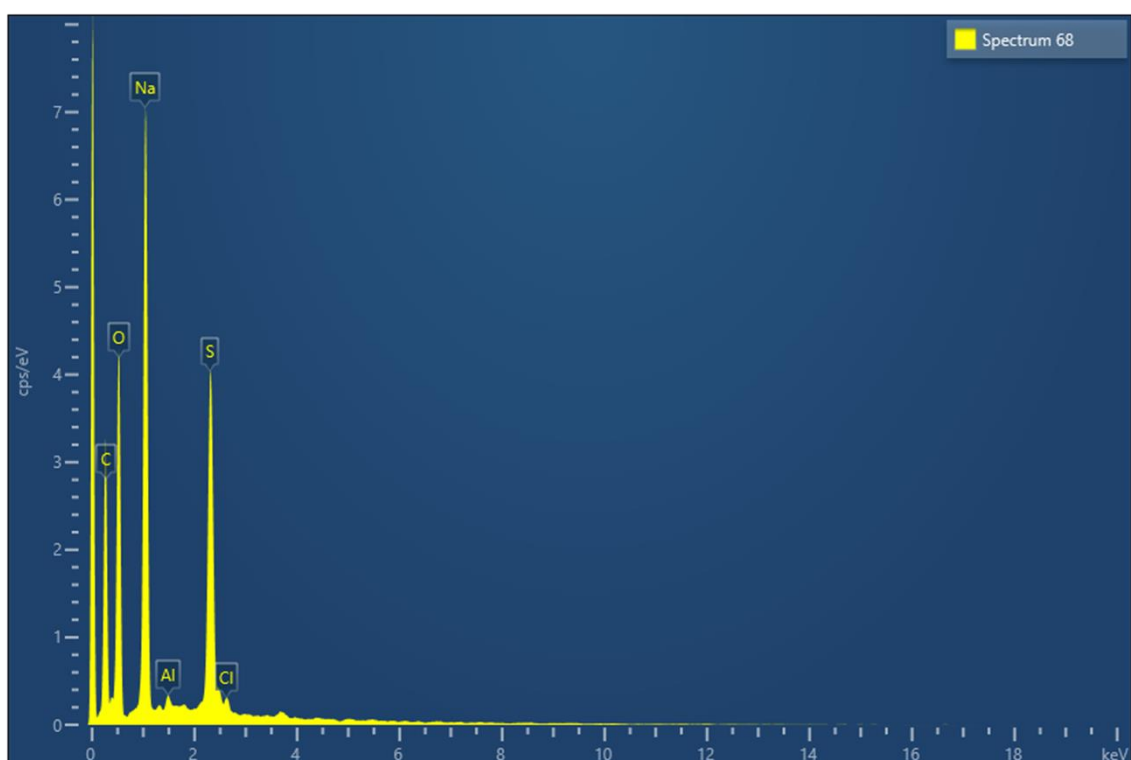


Figure S97 – Energy-dispersive X-ray spectrum showing elemental analysis of the xerogel imaged in Figure S93.

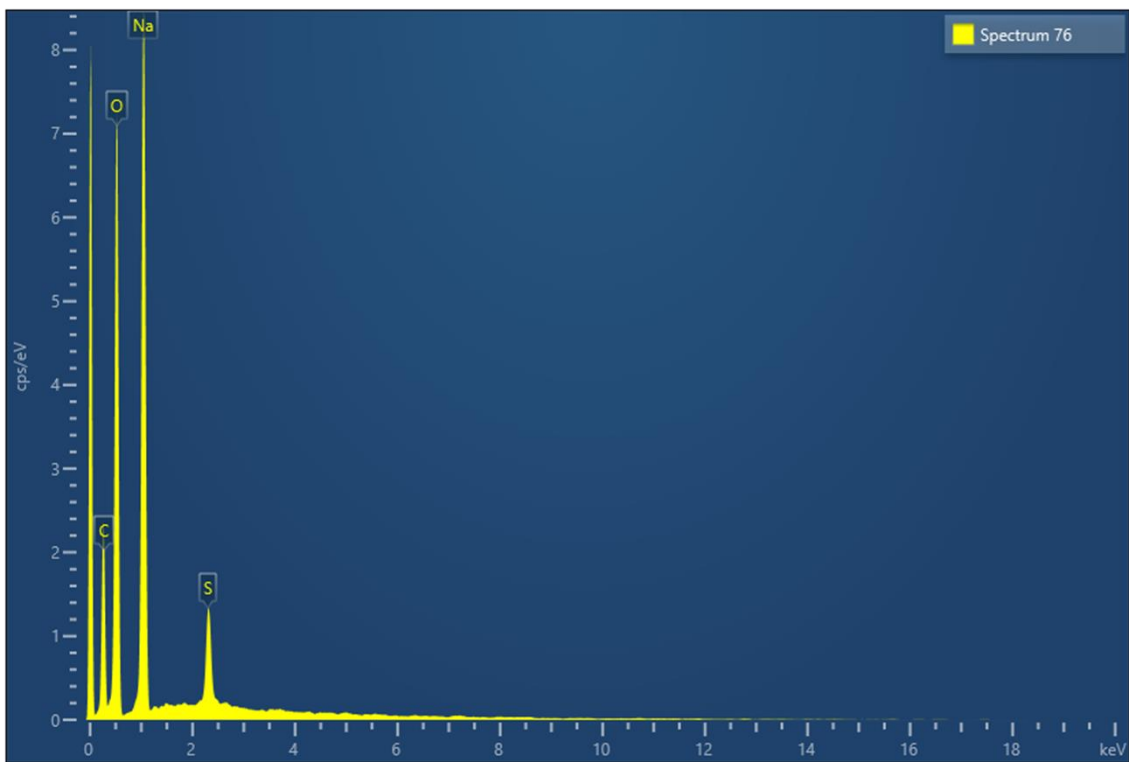


Figure S98 – Energy-dispersive X-ray spectrum showing elemental analysis of the xerogel imaged in Figure S93.

MIC₅₀ Growth Curves

USA 300 Methicillin-resistant *Staphylococcus aureus* (MRSA)

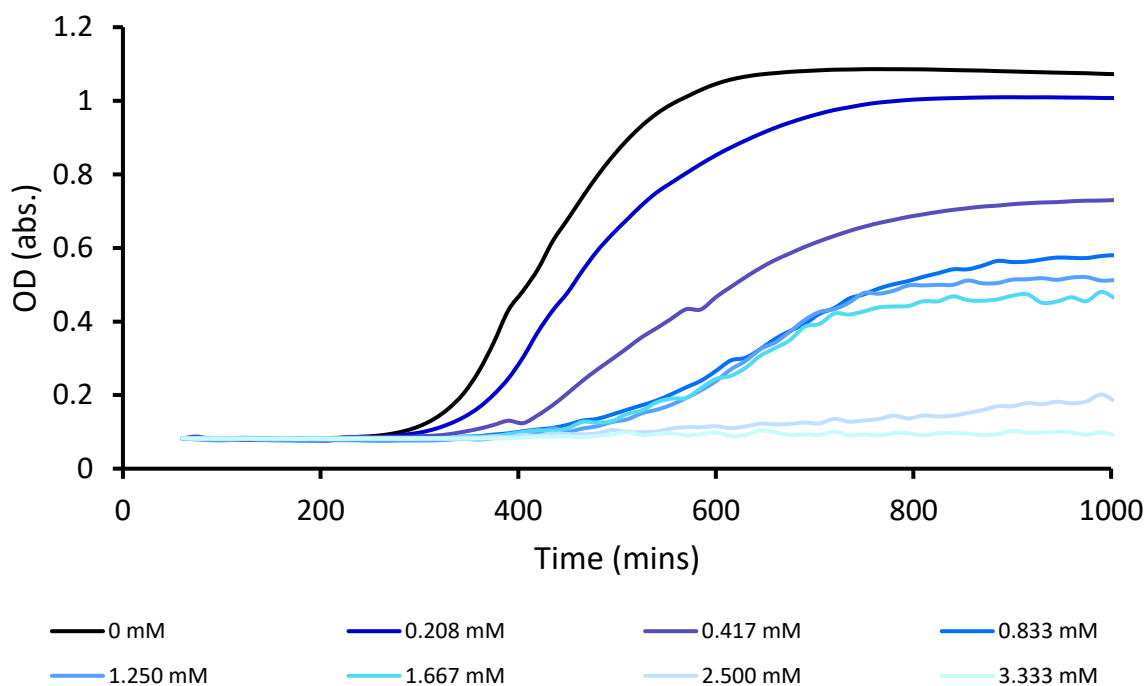


Figure S99 - Averaged growth curves created from absorbance readings of *S. aureus* in the presence of compound **1** at varying concentrations.

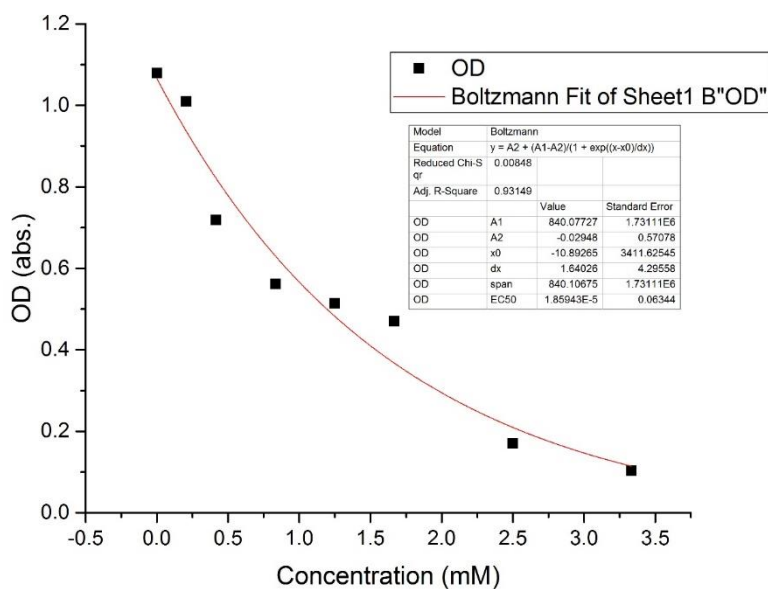


Figure S100 - Origin graph created using absorbance values at 900 minutes for compound **1** at varying concentrations.

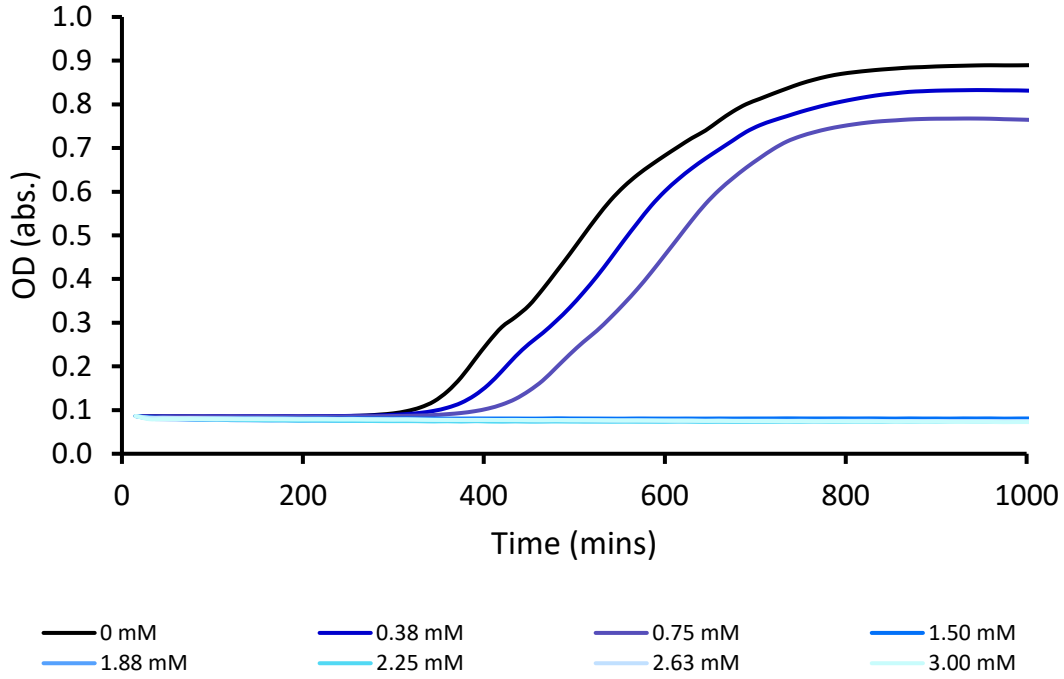


Figure S101 - Averaged growth curves created from absorbance readings of *S. aureus* in the presence of compound **2** at varying concentrations.

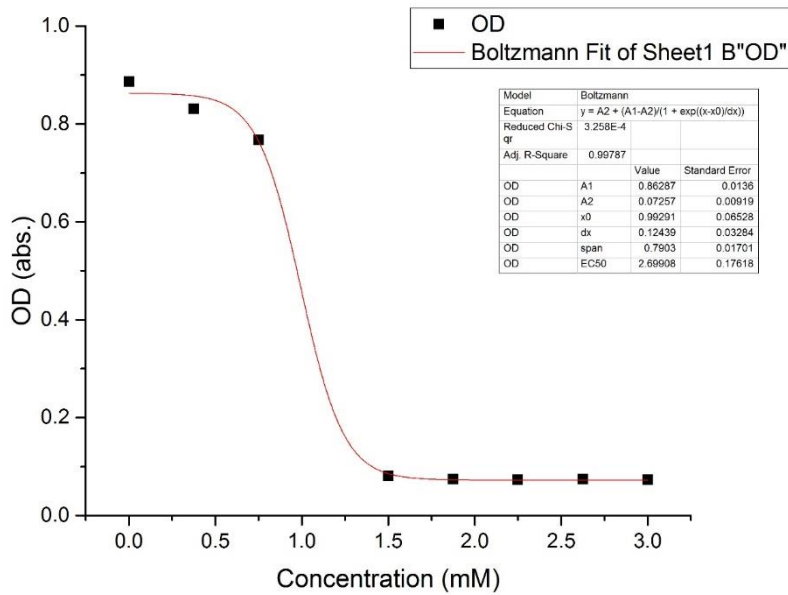


Figure S102 - Origin graph created using absorbance values at 900 minutes for compound **2** at varying concentrations.

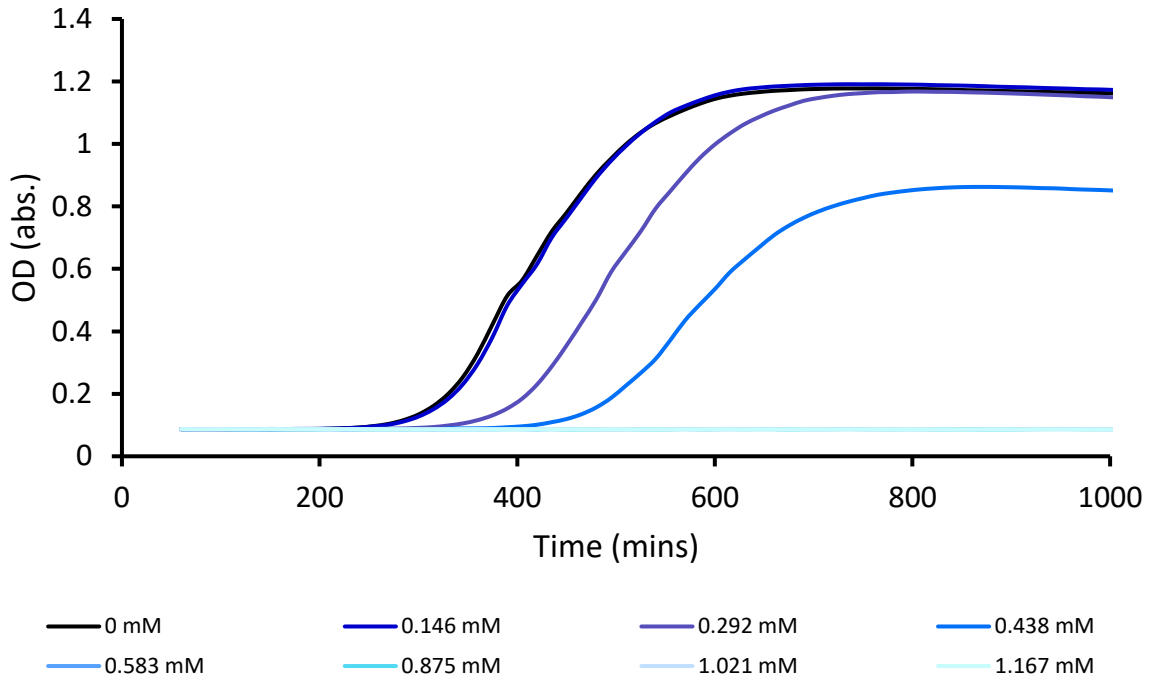


Figure S103 - Averaged growth curves created from absorbance readings of *S. aureus* in the presence of compound **3** at varying concentrations.

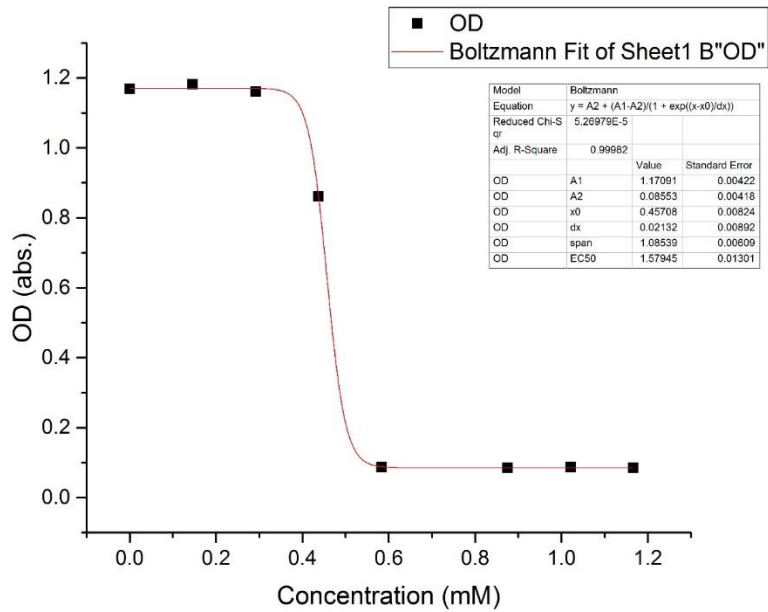


Figure S104 - Origin graph created using absorbance values at 900 minutes for compound **3** at varying concentrations.

***Escherichia coli* DH10β (*E. coli*)**

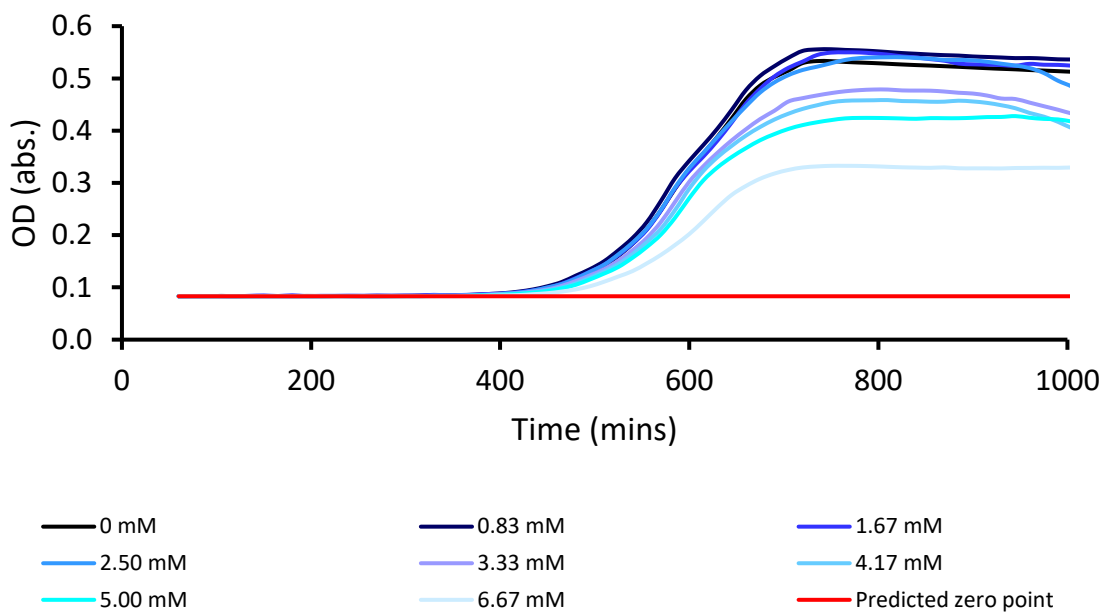


Figure S105 - Averaged growth curves created from absorbance readings of *E. coli* DH10β in the presence of compound **1** at varying concentrations. MIC₅₀ was calculated using predicted endpoint due to solubility.

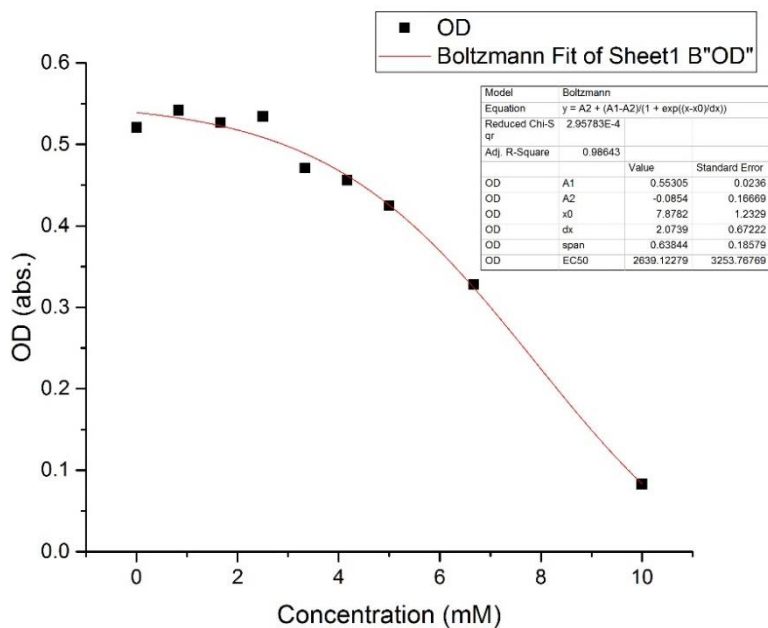


Figure S106 - Origin graph created using absorbance values at 900 minutes for compound **1** at varying concentrations.

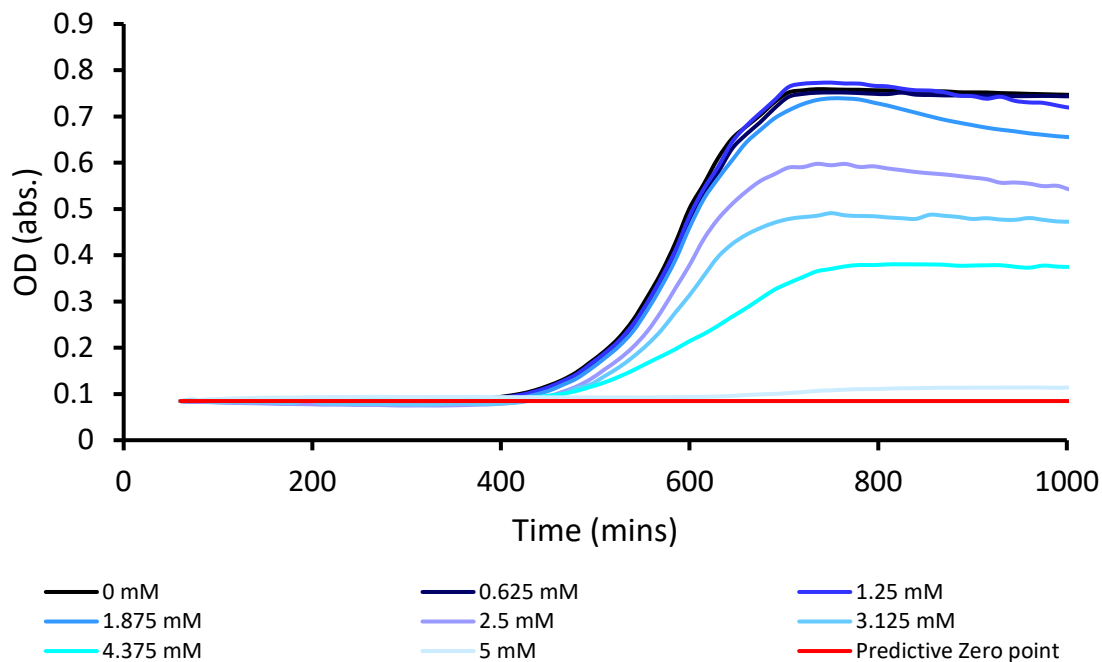


Figure S107 - Averaged growth curves created from absorbance readings of *E. coli* DH10 β in the presence of compound **2** at varying concentrations. MIC₅₀ was calculated using predicted endpoint due to solubility.

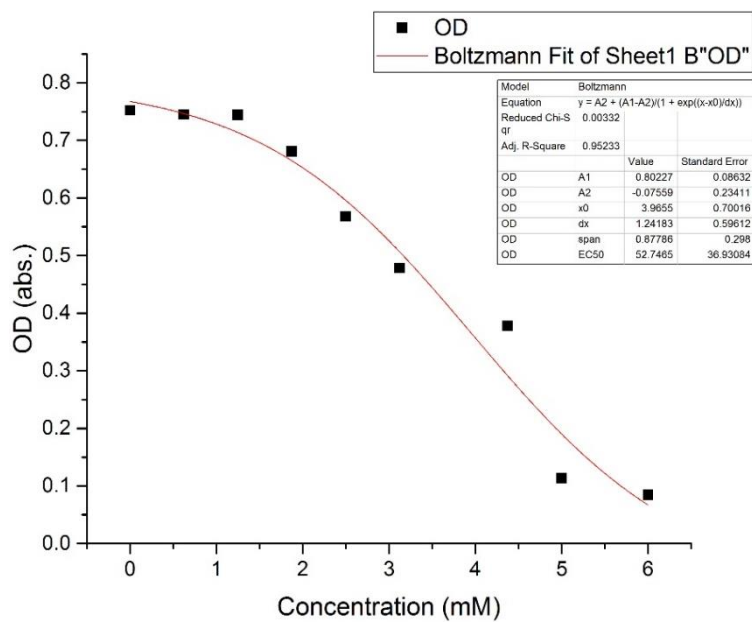


Figure S108 - Origin graph created using absorbance values at 900 minutes for compound **2** at varying concentrations.

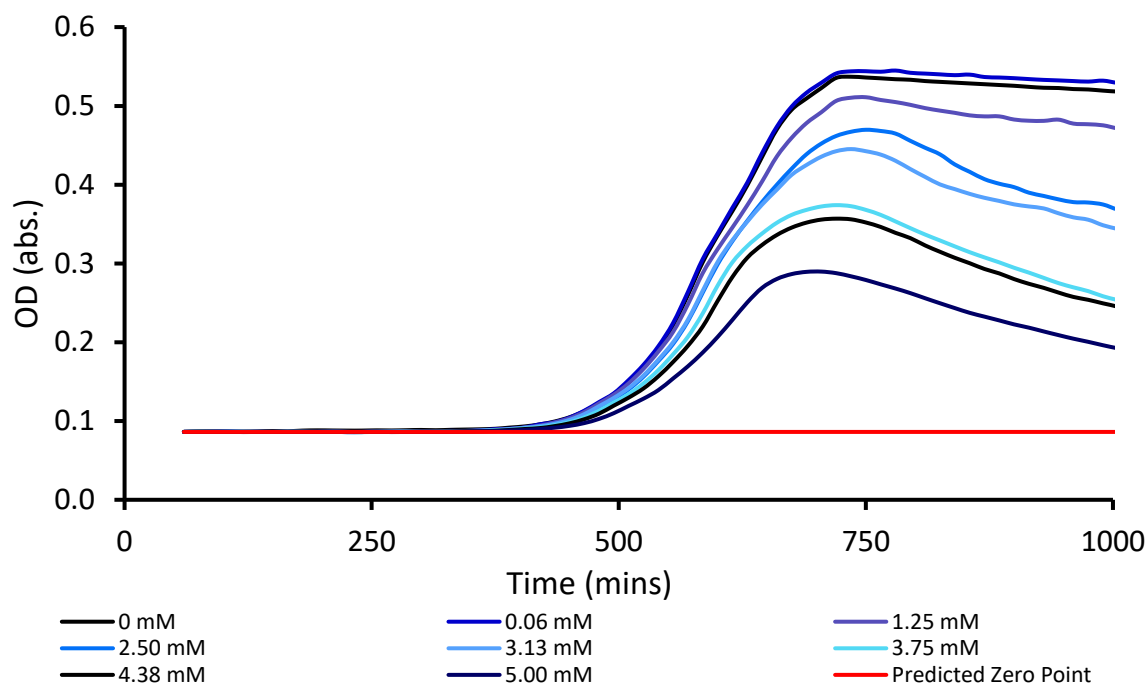


Figure S109- Averaged growth curves created from absorbance readings of *E. coli* DH10 β in the presence of compound **3** at varying concentrations. MIC₅₀ was calculated using predicted endpoint due to solubility.

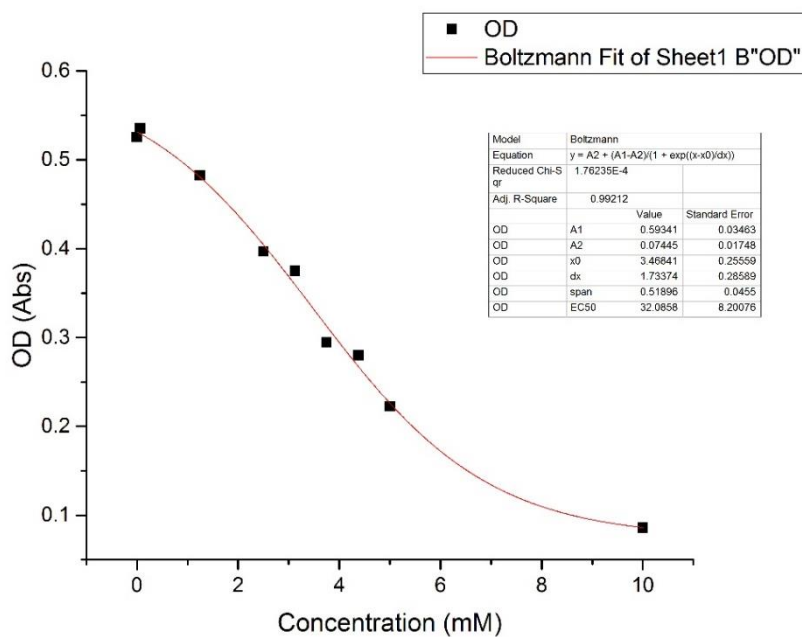


Figure S110 - Origin graph created using absorbance values at 900 minutes for compound **3** at varying concentrations.

Hydrogel antimicrobial efficacy experiments

Disc Diffusion assays *E. coli* DH10 β

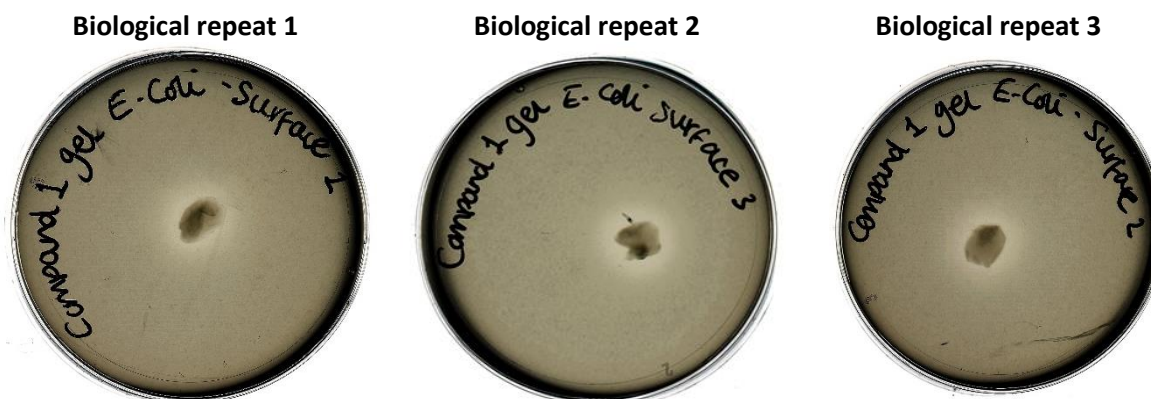


Figure S111 - Disc diffusion assays showing the zone of inhibition of growth of *Escherichia coli* DH10 β due to the presence of \approx 50 mg SSA hydrogel gel of **1** formed in NaCl solution (0.505 M) on the surface of the plate.

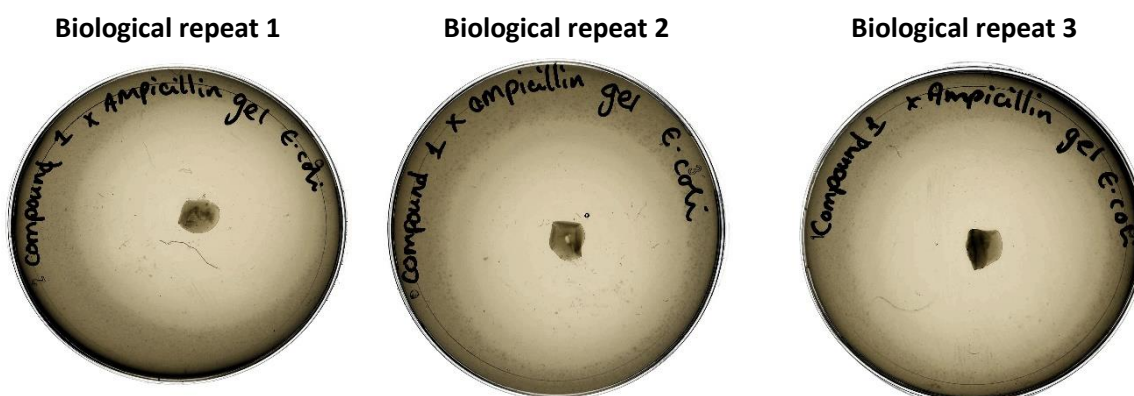


Figure S112 - Disc diffusion assays showing the zone of inhibition of growth of *Escherichia coli* DH10 β due to the presence of \approx 50 mg SSA hydrogel gel of **1** formed in NaCl solution (0.505 M) co-formulated in a 1 : 1 molar ratio with ampicillin, on the surface of the plate.

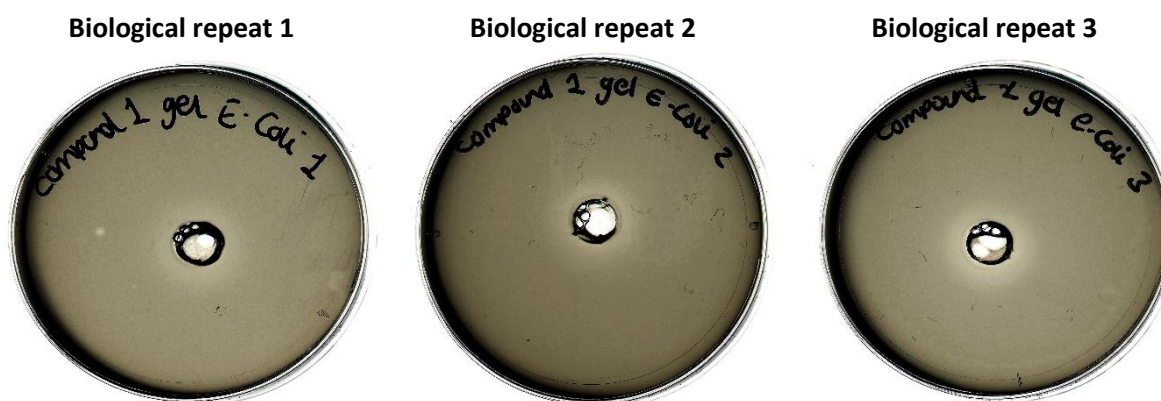


Figure S113 - Disc diffusion assays showing the zone of inhibition of growth of *Escherichia coli* DH10 β due to the presence of \approx 50 mg SSA hydrogel gel of **1** formed in NaCl solution (0.505 M) in a well in the plate.

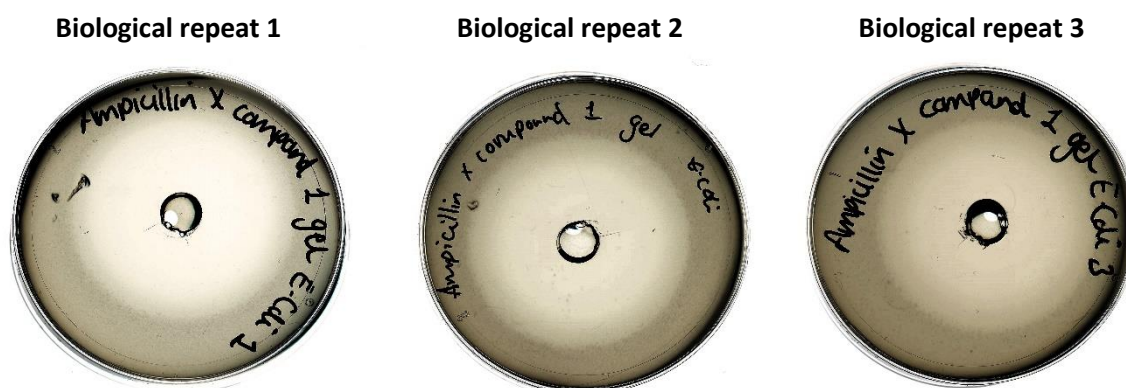


Figure S114 - Disc diffusion assays showing the zone of inhibition of growth of *Escherichia coli* DH10 β due to the presence of \approx 50 mg SSA hydrogel gel of **1** co-formulated in a 1 : 1 molar ratio with ampicillin, in a well in the plate.

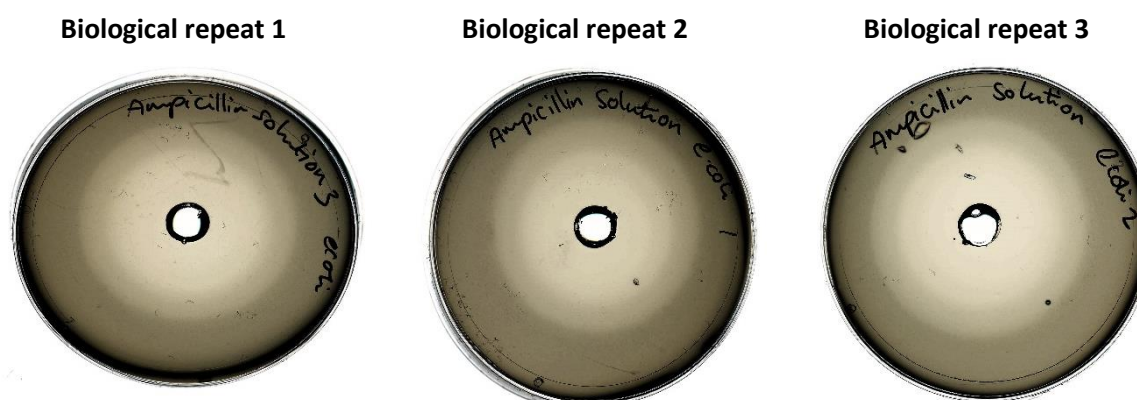


Figure S115 - Disc diffusion assays showing the zone of inhibition of growth of *Escherichia coli* DH10 β due to the presence of ampicillin solution (8.1 mM in a NaCl solution, 0.505 M) in a well in the plate.



Figure S116 - Disc diffusion assays showing the zone of inhibition of growth of *Escherichia coli* DH10 β due to the presence of NaCl solution (0.505 M) in a well in the plate.

Disc Diffusion Assays MRSA USA300



Figure S117 - Disc diffusion assays showing the zone of inhibition of growth of Methicillin resistant *Staphylococcus aureus* USA300 due to the presence of \approx 50 mg SSA hydrogel gel of **1** formed in NaCl solution (0.505 M) on the surface of the plate.

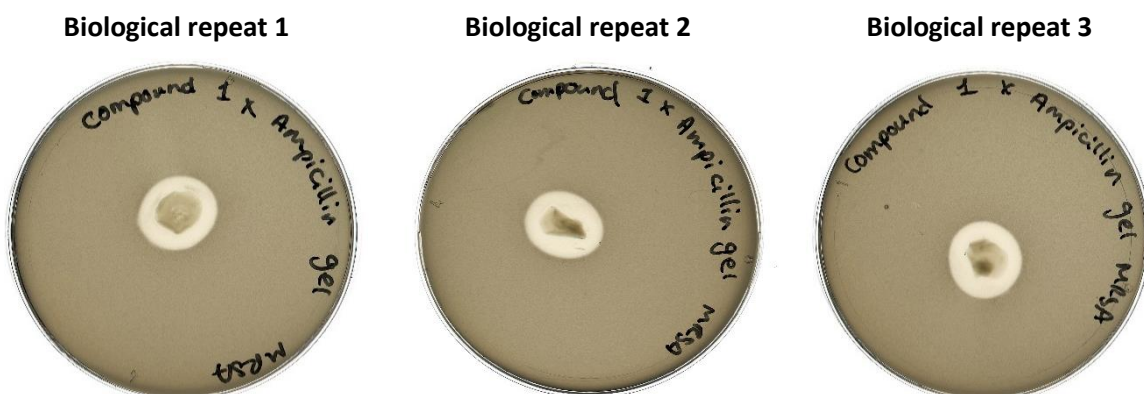


Figure S118 - Disc diffusion assays showing the zone of inhibition of growth of Methicillin resistant *Staphylococcus aureus* USA300 due to the presence of \approx 50 mg SSA hydrogel gel of **1** formed in NaCl solution (0.505 M) co-formulated in a 1 : 1 molar ratio with ampicillin, on the surface of the plate.

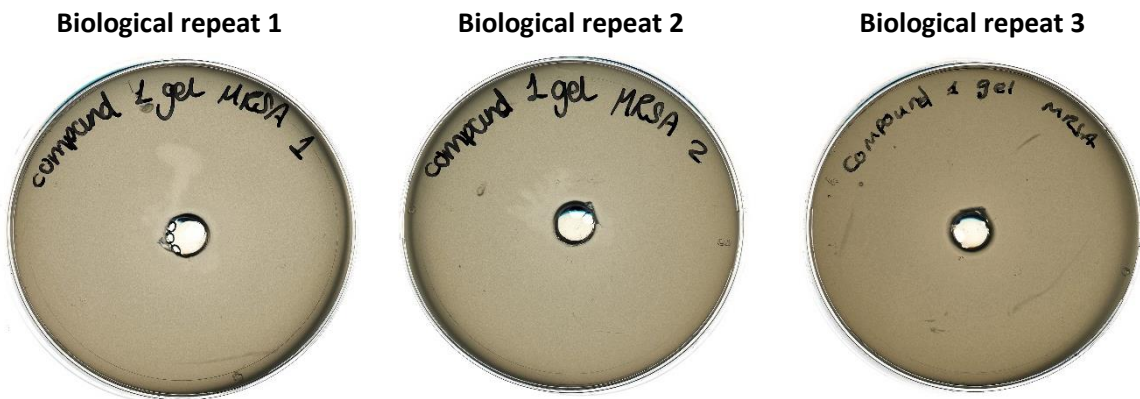


Figure S119 - Disc diffusion assays showing the zone of inhibition of growth of Methicillin resistant *Staphylococcus aureus* USA300 due to the presence of \approx 50 mg SSA hydrogel gel of **1** formed in NaCl solution (0.505 M) in a well in the plate.

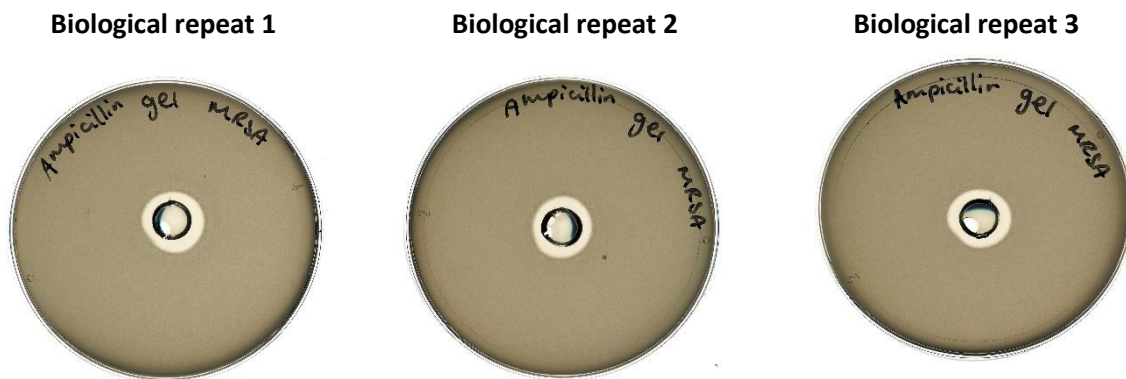


Figure S120 - Disc diffusion assays showing the zone of inhibition of growth of Methicillin resistant *Staphylococcus aureus* USA300 due to the presence of \approx 50 mg SSA hydrogel gel of **1** formed in NaCl solution (0.505 M) co-formulated in a 1 : 1 molar ratio with ampicillin, in a well in the plate.



Figure S121 - Disc diffusion assays showing the zone of inhibition of growth of Methicillin resistant *Staphylococcus aureus* USA300 due to the presence of ampicillin solution (8.1 mM in a NaCl solution, 0.505 M) in a well in the plate.



Figure S122 - Disc diffusion assays showing the zone of inhibition of growth of Methicillin resistant *Staphylococcus aureus* USA300 due to the presence of NaCl solution (0.505 M) in a well in the plate.

Table S2 - The measured zone of inhibition (diameter) in mm of the inhibition of growth in each experimental condition described in Figures S111-122.

Fig no.	Biological repeat 1	Biological repeat 2	Biological repeat 3	Mean average	Standard deviation
S111	13	18	14	14.8	1.92
S112	59	59	60	59.2	0.56
S113	13	21	19	17.4	3.52
S114	53	55	52	53.6	1.15
S115	51	51	56	52.3	2.34
S116	0	0	12	3.9	5.47
S117	17	16	14	15.9	1.19
S118	22	25	23	23.3	1.46
S119	15	13	13	13.8	0.63
S120	18	16	17	17.1	0.77
S121	16	16	14	15.3	0.613
S122	0	0	0	0	0

References

1. J. M. Andrews, *J. Antimicrob. Chemother.*, 2001, **48**, 5-16.
2. L. J. White, N. J. Wells, L. R. Blackholly, H. J. Shepherd, B. Wilson, G. P. Bustone, T. J. Runacres and J. R. Hiscock, *Chem. Sci.*, 2017, **8**, 7620-7630.
3. J. R. Hiscock, G. P. Bustone, B. Wilson, K. E. Belsey and L. R. Blackholly, *Soft Matter*, 2016, **12**, 4221-4228.

